UNIVERSITEIT VAN PRETORIA
UNIVERSITY OF PRETORIA
YUNIBESITHI YA PRETORIA
Denkleiers • Leading Minds • Dikgopolo tša Dihlalefi

# Microbial Precipitation of Pb(II) with Wild Strains of *Klebsiella pneumoniae* and *Paraclostridium bifermentans* Isolated From an Industrially Obtained Microbial Consortium

Olga Neveling

# Microbial Precipitation of Pb(II) with Wild Strains of *Klebsiella pneumoniae* and *Paraclostridium bifermentans* Isolated From an Industrially Obtained Microbial Consortium

by

**Olga Neveling**

A dissertation submitted in partial fulfilment of the requirements for the degree of

**Master of Engineering (Chemical Engineering)**

in the

Department of Chemical Engineering
University of Pretoria
South Africa

October 2022

# Abstract

The study focused on determining the microbial precipitation abilities of two bacterial strains, *Paraclostridium bifermentans* and *Klebsiella pneumoniae* isolated from an industrially obtained microbial consortium. Previous research has demonstrated the effectiveness of the consortium in the bioprecipitation of Pb(II). The bioremediation of Pb(II) provides an alternative and less costly method for lead removal from solution. A proof of concept was determined in a long duration study over 100 h wherein the bioprecipitation abilities of the strains were determined. It was concluded that approximately 84 % and 100 % of Pb(II) was removed from solution in experiments containing 80 mg $L^{-1}$ initial Pb(II) concentration over 100 h, with *P. bifermentans* and *K. pneumoniae* respectively. The mechanisms of precipitation were further investigated with a short-term study, since it was observed that precipitation occurred in under 18 h in the long duration study. This shorter study was conducted over 30 h with nine sampling intervals and indicated removal percentages of approximately 86 % and 91 % for samples containing 80 mg $L^{-1}$ initial Pb(II) concentration after 30 h for *P. bifermentans* and *K. pneumoniae* respectively. The precipitate identity was determined to be PbS and $Pb^0$ for samples containing *P. bifermentans* while samples containing *K. pneumoniae* contained precipitates of PbO and either PbCl or $Pb_3(PO_4)_2$. An investigation into the extracellular and intracellular Pb(II) concentration led to the observation that a rapid detoxification mechanism such as biosorption is present in the microbes within the first 6 h of the experiment. These mentioned factors provide a greater understanding of the mechanisms utilised by the bacteria in the bioprecipitation and adsorption of Pb(II), and can be used as a step towards applying the process on an industrial scale.

**Keywords**: lead; bioprecipitation; *K. pneumoniae*; *P. bifermentans*; bioremediation

# Acknowledgements

I would like to express my sincere gratitude to the following people and organisations for their contribution to the research in this dissertation:

1. The financial assistance of the National Research Foundation (NRF).
2. Prof H.G. Brink, my supervisor, and Prof E.M.N. Chirwa, my co-supervisor, for their guidance and support.
3. Inqaba Biotech for the BLAST analysis and generation of the phylogenetic trees of the isolated cultures.
4. Carla Cilliers and Job Tendenedzai, PhD students who provided my training and offered advice.
5. Thato Ncube and Ziyanda Ngxongo who provided immense laboratory assistance with the experiments.
6. Iain Ilott, Glenn and Celia Neveling and Teran and Kyle Benkenstein for their support throughout the year.
7. Glenn Neveling for the construction of the incubator used in all experiments.

# Nomenclature

$\mu$ Specific growth rate ($d^{-1}$)

$\mu_{max}$ Maximum specific growth rate ($d^{-1}$)

$\mu_X$ Mean for population X used in statistical inference, where X is equal to 1 or 2

$\overline{X}_X$ Mean of sample population X used in statistical inference, where X is equal to 1 or 2

$df$ Degrees of freedom used in statistical inference

$H_0$ Null hypothesis used in statistical inference

$H_1$ Alternative hypothesis used in statistical inference

$n_X$ Size of sample X used in statistical inference, where X is equal to 1 or 2

$S_p$ Pooled estimate of the common standard deviation of two populations used in statistical inference.

$s_X$ Sample standard deviation of sample population X used in statistical inference, where X is equal to 1 or 2

$t_g$ Generation time (d)

CFU Colony forming units

DMSO dimethyl sulfoxide

EDTA ethylenedinitrilotetraacetic acid disodium salt dihydrate

EMB Eosin methylene blue

LB Luria Bertani

MA Metabolic activity

MTC Maximum tolerance concentration

MTT 3-(4,5-dimethylthiazol-2-yl)-2,5-diphenyl tetrazolium bromide

$OD_{600}$ Optical density at 600 nm

WWTP Wastewater treatment plant

XPS X-ray photonelectron spectroscopy

# Contents

**Abstract** iii

**Acknowledgements** iv

**Nomenclature** v

**1 Introduction** 1

**2 Literature** 4

2.1 Lead pollution and the associated risks . . . . . 4

2.2 Lead consumption, production and reserves . . . . . 6

2.3 Conventional methods of lead removal in wastewater . . . . . 6

2.4 Lead bioremediation . . . . . 8

2.4.1 Mechanisms of lead resistance in microorganisms . . . . . 8

2.4.2 Previous studies done on lead bioremediation . . . . . 13

2.5 Microbiology . . . . . 22

2.5.1 Prokaryote metabolism - anaerobic respiration . . . . . 22

2.5.2 *Paraclostridium bifermentans* . . . . . 24

2.5.3 *Klebsiella pneumoniae* . . . . . 25

2.5.4 Growth conditions . . . . . 26

2.6 Experimental methods . . . . . 28

2.6.1 Preculture preparation . . . . . 28

2.6.2 Anaerobic batch reactors . . . . . 28

2.6.3 Aerobic batch reactors . . . . . 29

2.6.4 Anaerobic and aerobic spread and streak plates . . . . . 29
2.6.5 Microbial isolation . . . . . 30
2.6.6 Determination of extracellular and intracellular Pb(II) . . . . . 31
2.7 Analytical techniques . . . . . 31
2.7.1 Atomic Absorption Spectrometry . . . . . 31
2.7.2 Metabolic activity . . . . . 32
2.7.3 Nitrate removal . . . . . 33

**3 Experimental methods 34**

3.1 Materials . . . . . 34
3.2 Methods . . . . . 34
3.2.1 Preparation of lead nitrate solution . . . . . 34
3.2.2 Preculture preparation . . . . . 34
3.2.3 Anaerobic batch reactors . . . . . 35
3.2.4 Metabolic activity . . . . . 35
3.2.5 Nitrate removal . . . . . 36
3.2.6 $OD_{600}$ measurements . . . . . 36
3.2.7 Residual Pb(II) concentration measurements . . . . . 37
3.2.8 Determination of extracellular and intracellular Pb(II) . . . . . 37
3.2.9 Precipitate identity . . . . . 38
3.2.10 Preparation of anaerobic streak and spread plates . . . . . 38

**4 Bioprecipitation of lead using *P. bifermentans* and *K. pneumoniae*: long duration study 40**

4.1 Experimental methods . . . . . 40

4.2 Results and discussions . . . . . 41
4.2.1 Isolation of the strains . . . . . 41
4.2.2 Visual changes . . . . . 43
4.2.3 Microbial growth measurements . . . . . 44
4.2.4 Residual Pb(II) concentration . . . . . 45
4.2.5 Nitrate concentration . . . . . 49
4.3 Conclusions . . . . . 50

**5 Bioprecipitation of lead using *P. bifermentans* and *K. pneumoniae*: short duration study 52**

5.1 Experimental . . . . . 52
5.2 Results and discussions . . . . . 52
5.2.1 Visual changes . . . . . 52
5.2.2 Microbial growth measurements . . . . . 53
5.2.3 Residual Pb(II) concentration . . . . . 55
5.2.4 Nitrate concentration . . . . . 58
5.2.5 Comparison between metabolic activity measurements, nitrate concentration and residual Pb(II) concentration . . . . . 59
5.2.6 Extracellular and Intracellular Pb(II) concentration . . . . . 67
5.2.7 Specific growth rate . . . . . 68
5.2.8 Precipitate identity . . . . . 70
5.3 Conclusions . . . . . 71

**6 Bioprecipitation of lead using *P. bifermentans* and *K. pneumoniae*: an investigation into exponential growth and the influence of Pb(II) 73**

6.1 Experimental . . . . . 73

6.2 Results and discussions . . . . . 74
6.2.1 Visual changes . . . . . 74
6.2.2 Microbial growth measurements . . . . . 74
6.2.3 Residual Pb(II) concentration . . . . . 75
6.2.4 Correlation between CFU count, $OD_{600}$ and metabolic activity . . 76
6.2.5 Predicted values for metabolic activity and $OD_{600}$ . . . . . 79
6.2.6 Specific growth rate . . . . . 80
6.3 Conclusions . . . . . 82

**7 General conclusions and recommendations** **83**

**8 References** **84**

**A Appendix** **A.93**

# List of Figures


1 Classification of biosorption mechanisms according to dependence on cell metabolism, adapted from Perpetuo, Barbieri & Nascimento (2011) . . . 9

2 Classification of biosorption mechanisms based on the location within the cell and the metal removed, adapted from Perpetuo, Barbieri & Nascimento (2011) . . . 9

3 Serial dilution as adapted from Ogbu *et al* (2017). . . . 30

4 The description of the determination of the extracellular and intracellular Pb(II) as well as the expected species at each step. . . . 38

5 The method used for the preparation of the the streak plates. . . . 39

6 The phylogenetic tree indicating the identity of the *P. bifermentans* strain isolated from the microbial consortium (BPB21A). . . . 41

7 (a) The initial spread plate of the consortium and (b) the final streak plate containing the isolated strain *P. bifermentans*. . . . 42

8 The phylogenetic tree indicating the identity of the *K. pneumoniae* strain isolated from the microbial consortium (BKP21E). . . . 42

9 The plates used in the isolation experiment for *K. pneumoniae* with (a) the initial EMB agar plate and (b) the final LB broth agar plate used for identification of the strain. . . . 43

10 The bioreactors of (a) *P. bifermentans* and (b) *K. pneumoniae* at 0 h and the rapid visual changes observed for (c) *P. bifermentans* and (d) *K. pneumoniae* after 17 h. . . . 44

11 The metabolic activity of *P. bifermentans*, *K. pneumoniae* and the microbial consortium as observed over approximaterRly 100 h of the long duration precipitation study. . . . 45

12 The lead removal profiles of *P. bifermentans*, *K. pneumoniae* and the microbial consortium over approximately 100 h of the long duration precipitation study. . . . 46

13 The nitrate concentration of *K. pneumoniae*, *P. bifermentans* and the microbial consortium as observed over approximately 100 h of the long duration precipitation study. . . . . 50

14 The visual changes observed for each experiment in triplicate containing *P. bifermentans* over 30 h for (a) 80 mg $L^{-1}$, (b) 250 mg $L^{-1}$ and (c) 500 mg $L^{-1}$ initial Pb(II) concentration. . . . . 53

15 The visual changes observed for each experiment in triplicate containing *K. pneumoniae* over 30 h for (a) 80 mg $L^{-1}$, (b) 250 mg $L^{-1}$ and (c) 500 mg $L^{-1}$ initial Pb(II) concentration. . . . . 53

16 The metabolic activity as $A_{550}$ for both *P. bifermentans* and *K. pneumoniae* with varying initial Pb(II) concentrations compared with previously published data on the consortium from which the strains were isolated (Hörstmann, Brink & Chirwa, 2020). . . . . 54

17 The residual Pb(II) concentration over time for experiments containing both *P. bifermentans* and *K. pneumoniae* with (a) 80 mg $L^{-1}$, (b) 250 mg $L^{-1}$ and (c) 500 mg $L^{-1}$ initial Pb(II) concentration, compared to previously published data on the microbial consortium from which the strains were isolated (Hörstmann, Brink & Chirwa, 2020). . . . 57

18 The nitrate concentration over time for both *P. bifermentans* and *K. pneumoniae* with varying initial Pb(II) concentrations, compared to previously published data on the microbial consortium from which the strains were isolated (Hörstmann, Brink & Chirwa, 2020). . . . . 58

19 A comparison between metabolic activity as $A_{550}$ and the nitrate concentration for (a) 80 mg $L^{-1}$, (b) 250 mg $L^{-1}$, (c) 500 mg $L^{-1}$ initial Pb(II) concentration. A comparison between metabolic activity as $A_{550}$ and residual Pb(II) concentration for (d) 80 mg $L^{-1}$, (e) 250 mg $L^{-1}$, (f) 500 mg $L^{-1}$ initial Pb(II) concentration. A comparison between nitrate concentration and residual Pb(II) concentration of (g) 80 mg $L^{-1}$, (h) 250 mg $L^{-1}$ and (i) 500 mg $L^{-1}$ initial Pb(II) concentration for *P. bifermentans*. . . . . 60

20 A comparison between metabolic activity as $A_{550}$ and the nitrate concentration for (a) 80 mg $L^{-1}$, (b) 250 mg $L^{-1}$, (c) 500 mg $L^{-1}$ initial Pb(II) concentration. A comparison between metabolic activity as $A_{550}$ and residual Pb(II) concentration for (d) 80 mg $L^{-1}$, (e) 250 mg $L^{-1}$, (f) 500 mg $L^{-1}$ initial Pb(II) concentration. A comparison between nitrate concentration and residual Pb(II) concentration of (g) 80 mg $L^{-1}$, (h) 250 mg $L^{-1}$ and (i) 500 mg $L^{-1}$ initial Pb(II) concentration for *K. pneumoniae*. . . . . 61

21 The fitted curves using a four part sigmoidal curve for metabolic activity of (a) *P. bifermentans* and (b) *K. pneumoniae*, nitrate concentration of (c) *P. bifermentans* and (d) *K. pneumoniae* and residual Pb(II) concentration of (e) *P. bifermentans* and (f) *K. pneumoniae*. . . . . 62

22 The comparison between the first derivative curves of *P. bifermentans* for (a) metabolic activity and nitrate concentration, (b) metabolic activity and residual Pb(II) concentration, (c) nitrate and lead concentration for 80 mg $L^{-1}$ initial Pb(II) concentration, (d) metabolic activity and nitrate concentration, (e) metabolic activity and residual Pb(II) concentration, (f) nitrate and residual Pb(II) concentration for 250 mg $L^{-1}$ initial Pb(II) concentration, (g) metabolic activity and nitrate concentration, (h) metabolic activity and residual Pb(II) concentration, (i) nitrate and residual Pb(II) concentration for 500 mg $L^{-1}$ initial Pb(II) concentration. 63

23 The comparison between the first derivative curves of *K. pneumoniae* for (a) metabolic activity and nitrate concentration, (b) metabolic activity and residual Pb(II) concentration, (c) nitrate and lead concentration for 80 mg $L^{-1}$ initial Pb(II) concentration, (d) metabolic activity and nitrate concentration, (e) metabolic activity and residual Pb(II) concentration, (f) nitrate and residual Pb(II) concentration for 250 mg $L^{-1}$ initial Pb(II) concentration, (g) metabolic activity and nitrate concentration, (h) metabolic activity and residual Pb(II) concentration, (i) nitrate and residual Pb(II) concentration for 500 mg $L^{-1}$ initial Pb(II) concentration. 64

24 The comparison between the metabolic activity and the rate of change in metabolic activity for *P. bifermentans* with (a) 80 mg $L^{-1}$, (d) 250 mg $L^{-1}$ and (g) 500 mg $L^{-1}$ initial Pb(II) concentration. The comparison between the nitrate concentration and the rate of change in nitrate concentration for *P. bifermentans* with (b) 80 mg $L^{-1}$, (e) 250 mg $L^{-1}$ and (h) 500 mg $L^{-1}$ initial Pb(II) concentration. The comparison between the residual Pb(II) concentration and the rate of change in Pb(II) concentration for *P. bifermentans* with (c) 80 mg $L^{-1}$, (f) 250 mg $L^{-1}$ and (i) 500 mg $L^{-1}$ initial Pb(II) concentration . . . . . 66

25 The comparison between the metabolic activity and the rate of change in metabolic activity for *K. pneumoniae* with (a) 80 mg $L^{-1}$, (d) 250 mg $L^{-1}$ and (g) 500 mg $L^{-1}$ initial Pb(II) concentration. The comparison between the nitrate concentration and the rate of change in nitrate concentration for *K. pneumoniae* with (b) 80 mg $L^{-1}$, (e) 250 mg $L^{-1}$ and (h) 500 mg $L^{-1}$ initial Pb(II) concentration. The comparison between the residual Pb(II) concentration and the rate of change in Pb(II) concentration for *K. pneumoniae* with (c) 80 mg $L^{-1}$, (f) 250 mg $L^{-1}$ and (i) 500 mg $L^{-1}$ initial Pb(II) concentration . . . . . 67

26 The percentage composition of the samples in terms of extracellular, intracellular and solution Pb(II) concentration for *P. bifermentans* at (a) 80 mg $L^{-1}$ and (b) 250 mg $L^{-1}$ initial concentration Pb(II) and *K. pneumoniae* at (c) 80 mg $L^{-1}$ and (d) 250 mg $L^{-1}$ initial concentration Pb(II). . . . . 68

27 The specific growth rate, $\mu$, over time for *P. bifermentans* and *K. pneumoniae* with (a) 80 mg $L^{-1}$, (b) 250 mg $L^{-1}$ and (c) 500 mg $L^{-1}$ initial Pb(II) concentration. . . . . 69

28 The XPS profiles of the Pb-species for samples containing 80 mg $L^{-1}$ initial Pb(II) concentration with (a) *P. bifermentans* and (b) *K. pneumoniae*. . 71

29 The visual results of the experiment involving (a) *P. bifermentans* and (b) *K. pneumoniae* with 80 mg $L^{-1}$ initial concentration Pb(II). . . . . 74

30 Microbial growth of *P. bifermentans* and *K. pneumoniae* measured as CFU count for experiments containing no added Pb(II) and experiments containing 80 mg $L^{-1}$ initial concentration Pb(II). . . . . 75

31 Residual Pb(II) concentration for experiments containing *P. bifermentans* and *K. pneumoniae* with 80 mg $L^{-1}$ initial concentration Pb(II). . . . . 76

32 The relationship between metabolic activity and CFU count for *P. bifermentans* and *K. pneumoniae* with 80 mg $L^{-1}$ initial concentration Pb(II). 77

33 The relationship between metabolic activity and CFU count as well as $OD_{600}$ and CFU count for *P. bifermentans* with no added Pb(II). . . . . 77

34 The relationship between metabolic activity and CFU count as well as $OD_{600}$ and CFU count for *K. pneumoniae* with no added Pb(II). . . . . 78

35 The predicted values of metabolic activity for *P. bifermentans* and *K. pneumoniae* with 80 mg $L^{-1}$ initial concentration Pb(II). . . . . 79

36 The predicted values for metabolic activity and $OD_{600}$ for *P. bifermentans* and *K. pneumoniae* with no added Pb(II). . . . . 80

37 The fitted curves of the CFU count for experiments containing *P. bifermentans* with (a) 80 mg $L^{-1}$ Pb(II) and (b) no added Pb(II) and experiments containing *K. pneumoniae* with (c) 80 mg $L^{-1}$ Pb(II) and (d) no added Pb(II). . . . . 81

# List of Tables


1 The amount of dissolved lead found in the wastewater of various industries as well as in the influent and effluent of the wastewater treatment plant (WWTP) Leeuwkuil (Iloms *et al*, 2020) . . . . . 5

2 The amount of dissolved lead in wastewater of various municipalities in Limpopo, South Africa (Shamuyarira & Gumbo, 2014) . . . . . 5

3 The consumption, production and reserves of lead in South Africa and the world for 1984 and 2017 . . . . . 6

4 The conventional methods used in the removal of lead from wastewater with the related advantages and disadvantages . . . . . 7

5 The previous work done on the bioremediation of lead in wastewater by the Water Utilisation and Environmental Engineering Division of the University of Pretoria . . . . . 15

6 The optimum conditions for growth of *P. bifermentans*. . . . . 24

7 The optimum conditions for growth of *K. pneumoniae*. . . . . 25

8 The results for the tolerance of *K. pneumoniae* for various heavy metals, as reported by Oaikhena *et al* (2016) . . . . . 26

9 The recipes for LB broth and simulated LB broth. . . . . 26

10 The amounts of the components for LB broth agar and simulated LB broth agar . . . . . 29

11 Simulated LB broth as used in all experiments. . . . . 34

12 Amount of $Pb(NO_3)_2$ to be added to the reactors to obtain the desired Pb(II) solution. . . . . 35

13 The results of the statistical inference analysis to determine if there is a difference in the means of the populations indicating whether the bacterial species has a significant effect on the microbial precipitation of lead. . . . 48

14 The average percentage of Pb(II) removed from the reactors of each run at the final sampling time for the long duration study. . . . . 49

15 The calculated $t$ statistics of the inference analysis. . . . . 56

16 The percentage Pb(II) removed for each strain at the varying initial Pb(II) concentrations at the final sampling time of 30 h. . . . . 56

17 The value of the maximum specific growth rate ($\mu_{max}$) and the generation time ($t_g$) for all the experimental conditions observed for both strains. . . 70

18 Linear regression equations for a correlation between CFU, MA and $OD_{600}$ 78

19 The maximum specific growth rate, $\mu_{max}$, and the confidence interval and correlation coefficient of the fit for each experimental condition. . . . . 80

# 1 Introduction

The presence of lead in wastewater is a concern due to the health risks associated with the consumption of lead. These risks include neurodevelopmental alterations, neurodegeneration, the occurrence of diarrhoea and stomach pain, kidney damage and anaemia (Rigoletto *et al*, 2020; Lombó *et al*, 2013; Tao & T Zhang C, 2020). The concentrations of lead in wastewater is of particular concern in South Africa, where concentrations as high as 170 mg dissolved Pb(II) per kg dry mass of sewage has been recorded in the province of Limpopo (Shamuyarira & Gumbo, 2014).

Lead is introduced to the wastewater systems through anthropogenic sources such as battery waste, pesticides, fertilisers, mining waste and industrial wastewater effluents (Dongre, 2020). It is estimated that environmental Pb(II) concentrations have increased by three orders of magnitude in the last 300 years (Naik & Dubey, 2013).

While numerous conventional methods of lead removal exist, these methods are known to be costly, produce sludge and have a low selectivity for specific metals. These methods include ion exchange, electrowinning, electrocoagulation, cementation, reverse osmosis, electrodialysis, chemical coagulation and precipitation (Arbabi, Hemati & Amiri, 2015; Sylwan & Thorin, 2021). The bioremediation of lead is therefore an attractive alternative option.

The bioremediation of lead using a microbial consortium obtained from a battery recycling plant in Gauteng, South Africa has been previously researched by the Water Utilisation and Environmental Engineering division of the Department of Chemical Engineering at the University of Pretoria. These studies consisted of anaerobic and aerobic experiments using Luria-Bertani (LB) broth as the nutrient medium. Results reported by Hörstmann, Brink & Chirwa (2020), have shown removals of approximately 49 % and 93 % of 80 mg $L^{-1}$ initial Pb(II) concentration after 3 h and 12 d respectively. The same consortium removed 41 % and 72 % of 500 mg $L^{-1}$ initial Pb(II) concentration after 3 h and 12 d respectively.

The microbial consortium was analysed using 16S rDNA sequencing by Brink, Hörstmann & Peens (2020) and it was concluded that *Klebsiella pneumoniae* and *Paraclostridium bifermentans* are present in the consortium and are likely the main organisms responsible for the bioprecipitation of lead. It was demonstrated that the resulting precipitate included elemental Pb, which was concluded to be evidence for an anaerobic respiration mechanism which utilises Pb(II) as the terminal electron acceptor (Hörstmann, Brink & Chirwa, 2020).

The initial removal of Pb(II) as reported by Brink, Hörstmann & Peens (2020), was assumed to be due to a rapid detoxification mechanism, such as adsorption. Further investigation into the biosorption of Pb(II) by the same consortium was conducted and indicated that the biosorption abilities are improved by the sterilisation of the consortium using $NaN_3$ (van Veenhuyzen, Chirwa & Brink, 2021). A removal percentage of 62 % in reactors containing 80 mg $L^{-1}$ initial Pb(II) concentration was observed after 3 h. It was shown that metabolically active cells reduced the adsorption of Pb(II) to the cellular surface, indicating that the biosorption observed in the initial studies was most likely due to increased amounts of non-viable bacteria (van Veenhuyzen *et al*, 2021).

These results provide evidence for a mixed Pb(II) removal mechanism, which consists of a rapid biosorption stage followed by a slower metabolically dependent bioprecipitation stage. The utilisation of this mechanism would be ideal in industrial systems which are operated for extended periods of time since a significant amount of non-viable biomass will be accumulated.

The Pb(II) removal of the same consortium was investigated in a continuously operated upflow anaerobic sludge blanket (UASB) reactor. Removal efficiencies of between 90 and 100 % were recorded for this system with inlet Pb(II) concentrations varying between 80 and 200 mg $L^{-1}$. The maximum Pb(II) removed recorded for the UASB reactor was 1948.4 mg $L^{-1}$ (Chimhundi *et al*, 2021). These results affirm the potential of the system for the continuous removal of Pb(II), however a lack of understanding of the underlying removal mechanisms limits the scaling of the system.

The removal mechanisms of the consortium are investigated by isolating the main bioprecipitating strains. By obtaining more information about the removal mechanisms of the strains, the industrial application of the research becomes more attainable. The factors determined in this study which could be beneficial to an industrial application include: the time of initial precipitation, the amount of Pb(II) precipitated at varying initial Pb(II) concentrations, the duration of precipitation, the effect of certain nutrients on the mechanism, and the precipitate identity. The main objectives of the study are discussed in detail below.

The current research included the isolation of *Klebsiella pneumoniae* and *Paraclostridium bifermentans* from the consortium and the comparison of the effectiveness of microbial precipitation of the strains under various experimental conditions. In order to determine whether bioprecipitation occurs using the strains and if a significant difference exists between the bioprecipitation of lead using the isolated strains and the consortium, a long term study was conducted over 100 h and is described in Chapter 4.

A short term study was then conducted as described in Chapter 5 over 30 h with nine

sampling intervals. This study was completed to provide further clarification of the bioprecipitation mechanism and the influence of varying initial Pb(II) concentrations. The identity of the lead precipitate was determined for both strains with the use of XPS. The relationships between nitrate concentration, metabolic activity and the residual Pb(II) concentration was investigated.

A more comprehensive study into the exponential growth and the influence of the presence of Pb(II) on the individual strains was conducted as described in Chapter 6. This study was performed over 24 h with hourly sampling during the exponential phase and the stationary phase of the bacteria. This study provides an in depth understanding of the growth of the bacteria in environments with and without added Pb(II), with three methods of microbial growth measurements investigated.

# 2 Literature

## 2.1 Lead pollution and the associated risks

The consumption of lead through water sources is a serious concern due to the numerous associated health risks. Lead can be introduced to wastewater through anthropogenic sources such as battery waste, fertilisers, pesticides, industrial wastewater effluents and mining waste, among others (Dongre, 2020).

The metal is resistant to corrosion but oxidation of the metal does occur when it is exposed to air (Lenntech, 2021). Lead is commonly found in ore along with zinc, silver and copper, and is then extracted with these metals; it is uncommon to find lead in its elemental form in nature (Lenntech, 2021). Lead is primarily found in the form galena (PbS) and is persistent in wastewater due to the non-biodegradability of the metal and its toxic nature (Lenntech, 2021; Akpor, Ohiobor & Olaolu, 2014).

There are many health risks associated with lead pollution. The main concern of lead consumption is the effect that it has on the central nervous system. Lead has been shown to be detrimental to haemoglobin synthesis, with anaemia observed in children at lead blood levels above 40 µg $dL^{-1}$ (Baysal, Ozbek & Akman, 2013). It is possible that lead can cause kidney damage, and while some of these effects are reversible, chronic exposure to lead may result in decreased kidney function and possible renal failure (Baysal *et al*, 2013).

Lead has been shown to cause intellectual disabilities in children and may also have detrimental effects on the male and female reproductive systems (Tiquia-Arashiro, 2018). It has been observed that at blood lead levels exceeding 0.4 g $L^{-1}$ lead concentration, a reduced sperm count is present in men and at elevated blood lead levels in pregnant women, a higher occurrence of miscarriage, low birth weight and prematurity is observed (Tiquia-Arashiro, 2018).

In a study done by Iloms *et al* (2020), the concentrations of Pb(II) in different industrial wastewater and influents and effluents from the waste water treatment plant (WWTP) Leeuwkuil, Gauteng, South Africa were determined. These are shown in Table 1 and are compared to the allowable limit of dissolved lead in wastewater of 0.01 mg $L^{-1}$ as stipulated by The Department of Water Affairs, South Africa (Department of Water Affairs, 2013).

Table 1: The amount of dissolved lead found in the wastewater of various industries as well as in the influent and effluent of the wastewater treatment plant (WWTP) Leeuwkuil (Iloms *et al*, 2020)

| Source of wastewater | Dissolved Pb (mg $L^{-1}$) |
|---|---|
| Industry 1: Battery | $4.64 \pm 0.17$ |
| Industry 2: Iron/metal galvanising | $0.18 \pm 0.02$ |
| Industry 3: Iron/steel | $0.18 \pm 0.03$ |
| Industry 4: Tanking/car wash | $0.19 \pm 0.03$ |
| Industry 5: Iron/steel | $0.21 \pm 0.00$ |
| WWTP influent | $0.20 \pm 0.03$ |
| WWTP effluent | $0.19 \pm 0.03$ |

From the data in Table 1, there is a clear need for improved technologies and methods of lead removal from wastewater. All the industries analysed, as well as the effluent of the WWTP, contain levels of dissolved lead above the allowable limits.

The same conclusion is reached in research done by Shamuyarira & Gumbo (2014) on the assessment of heavy metals in municipal sewage sludge of various areas in Limpopo, South Africa. These values are shown in Table 2, and when compared to the allowable limit of dissolved lead of 100 mg (kg dry mass)$^{-1}$ (Shamuyarira & Gumbo, 2014), two of these municipalities have sewage sludge with dissolved lead over the limit.

Table 2: The amount of dissolved lead in wastewater of various municipalities in Limpopo, South Africa (Shamuyarira & Gumbo, 2014)

| Municipality | Dissolved Pb (mg (kg dry mass)$^{-1}$) |
|---|---|
| Thohoyandou | 34.56 |
| Polokwane | 102.8[1] |
| Tzaneen | 52.26 |
| Louis Trichardt | 171.9[1] |
| Musina | 21.28 |

[1] Over the allowable limit of 100 mg (kg dry mass)$^{-1}$ (Shamuyarira & Gumbo, 2014).

## 2.2 Lead consumption, production and reserves

Lead is currently used across the world in car batteries, pigments, chemicals and for various uses in the construction industry. The majority of lead used is found in car batteries (Fuller, 2009). Table 3 contains a comparison of lead production and reserves of South Africa and the world between 1984 and 2017. This data highlights the decrease in lead production and reserves over the time period and emphasises the importance of finding alternative sources of lead, such as the recovery of lead from wastewater.

Table 3: The consumption, production and reserves of lead in South Africa and the world for 1984 and 2017

| Year | 1984[1] | 2017[2] | Percentage difference (%) |
|---|---|---|---|
| South African reserves (Mt) | 5 | 0.3 | - 94 |
| South African production (kt) | 94.8 | 48 | - 49.4 |
| South African consumption (kt) | 50 – 55 | 57 | + 4 |
| World reserves (Mt) | 135 | 88 | - 34.8 |
| World production (Mt) | - | 4.97 | - |
| World consumption (Mt) | - | 11.6 | - |

[1] (Snodgrass, 1986)

[2] (Department of Mineral Resources: Republic of South Africa, 2019)

## 2.3 Conventional methods of lead removal in wastewater

The conventional methods of lead removal from wastewater include: ion exchange, electro-winning, electro-coagulation, cementation, reverse osmosis, electro-dialysis, adsorption, chemical coagulation/flocculation and chemical precipitation (Arbabi *et al*, 2015; Sylwan & Thorin, 2021).

These methods tend to be undesirable for use due to their limitations. These limitations

include the generation of sludge, a low percentage retention of metal ions, a high energy consumption and low selectivity for specific metals (Arbabi *et al*, 2015).

Table 4: The conventional methods used in the removal of lead from wastewater with the related advantages and disadvantages

| Method and Description | Advantages | Disadvantages |
|---|---|---|
| **Ion exchange** – The exchange of ions between the substrate and the surrounding medium. The ion exchange resin is insoluble in most aqueous and organic solutions and consists of a cross linked polymer matrix to which the charged functional groups are attached by covalent bonding (Hubicki & Kołodyńska, 2011). | High removal efficiency, rapid kinetics, high processing capability and a high selectivity of the process (Esmaeili & Foroutan, 2015). | High costs relating to the reduction phase and its current disposal and the low longevity of the resins with high levels of pollution (Esmaeili & Foroutan, 2015). |
| **Electrowinning** – Commonly used in the mining and metallurgical industry for heap leaching and acid mine draining. This method is also used in the electrical and electronic industries for the removal and recovery of lead ions (Arbabi *et al*, 2015). A DC current is laced in an ion solution with added anodes and cathodes. The difference in electrical potential causes the movement of cations towards the cathode (EMEW Clean Technologies, 2016). | Environmental compatibility - the electron acting as the reagent is a "clean reagent" (Stanković, 2007). | High costs associated with anode and cathode maintenance (Stanković, 2007). |
| **Electrocoagulation** – The electrochemical production of metal ions that act as destabilising agents which lead to neutralisation of electric charge for removing pollutants. The oppositely charged particles then bond together and form a mass (Didar-Ul Islam, 2019). | Reduced sludge production, ease of operation and a lack of chemicals required for the process (Didar-Ul Islam, 2019). | Costly maintenance and the replacement of electrodes. The consistency is difficult to achieve and the process is not passive which leads to higher operation costs (Chemtech International, 2020). |

| | | |
|---|---|---|
| **Cementation** – Lead is precipitated from a solution with the use of an electropositive metal. The metal is usually in a fixed bed of metal spheres or with a metal rod/disc (Nosier & Sallam, 2000). | Ease of control and the simplicity of the process (Nosier & Sallam, 2000). | Valuable metals are sacrificed (Nosier & Sallam, 2000). |
| **Reverse osmosis and electrodialysis** – Consists of selective membranes that are used between electrodes in electrolytic cells, the metal ion migrates under the electric current (Arbabi *et al*, 2015). | High selectivity of the metals (Arbabi *et al*, 2015). | High costs associated with the implementation and operation of the system and the generation of sludge (Arbabi *et al*, 2015). |
| **Chemical coagulation/flocculation and precipitation** – Coagulation is the charge neutralisation of colloids followed by the formation of clusters and flocculation is a process whereby small particles are combined by physical bonds (Sylwan & Thorin, 2021). In chemical precipitation, the chemicals react with heavy metal ions such as lead and form insoluble precipitates, which are separated from the water by sedimentation and filtration. Lead can be precipitated with the use of hydroxide precipitation which is a widely used precipitation method (Fu & Wang, 2011). | Low capital cost (Sylwan & Thorin, 2021). | Production of large volumes of a low density sludge (Sylwan & Thorin, 2021). |

## 2.4 Lead bioremediation

### 2.4.1 Mechanisms of lead resistance in microorganisms

The biological and chemical mechanisms employed by bacteria leading to lead resistance are applicable to the bioremediation process and can be utilised in the wastewater industry (Naik & Dubey, 2013; Tiquia-Arashiro, 2018). Biosorption mechanisms can be classified

according to whether the mechanism is dependent or independent on the cell metabolism, as well as according to the location within the cell and the metal removed.

The various mechanisms of biosorption by the microbial cell is shown in Figure 1 and Figure 2, which are adapted from a study published by Perpetuo, Barbieri & Nascimento (2011).

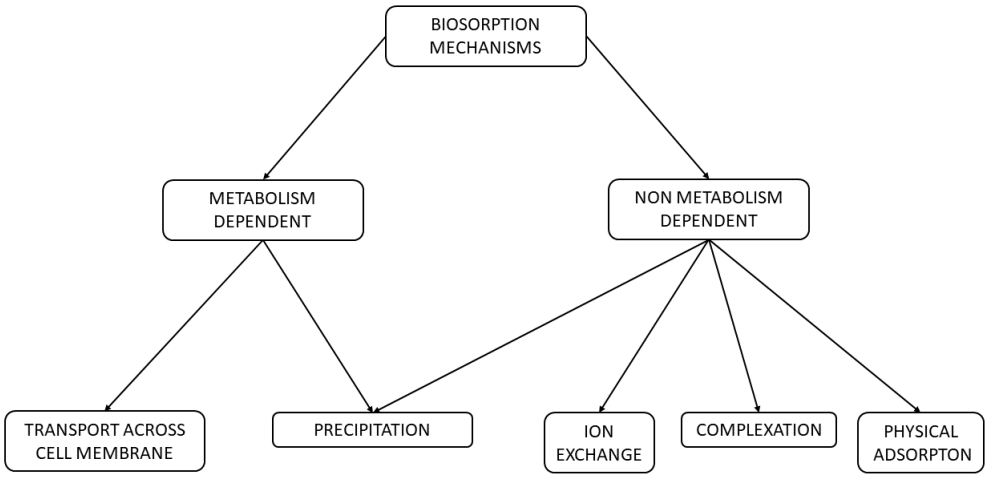


Figure 1: Classification of biosorption mechanisms according to dependence on cell metabolism, adapted from Perpetuo, Barbieri & Nascimento (2011)

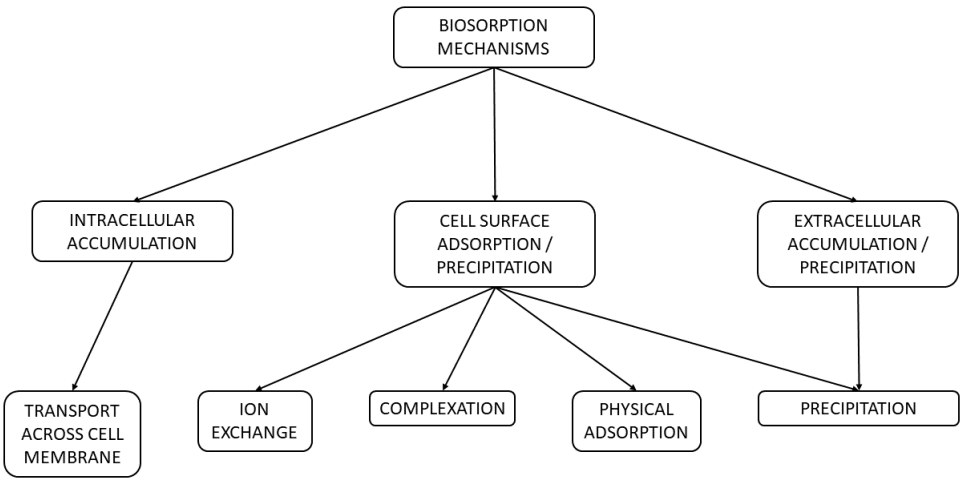


Figure 2: Classification of biosorption mechanisms based on the location within the cell and the metal removed, adapted from Perpetuo, Barbieri & Nascimento (2011)

**Efflux mechanism – Transport across cell membrane**

The efflux mechanism makes use of ATPases, which transport heavy metals across the cell membrane (Naik & Dubey, 2013). This maintains homeostasis of heavy metals in the cell, as the transporters prevent the over accumulation of heavy metals such as Pb(II), Cu(II), Ag(I), Zn(II) and Cd(II) in the cell (Naik & Dubey, 2013). The efflux mechanism only occurs in viable cells and is associated with an active defence mechanism.

**Intracellular bioaccumulation**

Intracellular bioaccumulation is a mechanism employed by bacteria to resist the toxic effects of heavy metals using the induction of metal binding proteins referred to as metallothioneins (MTs) (Naik & Dubey, 2013). MTs are low-molecular weight, cystein-rich proteins that facilitate the bioaccumulation of toxic metals in the cell, and therefore play an important role in the immobilisation of heavy metals (Naik & Dubey, 2013; Tiquia-Arashiro, 2018). The enzymes used in the metabolic processes of the bacterial cell are protected (Naik & Dubey, 2013).

This resistance mechanism is often plasmid-borne, which means that the MTs can be dispersed from one cell to another. MTs are synthesised in response to increased metal concentrations (Tiquia-Arashiro, 2018).

**Extracellular sequestration – Physical Adsorption**

The immobilisation of heavy metals in the cell is achieved by using extracellular high molecular weight biopolymers which are secreted by the bacterial cells (Naik & Dubey, 2013). The biopolymers are referred to as exopolysaccharides (EPS) and consist of macromolecules such as polysaccharides, proteins, nucleic acids, humic substances, lipids and other non-polymeric constituents which have a low molecular weight (Naik & Dubey, 2013). EPS are relevant to the bioremediation process due to their involvement in the flocculation and binding process of metal ions (Tiquia-Arashiro, 2018).

This binding process causes metal immobilisation, which in turn prevents the lead ions from entering the cell (Tiquia-Arashiro, 2018). The structural and compositional makeup of EPS is varied according to the phase of growth that the bacterial cell is experiencing (Tiquia-Arashiro, 2018). It has been shown that there is a higher removal of lead observed when the cell is in the stationary phase; this is due to the high net acidic sugar incorporation in the EPS (Tiquia-Arashiro, 2018).

According to Perpetuo *et al* (2011), physical adsorption is reversible, independent of metabolism and has many advantages in terms of treating large volumes of wastewater with low concentrations of contaminants.

There are various factors which influence the ability of the EPS to bind to the metal ions, these include (Tiquia-Arashiro, 2018):

- The initial metal concentrations;
- The pH; and
- The concentration of NaCl.

If the pH is low, then the active sites of the cell wall are associated with protons which will in turn restrict the approach of heavy metal cations and will result in a repulsive force (Perpetuo *et al*, 2011). If the pH is increasing then an increasing amount of active sites are replaced by negative charges which will increase the attraction of heavy metal cations leading to adsorption of the cations on the cell surface (Perpetuo *et al*, 2011).

In a study by Cui *et al* (2017), it was found that a high NaCl concentration significantly decreased the production of EPS. This was attributed to the different adaptive mechanisms to osmotic pressure under conditions lower or higher than the optimal growth salinity.

**Surface biosorption**

Surface biosorption is an extracellular sequestration mechanism of the toxic metals to prevent the entry of toxic metals in the bacterial cells. This helps to maintain metal homeostasis (Naik & Dubey, 2013). The biosorption of metals is facilitated by several mechanisms such as ion exchange, chelation, adsorption and diffusion through the cell walls and membranes (Naik & Dubey, 2013).

The functional groups of several macromolecules on the cell surface are able to bind metals. The cell walls carry a natural negative charge, which allows metal ions to bind to the cell surface and regulates the movement of metals across the cell membrane (Tiquia-Arashiro, 2018).

Gram-positive bacteria possess carboxyl groups as key binding sites for the metal cations, while gram-negative bacteria possess phosphate groups. The capacity of the absorption of Pb(II) on the cell surface is affected by the pH and the initial metal concentration (Tiquia-Arashiro, 2018).

**Complexation/Chelation**

Complexation is an extracellular mechanism which results from the electrostatic attraction between a metallic ion chelating agent and a polymer that is excreted by a microorganism (Perpetuo *et al*, 2011). Chelating agents contain pairs of electrons that present electrostatic attraction; if they cling to the metallic ions then there will be no transfer of electrons taking place (Perpetuo *et al*, 2011). The final structure of the complex has the electric charge of the sum of the individual charges of the components in the complex (Perpetuo *et al*, 2011).

**Ion exchange**

The cell walls of microorganisms contain polysaccharides and the bivalent metal ions can exchange with the counter ions in the polysaccharides which results in the biosorptive uptake of heavy metals (Perpetuo *et al*, 2011).

**Bioprecipitation**

The precipitation of toxic metals into insoluble complexes reduces the toxicity and the bioavailability of the metals (Naik & Dubey, 2013). This precipitation mechanism occurs extracellularly or intracellularly (Tiquia-Arashiro, 2018).

Bioprecipitation is either dependent or independent on the metabolism of the cell (Perpetuo *et al*, 2011). If the mechanism is dependent on cellular metabolism then the metal removed is often associated with the active defence mechanisms of the microorganisms (Perpetuo *et al*, 2011). If the mechanism is independent on cellular metabolism, it may be a consequence of the chemical interaction between the metal and the cell surface (Perpetuo *et al*, 2011).

Lead(II) has been known to react with the following anions (Tiquia-Arashiro, 2018):

- chlorides;
- phosphates;
- sulfides;
- carbonates; and
- hydroxyl groups

The bacterium *Enterobacter cloacae* has been shown to immobilise lead as insoluble lead phosphate (Tiquia-Arashiro, 2018). *Bacillus iodinium* GP13, *Bacillus pumilus* S3 and

*Klebsiella aerogenes* NCTC418 have all been shown to precipitate lead as lead sulfide (Tiquia-Arashiro, 2018).

According to Tiquia-Arashiro (2018), the pH plays an important role in the bioprecipitation of the metals. It has been shown that at a pH of 6.6 and higher, various lead phosphates and lead carbonates are precipitated (Tiquia-Arashiro, 2018). The complexation of metals decreases in increasing acidic conditions (Tiquia-Arashiro, 2018).

**Alteration in cell morphology**

The bacterial cell combats the environmental stresses placed on it by changing the cell shape (Naik & Dubey, 2013). This could be a cell reduction as seen for example when the lead resistant *E. cloacae* bacterial strain was exposed to 1.6 mM lead nitrate (Naik & Dubey, 2013).

**Reduction-oxidation reaction**

Microorganisms can mobilise or immobilise metal ions, metalloids and organometal compounds leading to the promotion of redox reactions (Perpetuo *et al*, 2011). The microorganisms can efficiently immobilise heavy metals through their ability to reduce metal ions thereby reducing them to a lower oxidation state (Perpetuo *et al*, 2011). This will give rise to metallic elements which will cause precipitation to occur (Perpetuo *et al*, 2011).

### 2.4.2 Previous studies done on lead bioremediation

**Studies not affiliated with the University of Pretoria**

In previous work done by Kang, Kwon & So (2016), the prospect of the bioremediation using bacterial mixtures was considered. The research was conducted using four bacterial strains obtained from mine soil. These strains were *Viridibacillus arenosi* B-21, *Sporosarcina soli* B-22, *Enterobacter cloacae* KJ-46 and *E. cloacae* KJ-47. The experiments were done with various combinations of the bacterial strains under aerobic conditions. For this study, the heavy metal stock solutions were prepared using $CdCl_2.5H_2O$, $PbCl_2$ and $CuCl_2$ to make solutions of 1 M. The experiments were carried out using a yeast extract broth containing 12 g $L^{-1}$ yeast extract and 10 g $L^{-1}$ ammonium sulphate, at a pH of 7.0. The study concluded that the bacteria is more efficient at bioremediation when grouped together as a consortium, as opposed to the individual bacteria. After 48 h, remediation of 98.3 % Pb, 85.4 % Cd and 5.6 % Cu was observed.

The work done by Li *et al* (2016) focused on the bioremediation of lead in contaminated soil. The bacteria used was *Rhodobacter sphaeroides* and it was concluded that the species

did not decrease the total amount of lead in the soil but rather changed the speciation of the lead. Results of the study indicated that Pb contaminated soil was treated by the precipitation mechanism resulting in formation of lead sulphate and lead sulfide.

In a study done by K Zhang *et al* (2021), the biomineralization of lead in wastewater was investigated with the use of *Lysinibacillus*, which proved to immobilize Pb(II) ions at a pH greater than 2. According to K Zhang *et al* (2021), the current studies on biomineralization indicate that the cell is used as the nucleation site and is then encapsulated by the metal minerals until the cell is inactivated. This research was focused on the reutilization of mineralized cells and the recovery of metals, by first determining a quick method to achieve the reutilization of mineralized bacteria, to study the reutilization mechanism and to investigate the time scale evolution of the oxidative damaging effect of cells (K Zhang *et al*, 2021).

**Studies completed by the University of Pretoria**

There have been numerous studies done on lead bioremediation by the University of Pretoria, Department of Chemical Engineering, Water Utilisation and Environmental Engineering Division all of which are highlighted and described in Table 5. These studies have focused on the bioremediation of lead using two consortia of bacteria obtained from a lead mine and from a battery recycling plant. The studies have determined the influence of the following aspects on the bioprecipitation of lead:

- Elevated lead concentrations;
- Presence of glucose;
- Various growth substrates such as LB broth, glucose and xylose;
- Presence of Zn(II) and Cu(II); and
- The effects of aeration conditions

Various other factors were also investigated such as the minimum inhibitory concentration and the precipitate identity as well as the effect of nutrient conditions such as the implementation of yeast extract autolyzed from *Saccharomyces cerevisiae*.

From a study done by Brink, Hörstmann & Peens (2020), the precipitate identity and method of precipitation was determined and proposed. In this study, SEM-EDX and XPS analysis determined that the precipitate was formed on the surface of the microbial cell. This led to the hypothesis of a surface electron transfer mechanism occurring which

causes the direct reduction of Pb(II) ions. The sulphur-containing amino acids could also be metabolised intracellularly leading to the excretion of sulphide into the medium which would cause the precipitation of PbS on contact with the dissolved Pb(II) ions in the medium (Brink, Hörstmann & Peens, 2020).

The XPS results reported by Brink, Hörstmann & Peens (2020) describe the aerobic runs to contain exclusively PbO and elemental Pb, while the anaerobic runs contain significant fractions of PbS with PbO and elemental Pb. The authors attribute the lack of PbS in the aerobic runs to the oxidation of $S^{2-}$ ions intracellularly or that aerobic conditions inhibit the metabolism of sulphur-containing amino acids.

The presence of PbO is hypothesised to be due to the oxidation of elemental Pb in aerobic runs or as a result of exposure to oxygen during sample preparation in the anaerobic runs (Brink, Hörstmann & Peens, 2020).

The study concludes that the Pb(II) initially loaded into the batch reactors will act as an electron acceptor to the electrons released during the catabolism of carbon sources to $CO_2$.

**Summary of the studies conducted by this research team at the University of Pretoria**

Table 5: The previous work done on the bioremediation of lead in wastewater by the Water Utilisation and Environmental Engineering Division of the University of Pretoria

| Lead Removal Using Industrially Sourced Consortia: Influence of Lead and Glucose Concentrations (Brink, Lategan, *et al*, 2017) |
|---|
| Description<br>• Study aimed at exploring the lead removal capabilities of two locally sourced industrial consortia with the use of batch fermentation.<br>• The experiments took place under anaerobic conditions with two different lead concentrations: 80 mg $L^{-1}$ and 160 mg $L^{-1}$.<br>• The effect of glucose on the precipitation of lead was also studied. |

Main findings

- Consortium can effectively remove lead with main limitation being substrate availability.
- The changes in absorbance were minimal which indicates that a non-growth removal mechanism is present. The removal is as a result of a defence mechanism of the organism.
- The presence of glucose caused severe substrate inhibition which reduced the effectiveness of lead removal.

---

Microbial Pb(II) precipitation: the influence of elevated Pb(II) concentrations (Peens, Wu & Brink, 2018)

---

Description

- The study aimed at determining the effect that elevated lead(II) concentrations have on the precipitation of Pb(II) by an industrially obtained consortium.
- The study was done under anaerobic conditions with LB broth and simulated LB broth (reduced NaCl) as the growth medium.
- Lead(II) concentrations ranged from 80 mg $L^{-1}$ to 1000 mg $L^{-1}$.

Main findings

- 99 % removal of lead with 500 mg $L^{-1}$ lead after 11 d and 87 % removal of lead with 1000 mg $L^{-1}$ lead after 22 d. This indicates that the consortium is able to precipitate lead concentrations up to 1000 ppm.
- The simulated broth led to no precipitation of $PbCl_2$.

---

Microbial Lead(II) precipitation: the influence of growth substrate (Brink & Mahlangu, 2018)

---

Description

- The study aimed at exploring the influence of various growth substrates on the removal of lead(II) from solution.
- The fermentation media tested was glucose and xylose supplemented LB broth, with and without $CaCO_3$ as a pH buffer.
- Various components of LB broth were also tested, this includes yeast extract, tryptone and NaCl.

Main findings

- The glucose and xylose supplemented experiments indicated a significant removal of lead but without the precipitation of lead. A significant gas build up was observed in all runs with a drop in pH of the unbuffered runs and this could indicate an anaerobic digestion mechanism with either internal or external sequestration of lead.
- The LB broth experiments indicated that the commercial growth medium LB broth performed the best in terms of lead(II) removal, with the yeast extract NaCl complex medium performing nearly as well.

---

Microbial Pb(II) Precipitation: Minimum Inhibitory Concentration and Precipitate Identity (Brink, Hörstmann & Feucht, 2019)

---

Description

- The study aimed to determine the minimum inhibitory concentration (MIC) at which the industrially obtained consortium would cease growth and/or would cease precipitation of Pb(II). The study also aimed to determine the identity of the precipitate formed.

Main findings

- The industrially obtained consortium has the ability to grow in high amounts of lead(II). The consortium has significant biological Pb(II) reducing capabilities.

---

Microbial lead(II) Precipitation: The Influence of Aqueous Zn(II) and Cu(II) (Hörstmann & Brink, 2019b)

---

Description

- The study was aimed to determine the effect that the presence of Zn(II) and Cu(II) have on the Pb(II) precipitation capabilities and metabolic activity of an industrially obtained consortium.

Main findings

- Growth was inhibited in the reactors containing only Cu(II). The consortium was capable of removing a significant amount of Cu(II) in the presence of Pb(II). Pb(II) concentrations did not decrease as much as the Cu(II) concentrations and this could indicate a competitive removal mechanism.
- For the reactors containing Pb(II) and Zn(II) a higher amount of lead was removed in the reactor containing only Pb(II), followed by reactors containing Pb(II) and Zn(II) at lower concentrations of Zn(II).
- Pb(II) promotes metabolic activity and Zn(II) and Cu(II) inhibit metabolic activity, most probably due to the inhibition of the lead precipitating mechanism.
- Zn(II) and Cu(II) ions need to be removed before any precipitation of Pb(II) can take place.

---

Microbial Pb(II) Precipitation: The effects of Aeration Conditions and Glucose Presence on a Lead-Mine Consortium (Hörstmann & Brink, 2019a)

---

Description

- The purpose of the study was to quantify the effects of aerobic and anaerobic conditions as well as the presence of glucose, on the effectiveness of an industrially obtained consortium at precipitating aqueous lead(II), using batch conditions.

| | |
|---|---|
| Main findings | • The biological activity was increased under aerobic conditions but this did not lead to increased Pb(II) removal.<br>• Increased amount of Pb(II) is removed in the systems without glucose than in the systems containing glucose. This is because the glucose leads to a fermentation mechanism that provided an alternative energy producing mechanism, which in turn prevented dissimilatory reduction as an energy generating process, leading to less lead(II) precipitation.<br>• The optimal dissimilatory reduction of Pb(II) requires anaerobic conditions in the absence of glucose. |

| Microbial Pb(II)-precipitation: the influence of oxygen on Pb(II)-removal from aqueous environment and the resulting precipitate identity (Brink, Hörstmann & Peens, 2020) | |
|---|---|
| Description | • The study focused on the quantification of the lead(II) bio-precipitation effectiveness, and the produced precipitate identities of industrially obtained consortia under anaerobic and aerobic conditions. |
| Main findings | • Precipitation and removal of lead in both anaerobic and aerobic experiments was successful.<br>• Majority of the lead removal in the aerobic runs took place in the first 48 h.<br>• The XPS analysis of the precipitates indicated the presence of PbO and elemental lead in the aerobic runs and PbO, PbS and elemental lead in the anaerobic runs.<br>• An oxidation-reduction mechanism with lead(II) as the electron acceptor is observed for both aerobic and anaerobic runs, while a sulphide-liberation catabolism of sulphur-containing amino acids was observed for the anaerobic runs only. |

Pb(II) Bio-Removal, Viability, and Population Distribution of the Industrial Microbial Consortium: The Effect of Pb(II) and Nutrient Concentrations (Hörstmann, Brink & Chirwa, 2020)

Description

- The effect of aqueous Pb(II) and nutrient concentrations on the Pb(II)-removal, biomass viability, active species identities and the population distribution of an industrial Pb(II) resistant consortium was investigated.

Main findings

- Approximately 50 % of Pb(II) was removed in the first 3 h of the runs, for all conditions tested. After 3 h, a slower rate of Pb(II) removal occurs with a dark precipitate forming.
- Pb(II) removal was independent of the microbial growth, while the growth was found to be dependent on the concentration of Pb(II), nutrients, and the nitrates in the system.
- Scanning electron microscope results show viable bacilli embedded in the precipitate and this is an indication that precipitation occurs on the surface of the biomass and not as a result of an internal excretion mechanism.
- Microbial characterisation indicated that *Klebsiella pneumoniae* was the only active species in the sample directly contributing to the bioprecipitation of Pb(II). The other species identified are lead resistant organisms and could be responsible for the initial biosorption of Pb(II) noticed in the first 3 h of the runs.

Microbial Pb(II) precipitation: Yeast Extract Autolyzed from Saccharomyces Cerevisiae as a Sustainable Growth Substrate (Hörstmann, Naidoo, *et al*, 2020)

Description

- The study aimed to determine the effectiveness of yeast extract as a growth medium for a Pb(II) removing consortium. The experiments took place under anaerobic batch conditions with 80 mg $L^{-1}$ lead.

Main findings

- Pb(II) initially removed rapidly within the first 7 min of the runs, with the rest of the Pb(II) removed from solution in 24 h.
- Metabolic activity increased slowly for the first 8 h with a greater increase between 8 and 48 h.
- The optical density had a slow increase from 0 to 16 h with a sharp increase between 16 and 24 h.
- A dark precipitate was observed in all runs.
- The initial drop of Pb(II) can be attributed to a biosorption mechanism.
- The large metabolic activity and optical density increases can correspond to low Pb(II) concentrations, which is caused by a Pb(II) inhibitory effect or by the slow access to more complex components in the yeast.

---

Microbial Removal of Pb(II) Using an Upflow Anaerobic Sludge Blanket (UASB) Reactor (Chimhundi *et al*, 2021)

---

Description

- The study was focused on the design and implementation of a upflow anaerobic sludge blanket (UASB) reactor to be used in the biorecovery and bioreduction of Pb(II) using an industrially obtained consortium as a biocatalyst and yeast extract as the sole growth medium.

Main findings

- The UASB reactor demonstrated removal efficiencies of between 90 and 100 % for inlet concentrations of lead varying between 80 and 2000 mg $L^{-1}$.
- A maximum removal rate of 1948.4 mg $L^{-1}$ $d^{-1}$ was reported.
- An XRD and XPS analysis of the precipitate formed in the study was identified to contain: $Pb^0$, PbO, PbS and $PbSO_4$.

---

Insight into the Metabolic Profiles of Pb(II) Removing Microorganisms (Hörstmann, Chirwa & Brink, 2021)

---

Description

- The purpose of this study was to investigate the metabolic pathways of lead-resistant microorganisms known to employ bioprecipitation as a resistance mechanism.
- The study made use of anaerobic batch experiments with LB broth as a growth medium, over 33 h with varying concentrations of lead.
- Metabolic profiling was achieved using liquid chromatography coupled with tandem mass spectrometry (UPLC-HDMS) and high-performance liquid chromatography.

Main findings

- Lead measurements decreased dramatically within the first 3 h of sampling with no decrease in nitrates and no increase in growth, this indicates a possible biosorption mechanism.
- After 3 h, substantial growth is observed that is gradually dependent on the availability of nitrates.
- Four main compounds were identified and the proposed pathways for their catabolism by the bacterial consortium were presented. These include: piperidine, indoline, indoleacrylic acid and leucylproline.
- Calculated energy productions were 4.87, 0.68, 3.36 and 1.49 mmol $L^{-1}$ for indoleacrylic acid, leucylproline, indoline and piperidine respectively.
- The amount of theoretical NADH produced by the compounds was 10.4 mmol $L^{-1}$.

---

## 2.5 Microbiology

### 2.5.1 Prokaryote metabolism - anaerobic respiration

Anaerobic respiration is achieved when a molecule other than oxygen is used as the final electron acceptor in the electron transport chain (Slonczewski & Foster, 2011). Various methods of anaerobic respiration are utilised by bacteria, this includes denitrification and the reduction of sulphur and sulphate.

Denitrification is the reduction of the ionic nitrogen oxides (nitrate and nitrite) to the gaseous oxides (NO and $N_2O$). The gaseous oxides can be further reduced to $N_2$ (Knowles, 1982). The reactions of the denitrification process are as follows:

$$NO_3^- + 2\,H^+ + 2\,e^- \xrightarrow{\text{nitrate reductase}} NO_2^- + H_2O$$

$$NO_2^- + 2\,H^+ + e^- \xrightarrow{\text{nitrite reductase}} NO + H_2O$$

$$2\,NO + 2\,H^+ + 2\,e^- \xrightarrow{\text{nitric oxide reductase}} N_2O + H_2O$$

$$N_2O + 2\,H^+ + 2\,e^- \xrightarrow{\text{nitrous oxide reductase}} N_2 + H_2O$$

Denitrification is a bacterial process which is triggered by low oxygen and the availability of a nitrogen oxide. The process is nearly exclusively a facultative trait and is therefore used by facultative anaerobes (Zumft, 1997). These organisms have the ability to respire in aerobic conditions and anaerobic conditions.

The nitrate reductase enzyme catalyses the reaction of $NO_3^-$ to $NO_2^-$ and is membrane-bound (Morena-Vivián *et al*, 1999). The enzyme is composed of three subunits. These subunits include a catalytic $\alpha$ subunit, a soluble $\beta$ subunit and a membrane $b$ quinol-oxidising $\gamma$ subunit. The $\alpha$ and $\beta$ subunits are anchored to the cytoplasmic side of the membrane by the $\gamma$ subunit (Morena-Vivián *et al*, 1999).

The nitrite reductase enzyme is responsible for catalysing the reaction of $NO_2^-$ to NO (Rinaldo & Cutruzzolá, 2007). There are two distinct classes of nitrite reductase that yield NO as the main product, these have either copper (CuNIR) or heme ($cd_1$NIR) as the cofactors (Rinaldo & Cutruzzolá, 2007).

Nitric oxide reductase is the enzyme which catalyses the reaction of NO to $N_2O$ in the denitrification process. Two types of bacterial nitric oxide reductases have been characterised, one being a cytochrome *bc*-complex (cNOR) that receives electrons from redox proton donors, and the other lacking the cytochrome c component and uses quinol as the electron donor in the reaction (Hendriks *et al*, 2000).

The final reaction in the denitrification process, the reaction of $N_2O$ to $N_2$, is catalysed by nitrous oxide reductase. The enzyme has two copper centres, a CuZ centre which is a unique tetranuclear copper centre possessing either one or two sulfide bridges, and a binuclear CuA centre (Pauleta, Dell'Acqua & Moura, 2013).

Another method of anaerobic respiration of bacteria is the reduction of sulphate (Ayangbenro, Olanrewaju & Babalola, 2018). Sulphate is used as an electron acceptor and is

converted to hydrogen sulphide. This method is currently being harnessed in the field of bioremediation of wastewater, to remove toxic metals (Ayangbenro *et al*, 2018). Many toxic metals form insoluble sulphides and can therefore be removed from the water. This process is favourable due to its low costs.

In research conducted by Pfennig & Biebl (1976), a bacterium that is able to obtain energy from anaerobic sulfur respiration is described. The bacterium, *Desulfuromonas acetoxidans*, is one of many species which have their oxidation to $CO_2$ linked to the reduction of elemental sulfur to sulfide (Pfennig & Biebl, 1976).

### 2.5.2 *Paraclostridium bifermentans*

*Paraclostridium* is a genus of gram-positive and rod shaped bacteria (Rai *et al*, 2020). These cells are motile and have either peritrichous flagella or pseudo filaments. The species of this genus reproduce by binary fission and produce endospores (Rai *et al*, 2020). *Paraclostridium* are catalase- and oxidase-negative and are obligate anaerobes, meaning that the cells cannot utilise aerobic respiration in the energy generation process (Rai *et al*, 2020).

*Paraclostridium* function well in mesophilic conditions, which is to say that these organisms thrive in moderate temperatures instead of extreme conditions (Rai *et al*, 2020). The metabolic activities of the organisms such as indole and $H_2S$ production, starch and gelatin hydrolysis and nitrate reduction vary within the species (Rai *et al*, 2020).

According to Rai *et al* (2020), *Paraclostridium bifermentans* cannot utilise D-mannitol, starch, cellobiose, D-mannose, D-sorbital, benzoate or fumarate for growth. The species rather breaks down levulose to provide for its energy needs. This species is able to produce indolic compounds from L-tryptophan and does not reduce $NO_3$. The optimum growth conditions of *P. bifermentans* are shown in Table 6.

Table 6: The optimum conditions for growth of *P. bifermentans*.

| Characteristic | Value |
|---|---|
| Optimum temperature (°C) | 30 – 37 |
| Optimum pH | 6 – 7 |
| NaCl required (% w/v) | 0 – 1 |

In a review done by Rai *et al* (2020), it is stated that the strain of *P. bifermentans* used (JCM $1386^T$) does not produce $H_2S$. This is countered in the work done by Kutsuna *et al* (2018) where two versions of the same strain (PAGU $2008^T$ and PAGU $2078^T$) were noted

to produce $H_2S$, but where strain PAGU $1678^T$ was negative for the production of $H_2S$. The authors concluded that *P. bifermentans* should be described to be $H_2S$ producing but that strain PAGU $1678^T$ can be identified with its characteristic of not producing $H_2S$.

### 2.5.3 *Klebsiella pneumoniae*

*Klebsiella pneumoniae* is a gram-negative, encapsulated and non-motile bacterium that was first described by Carl Friedlander in 1882 after isolating the bacterium from the lungs of pneumonia patients (Ashurst & Dawson, 2021). *K. pneumoniae* is not indole or hydrogen sulfide producing but does make use of D-mannitol, sucrose, lactose and D-sorbitol fermentation (Tankeshwar, 2019). The bacteria is facultative anaerobic, which means that it can function in both aerobic and anaerobic conditions (Tankeshwar, 2019).

The optimum growth temperature and pH of *K. pneumoniae* was determined by Tsuji *et al* (1982) and is shown in Table 7. The optimum NaCl conditions for *K. pneumoniae* is shown in Table 7, as described by Linke, Sánchez-Cordero & Hoffman (1980).

Table 7: The optimum conditions for growth of *K. pneumoniae*.

| Characteristic | Value |
|---|---|
| Optimum temperature (°C) | 35 |
| Optimum pH | 6 – 7.5 |
| NaCl required (% w/v) | 2 |

In a study done by Oaikhena *et al* (2016), five heavy metal tolerant bacteria were isolated from a petroleum refinery effluent, including *K. pneumoniae*. Each isolate was inoculated into different concentrations of cadmium, chromium, nickel and zinc to determine what the maximum tolerance of the bacteria for each heavy metal is. These results for *K. pneumoniae* are shown in Table 8.

Table 8: The results for the tolerance of *K. pneumoniae* for various heavy metals, as reported by Oaikhena *et al* (2016)

| Heavy metal | Maximum Tolerance Concentration (MTC) (mg $L^{-1}$) |
|---|---|
| Cadmium | 0.7 |
| Chromium | 4 |
| Nickel | 2 |
| Zinc | 5 |

### 2.5.4 Growth conditions

#### Growth media

The growth media used in previous research by this team was the Miller Luria Bertani Broth (LB Broth). LB broth is a rich growth medium that is commonly used to culture *Enterobacteriaceae* but has shown to be effective for the bacteria used in previous research by this team. The recipe for LB broth as described by MacWilliams & Liao (2006) can be seen in Table 9.

The presence of NaCl in the broth causes the precipitation of $PbCl_2$. Therefore, in work done by Peens *et al* (2018), a simulated LB broth was used for conditions of high Pb(II) concentration. The recipe for the simulated LB Broth is shown in Table 9.

Table 9: The recipes for LB broth and simulated LB broth.

| | LB Broth | Simulated LB Broth |
|---|---|---|
| Yeast extract (g $L^{-1}$) | 5 | 10 |
| Tryptone (g $L^{-1}$) | 10 | 20 |
| NaCl (g $L^{-1}$) | 10 | 1 |

Yeast extract is the product of yeast cells and has been used as a nutritional source for bacterial growth (Zarei, Dastmalchi & Hamzeh-Mivehroud, 2016). Yeast extract provides vitamins and trace elements to the bacteria (Interchim, 2015).

Tryptone is another nutritional source for bacterial growth that acts as a nitrogen and carbon source (Interchim, 2015). In work done by Christensen *et al* (2017), tryptone

was determined to increase glucose consumption, cell growth rate and growth yield in *Escherichia coli*.

The presence of NaCl is important as it provides sodium ions for transport and osmotic balance (Interchim, 2015).

In previous work done by this research team, the effect of NaCl, yeast extract and tryptone on the growth of the investigated consortium was determined (Brink & Mahlangu, 2018). The results indicated that the yeast extract is essential for growth while having a yeast extract only medium performed poorly. This indicates a possible requirement of NaCl for growth (Brink & Mahlangu, 2018).

**Effect of temperature and pH on growth**

Temperature plays an important role in microbial growth. If the temperature is too low the membranes of the bacteria lose their fluidity, proteins become too rigid to catalyse reactions and may also undergo denaturation and, chemical reactions and diffusion processes slow down considerably (Parker *et al*, 2016). High temperatures denature proteins and nucleic acids and cause an increase in fluidity of the cell which impairs metabolic processes occurring in the cell membrane (Parker *et al*, 2016).

Bacterial organisms can be classified according to the optimum temperature at which they survive. Mesophiles are adapted to have optimal growth at 20 – 45 °C, psychrotrophs thrive in ranges of 4 – 25 °C, psychrophiles are best suited to ranges of 0 – 15 °C and thermophiles are adapted to ranges of 50 – 80 °C (Parker *et al*, 2016).

The protein motive force that is responsible for the production of ATP in both anaerobic and aerobic cellular respiration is driven by the concentration gradient of $H^+$ ions across the plasma membrane (Parker *et al*, 2016). For this reason the pH of conditions surrounding the bacterial cell is important.

Changes in the pH can also cause the modification and ionisation of amino acid functional groups, which leads to a disruption in the hydrogen bonding. This will then cause changes in the folding of the protein molecule and will lead to denaturation of the proteins in the bacterial cell (Parker *et al*, 2016).

Due to these reasons, it is important that the growth conditions are kept at the optimal temperature and pH for the desired bacteria to grow in the experiment.

## 2.6 Experimental methods

### 2.6.1 Preculture preparation

The preparation of precultures is described by Brink, Hörstmann & Feucht (2019) in research done by this research team on the determination of the minimum inhibitory concentration of a consortium obtained from a borehole at an automotive-battery recycling plant.

The initial culture was prepared by adding 1 g of the contaminated soil from the borehole of the recycling plant to sterile LB broth in a 100 mL serum bottle containing 80 mg $L^{-1}$ Pb(II) and incubated for 24 h at 35 °C in a shaker at 120 rpm under anaerobic conditions. The sample was stored with 20 v/v% glycerol at -77 °C.

The preculture was prepared using the stored inoculum by adding one loop of the inoculum to a 100 mL serum bottle containing LB broth and lead at 80 mg $L^{-1}$. The serum bottle was purged with $N_2$ gas for 3 min and sealed. The serum bottle was placed in an incubator at 120 rpm and 35 °C for a sufficient duration of time until bacterial growth was observed.

### 2.6.2 Anaerobic batch reactors

Previous research focusing on microbial Pb(II) precipitation by Hörstmann & Brink (2019a) of this research team describes the experimental procedure for the preparation of anaerobic batch reactors using LB broth and a bacterial consortium obtained from a lead-mine. The lead stock solution and the LB broth solutions were prepared separately and autoclaved. Once the solutions had cooled down, the lead stock solution was added to the growth media in serum bottles to reach the desired concentration of lead.

It is important that the lead is added to the broth solution at a slightly higher temperature. The precipitation of $PbCl_2$ occurs at lower temperatures, since the solubility of $PbCl_2$ increases with an increase in temperature. This is shown by Hwang & Oweimreen (2003), where the $K_{sp}$ value of $PbCl_2$ is seen to decrease with a decrease in temperature. However, it is important that the solutions are not too hot to ensure that the denaturation of the proteins in the bacteria does not take place (Parker *et al*, 2016).

The serum bottles containing the LB broth and lead solutions were inoculated using a loop from the prepared culture. The bottles were then purged with $N_2$ gas for 3 min and then sealed with a rubber stopper and metal cap, this is done to ensure anaerobic conditions. The serum bottles were placed in a shaker at 120 rpm and 32 °C for 9 d.

### 2.6.3 Aerobic batch reactors

The method described in Chapter 2.6.2 is similar to the method for the aerobic batch reactors. This method is also obtained from work done by Hörstmann & Brink (2019a).

The aerobic batch reactors were prepared using Erlenmeyer flasks, in which the LB broth and lead solutions were added. The lead solution and the broth is autoclaved separately before being added together in a biological safety cabinet in the presence of an open flame.

The flasks were inoculated using a loop of the preculture and were then sealed with sterile cotton wool. The cotton wool ensures the movement of air through the flasks. The batch reactors were then placed on a shaker at 120 rpm for 32 °C for 9 d.

### 2.6.4 Anaerobic and aerobic spread and streak plates

Previous research done by Brink, Hörstmann & Feucht (2019) of this research group focused on determining the minimum inhibitory concentration of microbial Pb(II) precipitation using a lead resistant consortium obtained from an automotive-battery recycling plant in Gauteng, South Africa.

The agar plates prepared from this work made use of a base agar consisting either of LB broth agar or simulated LB broth agar, as seen in Table 10. The required amount of lead is added to the agar after the solutions have been autoclaved separately.

Table 10: The amounts of the components for LB broth agar and simulated LB broth agar

| | LB Broth | Simulated LB Broth |
|---|---|---|
| Yeast extract (g $L^{-1}$) | 5 | 10 |
| Tryptone (g $L^{-1}$) | 10 | 20 |
| NaCl (g $L^{-1}$) | 10 | 1 |
| Agar (g $L^{-1}$) | 15 | 15 |

Either spread or streak plates can be prepared, with the methods described by Sanders (2012). The streak plate is done using a sterilised loop. The loop is placed in the sample and then moved across the agar plate that has been left to cool and set. The loop is moved over the surface of the agar medium in a back and forth motion from the rim of

the plate to the centre. The agar plate is then rotated 90 ° and the loop is touched to the first quadrant near the end of the last streak. The same back and forth movement is used from the first quadrant to the second quadrant. This procedure is repeated four times.

The spread plates are prepared using a glass rod bent in a hockey stick shape. The sample is diluted in a serial dilution in ultra-pure water to the desired dilution. An example of a serial dilution is shown in Figure 3, as adapted from Ogbu *et al* (2017).

A sample volume of between 0.1 and 0.2 mL is dispensed onto the centre of the agar. The sample is then spread across the plate using a sterile hockey-stick shaped glass rod.

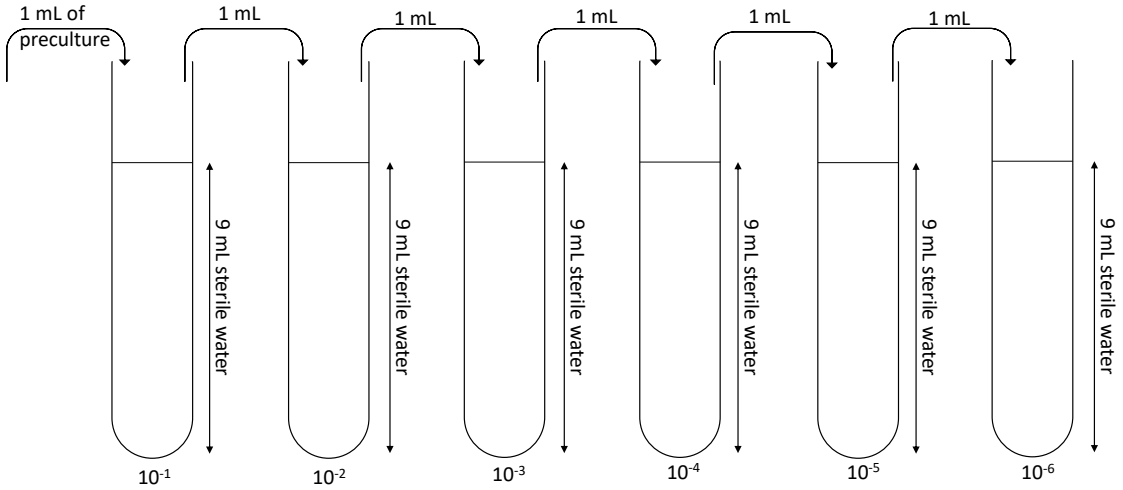


Figure 3: Serial dilution as adapted from Ogbu *et al* (2017).

Once the plates have been prepared they are sealed with parafilm and placed in a glass jar as described by Brink, Hörstmann & Feucht (2019). If aerobic growth is required this jar is placed in the incubator without further alteration, if anaerobic growth is required then the jar is tightly sealed with an AneroGen$^{TM}$ anaerobic environment generation sachet placed in the jar. The plates are incubated for a week at 35 °C.

### 2.6.5 Microbial isolation

Future research by this research group will be aimed to determine the performance of the individual bacterial species on lead precipitation. The consortium used in the past indicated high percentages of *Klebsiella pneumoniae*, *Clostridium tertium* and *Paraclostrid-*

*ium bifermentans* (Hörstmann, Brink & Chirwa, 2020). It is of interest to isolate these bacterial strains and determine the abilities of the individual strains on microbial precipitation of lead.

Isolation of *K. pneumoniae* can be achieved with the use of eosin methylene blue agar (EMB) (Lal & Cheeptham, 2007). This is a selective and differential medium containing peptone, lactose, sucrose and the dyes eosin Y and methylene blue (Lal & Cheeptham, 2007). EMB agar is selective for gram-negative bacteria since methylene blue inhibits the growth of gram-positive bacteria (Lal & Cheeptham, 2007). Eosin responds to a change in pH by undergoing a colour change from colourless to black under acidic conditions. Lactose-fermenting gram-negative bacteria will acidify the medium and will produce a dark purple complex with a metallic sheen under acidic conditions (Lal & Cheeptham, 2007).

Since *K. pneumoniae* is gram-negative and lactose fermenting, it is expected to grow on the EMB agar and produce a metallic shine, while both *Clostridium tertium* and *Paraclostridium bifermentans* should be inhibited on EMB because they are gram-positive (Tankeshwar, 2019; Rai *et al*, 2020; Miller *et al*, 2001).

### 2.6.6 Determination of extracellular and intracellular Pb(II)

In the previously mentioned work done by K Zhang *et al* (2021), which focused on the biomineralization of lead in wastewater, the extracellular and intracellular concentrations of Pb(II) were investigated.

The extracellular Pb(II) was extracted using 20 mmol $L^{-1}$ EDTA solution with a contact time of 30 s. The intracellular Pb(II) was extracted by digesting the cells with 1.0 mol $L^{-1}$ $HNO_3$ solution at 100 °C for 30 min.

## 2.7 Analytical techniques

### 2.7.1 Atomic Absorption Spectrometry

According to Skoog, Holler & Crouch (2018), atomic absorption spectrometry (AAS) has been the most widely used method of detecting and quantifying single elements in a sample for half a century. AAS works by measuring the absorbed radiation by the element of interest in the sample (García & Báez, 2012).

When samples are exposed to radiation, the atoms absorb ultraviolet or visible light and make transitions to higher energy levels (García & Báez, 2012). The amount of energy in the form of photons of light that are absorbed by the sample are measured (García & Báez, 2012).

A detector is used to measure the wavelengths of light that are transmitted by the sample and these are compared to the wavelengths which had originally passed through the sample (García & Báez, 2012). A signal processor is used to integrate the changes in wavelength absorbed, which then appear in the readout as peaks of energy absorption at discrete wavelengths (García & Báez, 2012).

When the electrons are excited and move to a higher energy level, a photon is emitted (García & Báez, 2012). The atoms of each element emit a characteristic spectral line, where every atom has its own pattern of wavelengths at which energy is absorbed (García & Báez, 2012). This is due to the unique configuration of electrons in the outer shell of the atom and enables qualitative analysis (García & Báez, 2012).

The flame atomic absorption methods can also be referred to as direct aspiration determinations (García & Báez, 2012).

### 2.7.2 Metabolic activity

In previous research done by this research group, the metabolic activity of the samples was measured. This method as described by Hörstmann, Brink & Chirwa (2020) is as follows.

The metabolic activity was measured with the use of 3-(4,5-dimethylthiazol-2-yl)-2,5-diphenyl tetrazolium bromide (MTT), which is a water-based yellow dye. MTT is reduced to water-insoluble purple formazan crystals by the dehydrogenase enzymes in viable cells (Hörstmann, Brink & Chirwa, 2020).

The reduction mechanism primarily takes place in the cell cytoplasm; the reductase activity of the endoplasmic reticulum is highly dependent on the concentration of the intracellular NADH and NADPH (Kupcsik, 2011). According to Kupcsik (2011), the abundance of NADH and NADPH is related to the availability of extracellular glucose. If the cell culture medium is exhausted, lower MTT absorbance readings may be noted due to the low glucose concentration (Kupcsik, 2011).

Due to the described metabolic processes, the formation of dark purple needle-like crystals occurs from the cells after a few hours (Kupcsik, 2011). The formazan crystals formed

can be solubilised by mixing the crystals with an organic solvent (Kupcsik, 2011). The absorbance of the solubilised crystals is then measured around a peak broad wavelength of between 570 and 590 nm (Kupcsik, 2011). The absorbance of the crystals is directly proportional to the cell number (Kupcsik, 2011).

In work done by Hörstmann, Brink & Chirwa (2020), the formazan crystals were solubilised with the use of dimethyl sulfoxide (DMSO). The metabolic activity was determined directly after sampling, where two sets of analyses were completed: one not containing biomass and one containing biomass. According to Hörstmann, Brink & Chirwa (2020), this is to account for background interference and medium interaction with MTT and DMSO.

To remove the biomass, the samples were filtered with 25 mm nylon syringe filters with 0.45 µm pores. The sample (with or without biomass) was diluted and MTT was added. The samples were then incubated for 1 h at 35 °C. After incubation, the samples were solubilised with DMSO and the absorbance at 550 nm was measured (Hörstmann, Brink & Chirwa, 2020).

### 2.7.3 Nitrate removal

Previous work done by this research team focused on determining the microbial precipitaion of lead using a bacterial consortium (Hörstmann, Brink & Chirwa, 2020). In this research, the nitrate content of the samples was measured to determine if denitrification is taking place. Denitrification is a mechanism of anaerobic respiration where nitrate is used as an electron acceptor (Hörstmann, Brink & Chirwa, 2020).

The method used by Hörstmann, Brink & Chirwa (2020) consisted of using previously stored samples and a nitrate testing kit. The nitrate ions are reduced with a form of benzoic acid in sulpheric acid and this forms a red nitro solution. This solution was measured photometrically using the spectroquant Nova 600 (Hörstmann, Brink & Chirwa, 2020).

Results from this research indicated that a rapid decline in nitrates was observed between 6 h to 1 d, with all the reactors reaching a limit after the first day. In runs involving a longer time frame, the limit was reached after 3 d where a nearly depleted nitrate reading was observed (Hörstmann, Brink & Chirwa, 2020).

# 3 Experimental methods

## 3.1 Materials

All batch reactors were prepared using simulated Luria-Bertani (LB) broth as shown in Table 11. Metabolic activity was determined using 3-(4,5-dimethylthiazol-2-yl)-2,5-diphenyl tetrazolium bromide (MTT) (Sigma Aldrich, St Louis, MO, USA) and dimethyl sulfoxide (DMSO) (Sigma Aldrick, St. Louis, MO, USA). The lead nitrate solution was prepared using 16 g $L^{-1}$ $Pb(NO_3)_2$ (Glassworld, South Africa) in distilled water, to produce a stock solution of 10 000 mg $L^{-1}$ Pb(II). All agar plates were made using simulated LB broth as shown in Table 11 with 15 g $L^{-1}$ added agar (Sigma Life Science, Spain).

Table 11: Simulated LB broth as used in all experiments.

| Constituents of broth | Amount (g $L^{-1}$) |
|---|---|
| Yeast extract (Merck, Modderfontein, South Africa) | 10 |
| Tryptone (Sigma Aldrich, St Louis, MO, USA) | 20 |
| NaCl (Glassworld, South Africa) | 1 |

## 3.2 Methods

### 3.2.1 Preparation of lead nitrate solution

The solution of $Pb(NO_3)_2$ was prepared using 1.6 g of lead nitrate (Glassworld, South Africa) added to 100 mL distilled water. This produces a solution of 10 000 mg $L^{-1}$ Pb(II).

### 3.2.2 Preculture preparation

Once the bacterial strains were isolated as described in Chapter 4, an anaerobic batch reactor was prepared using LB broth. A loop inoculation occurred using the plate containing the isolated strain. The reactor was incubated at 35 °C for 24 h and a sample was stored in a sterile 2 mL vial containing 20 v/v % glycerol at -40 °C.

### 3.2.3 Anaerobic batch reactors

The anaerobic batch reactors were prepared using simulated LB broth as described by Hörstmann, Brink & Chirwa (2020). The amounts of the components of the broth are shown in Table 11.

The broth was prepared in a volumetric flask with distilled water and 100 mL of this solution was added to serum bottles in triplicate. A set amount of broth was removed from each reactor corresponding to the desired Pb(II) concentration and the reactors were autoclaved at 121 °C for 15 min along with the lead solution. The reactors were left to cool down and lead nitrate solution was added to each reactor the amounts of $Pb(NO_3)_2$ added correspond to the desired concentration of Pb(II) and are shown in Table 12.

Table 12: Amount of $Pb(NO_3)_2$ to be added to the reactors to obtain the desired Pb(II) solution.

| Desired Pb(II) concentration (mg $L^{-1}$) | Amount of Pb(II) added (mL) |
|---|---|
| 80 | 0.8 |
| 250 | 2.5 |
| 500 | 5 |
| 900 | 9 |

The reactors were then inoculated with 0.2 mL stored preculture containing 20 v/v% glycerol. After inoculation the reactors were purged with nitrogen gas for 3 min and sealed to ensure anaerobic conditions. The reactors were then placed in an incubator at 120 rpm and 35 °C.

Sampling was done using sterile hypodermic needles and syringes. The sample was added to a sterile 2 mL vial and stored at -40 °C.

### 3.2.4 Metabolic activity

Metabolic activity of the samples was determined immediately after sampling using the method described by Brink, Hörstmann & Peens (2020). The method makes use of 3-(4,5-dimethylthiazol-2-yl)-2,5-diphenyl tetrazolium bromide (MTT) (Sigma Aldrich, St Louis, MO, USA), a yellow dye that is reduced to purple formazan crystals. This reduction occurs with the use of the dehydrogenase enzymes which are found in bacterial cells. A

colour change occurs as reduction takes place and this is indicative of the amount of viable bacterial cells (Brink, Hörstmann & Peens, 2020). The formazan crystals are then extracted with the use of dimethyl sulfoxide (DMSO) (Sigma Aldrich, St, Louis, MO, USA) which is an organic solvent.

The MTT solution was prepared by adding 5 g $L^{-1}$ of MTT to distilled water in a volumetric flask. The solution was filtered into a sterile 2 mL vial using a 25 mm nylon syringe filter with 0.45 µm pores. These vials were stored in a dark container at -40 °C.

The samples were centrifuged at 7711 × $g$ for 10 min and 0.5 mL of each sample was filtered with a 25 mm nylon syringe filter with 0.45 µm pores. The filtered sample is a representative of a sample without biomass. An amount of 0.5 mL was not filtered and these two results are subtracted to represent the sample without noise. The two 0.5 mL samples were added to 1.5 mL sterile distilled water in separate 15 mL tubes. The solution was mixed and 0.9 mL of the diluted solution was added to a sterile 2 mL vial. Thereafter, 0.1 mL of MTT solution was added to each vial and the vials were incubated at 35 °C for 1 h. The samples were then diluted with 1 mL DMSO and the absorbance of the samples were measured at 550 nm on a UV/Vis spectrometer (WPA-Lightwave II, Labotech, South Africa).

### 3.2.5 Nitrate removal

The extent of nitrate removal was determined using a nitrate test (Spectroquant Nitrate Test, Supelco, Germany). The nitrate ions react with a benzoic acid derivative in concentrate sulfuric acid and this forms a red nitro compound that is determined photometrically.

The two reagents in the test were mixed with 1.5 mL of prepared sample and the reaction occurred for 10 min. The amount of nitrates in the sample was then determined using the photometer (Spectroquant NOVA 60, Merck).

The samples were prepared by centrifugation at 7711 × $g$ for 10 min, followed by dilution with distilled water.

### 3.2.6 $OD_{600}$ measurements

The optical density was determined spectrophotometrically using a UV/Vis spectrometer at 600 nm. The reading was done by placing 2 mL of the unaltered sample in a curvette.

If the reading is larger than 2.5, which is beyond the limitations of the instrumentation, the sample was diluted using distilled water.

### 3.2.7 Residual Pb(II) concentration measurements

The original samples obtained from the bioreactors were prepared by centrifugation at 7711 $\times$ $g$ for 10 min. The supernatant was then decanted into sterile 2 mL vials. The samples were diluted in distilled water to a range between 0 – 10 mg $L^{-1}$ Pb(II) concentration as this is the range of the analytical instrumentation. Measurements of the supernatant were done using an atomic absorption spectrometer with a Pb lumina hollow cathode lamp (PerkinElmer AAnalyst 400, Waltham, Massachusetts). The measurements are done using the calibration curve method of a direct aspiration determination. This method includes the preparation of three different concentrations of lead and the absorbance of the standard solutions is then measured, a calibration curve is prepared from these values and the sample concentrations are determined based on this calibration curve (García & Báez, 2012).

### 3.2.8 Determination of extracellular and intracellular Pb(II)

The extracellular and intracellular concentration of Pb(II) was determined using a previously described method by (K Zhang *et al*, 2021). The original samples were centrifuged at 7711 $\times$ $g$ for 10 min and the supernatant Pb(II) concentration was determined as described in Chapter 3.2.7. The pellet was then dissolved in 1 mL 20 mmol $L^{-1}$ ethylenedinitrilotetraacetic acid disodium salt dihydrate (EDTA) solution (Supelco, Germany), with a contact time of 30 s.

The dissolved pellet was then centrifuged at 7711 $\times$ $g$ for 10 min and the supernatant concentration, which is the extracellular Pb(II) concentration, was determined using the atomic absorption spectrometer. The pellet was dissolved with 55 % $HNO_3$ solution and the intracellular Pb(II) concentration was determined. A description of the process along with the expected concentrations and expected species obtained at each step is shown in Figure 4.

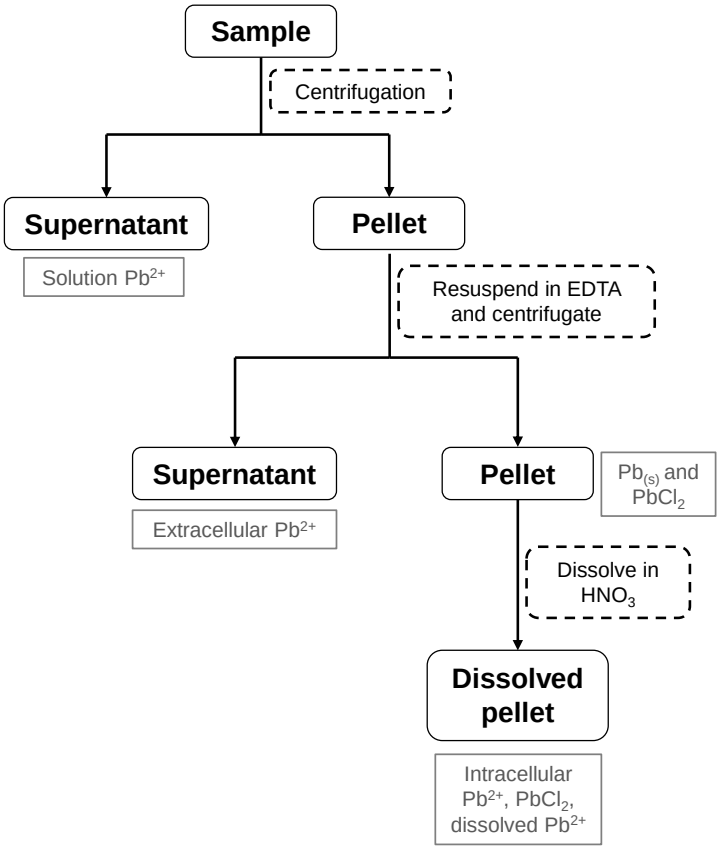


Figure 4: The description of the determination of the extracellular and intracellular Pb(II) as well as the expected species at each step.

### 3.2.9 Precipitate identity

The precipitate samples were characterised by X-ray photonelectron spectroscopy (XPS) (Thermo ESCAlab 250, Xi, Waltha, MA) (Brink, Hörstmann & Peens, 2020). Sample preparation involved the centrifugation of the original samples obtained from the bioreactors at 7711 $\times$ $g$ for 10 min. The samples were then dried anaerobically to ensure that minimum oxidation of the precipitate occurs. The drying process involved placing the samples in a sealed jar containing silica crystals and an AnaeroGen$^{TM}$ anaerobic environment generation sachet (Thermo scientific, UK) for 24 h. The XPS data was deconvoluted using OriginPro 2022 (OriginLab Corporation, Northampton, Massachussetts, USA) and analysed using the NIST CPS database (National Institute of Standards and Technology, 2002).

### 3.2.10 Preparation of anaerobic streak and spread plates

The agar used in the preparation of the anaerobic plates was prepared using the amount of LB broth shown in Table 11 with added 15 mg $L^{-1}$ agar. This solution is prepared

using distilled water and autoclaved at 121 °C for 15 min.

The agar was distributed into plastic agar plates and set to cool. Once the agar had cooled the plates were prepared using either the streak method or the spread method.

For the spread method, the sample was diluted to a factor of either $10^{-4}$, $10^{-5}$ or $10^{-6}$ - depending on the stage of growth at the time of measurement. The dilution was done using sterile distilled water in sterile tubes. Thereafter, 0.1 mL of the diluted sample was placed onto an agar plate and a sterile hockey-stick shaped glass rod was used to spread the sample across the plate.

In the streak plate method, a sterile loop was dipped into the sample and the loop was streaked across the plate, as shown in Figure 5.

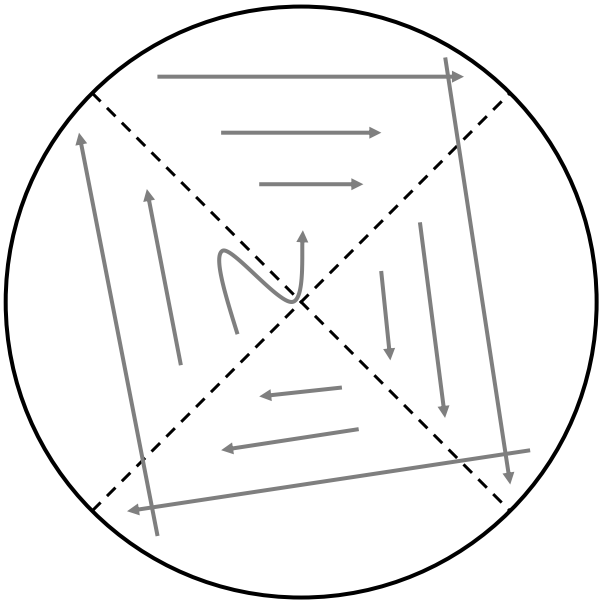

Figure 5: The method used for the preparation of the the streak plates.

For both methods, the plates were sealed with parafilm and placed inside an autoclaved 3 L jar with an AnaeroGen$^{TM}$ anaerobic environment generation sachet (Thermo scientific, UK) and an anaerobic indicator (Thermo scientific, UK). The jars were sealed and placed in an incubator at 35 °C for the required time specific to the experiment.

# 4 Bioprecipitation of lead using *P. bifermentans* and *K. pneumoniae*: long duration study

A long duration study was done as a proof of concept to determine if the pure cultures isolated from the microbial consortium are able to precipitate Pb(II) from solution, and to determine if there is a difference in the abilities of the two strains.

The work presented in this chapter has been accepted for publication in *International Journal of Molecular Sciences* under the title "Microbial Precipitation of Pb(II) with Wild Strains of *Paraclostridium bifermentans* and *Klebsiella pneumoniae* Isolated From an Industrially Obtained Microbial Consortium".

Part of the work presented in this chapter on the bioprecipitation of *K. pneumoniae* has been published in *Chemical Engineering Transactions* under the title "Microbial Pb(II) Removal by Precipitation and Adsorption Mechanisms with *Klebsiella Pneumoniae* Isolated from an Industrially Obtained Consortium" (Neveling *et al*, 2022).

## 4.1 Experimental methods

The strains were isolated with a series of spread and streak plates. The isolation of *P. bifermentans* was done using Luria-Bertani (LB) broth agar, with sequential rounds of streak and spread plates. The first round of plates consisted of spread plates made with an dilution factor of $10^{-5}$ using the method described in Chapter 3.2.10 and the stored microbial consortium. Two rounds of streak plates were then performed using visually desirable colonies from the previous plates. The final streak plate was analysed using 16S rDNA sequencing by Inqaba Biotech (South Africa).

For the isolation of *K. pneumoniae*, the strain was streaked across an agar plate consisting of eosin methylene blue agar (EMB) (Oxoid, Hants, UK). This is agar is selective for gram-negative microbes. A colony from the EMB plate was then streaked onto LB agar plates containing 80 mg $L^{-1}$ Pb(II). From these plates batch reactors were prepared using the method described in Chapter 3.2.3, with the exception that these reactors were grown aerobically to inhibit the growth of the obligate anaerobe *P. bifermentans*. The batch reactors were then used to streak LB agar plates containing 80 mg $L^{-1}$ Pb(II) and these final plates were analysed using 16S rDNA sequencing by Inqaba Biotech (South Africa).

The isolated strains were grown in triplicate anaerobic batch reactors prepared using the method described in Chapter 3.2.3. Metabolic activity measurements were done using

the method in Chapter 3.2.4. Nitrate measurements were done using the method in Chapter 3.2.5, and the residual Pb(II) concentration was determined using the method described in Chapter 3.2.7. The same experiment was conducted using the microbial consortium, this was done to compare the performance of the individual strains with the consortium from which they were isolated.

## 4.2 Results and discussions

### 4.2.1 Isolation of the strains

The isolated strain was identified as *Paraclostridium bifermentans* with the use of 16S rDNA sequencing and the phylogenetic tree indicating the identity of the strain *P. bifermentans* (BPB21A) is shown in Figure 6. The initial spread plate of the consortium and the final streak plate of *P. bifermentans* is shown in Figure 7.

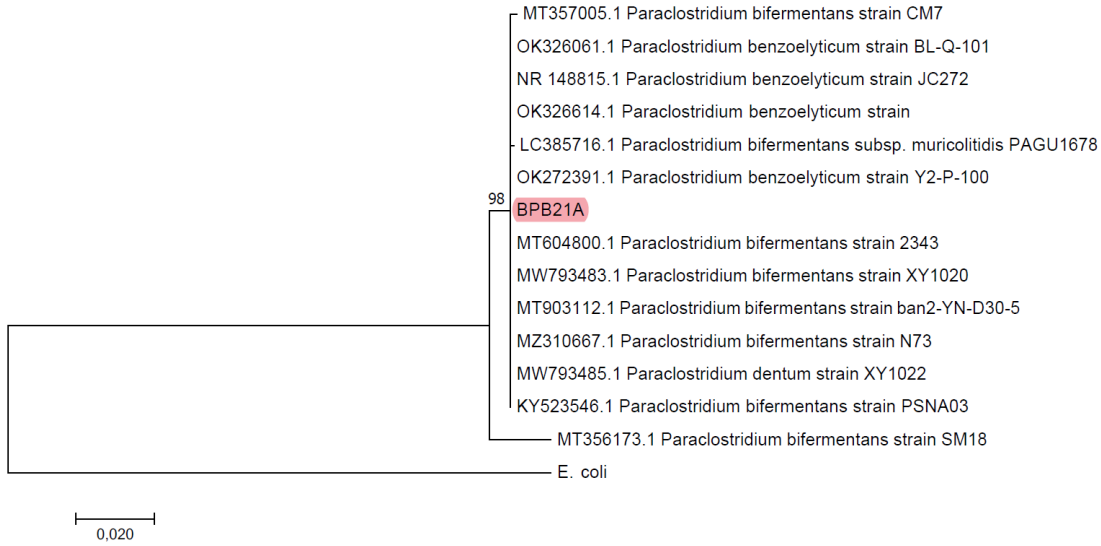


Figure 6: The phylogenetic tree indicating the identity of the *P. bifermentans* strain isolated from the microbial consortium (BPB21A).

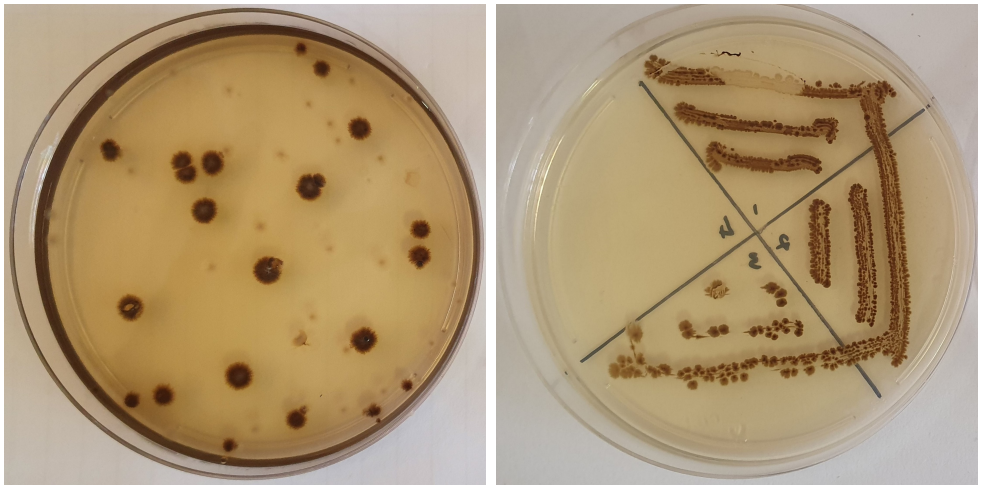

(a) (b)

Figure 7: (a) The initial spread plate of the consortium and (b) the final streak plate containing the isolated strain *P. bifermentans*.

It was possible to isolate *K. pneumoniae* from the consortium, and the phylogenetic tree indicating the identity of the strain *K. pneumoniae* (BKP21E) is shown in Figure 8. The initial EMB plate and the final LB broth agar plate used in the isolation of the strain is shown in Figure 9.

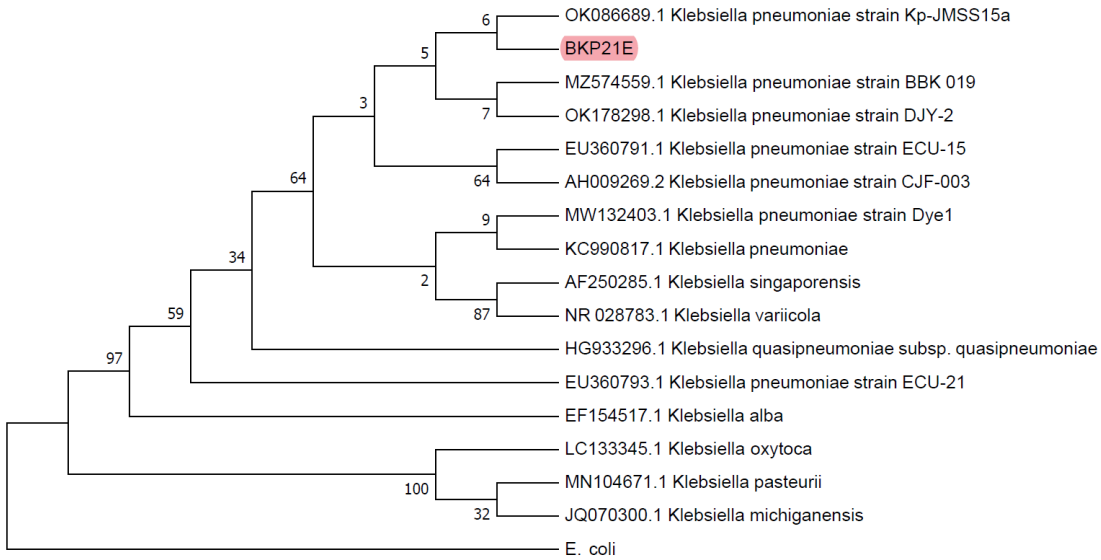


Figure 8: The phylogenetic tree indicating the identity of the *K. pneumoniae* strain isolated from the microbial consortium (BKP21E).

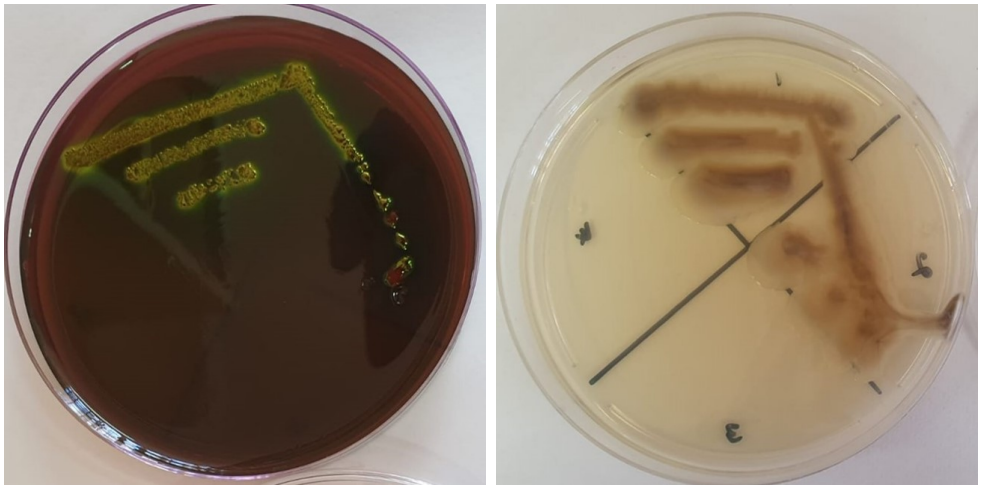

(a) (b)

Figure 9: The plates used in the isolation experiment for *K. pneumoniae* with (a) the initial EMB agar plate and (b) the final LB broth agar plate used for identification of the strain.

### 4.2.2 Visual changes

Visual changes were observed in the reactors due to the precipitation of Pb(II), thereby serving as a preliminary indication that the experiment was successful. The visual changes observed in the long duration study for *P. bifermentans* and *K. pneumoniae* are shown in Figure 10. From these results it is clear that precipitation occurs in under 18 h for both bacterial strains. A slight variance in the intensity of the colour of precipitate is observed between the strains. This could be due to a difference in precipitate identity which is further discussed in Chapter 5. The colour difference could also be an indication of the location of the Pb(II) precipitate, that is, if it is found extracellularly or intracellularly.

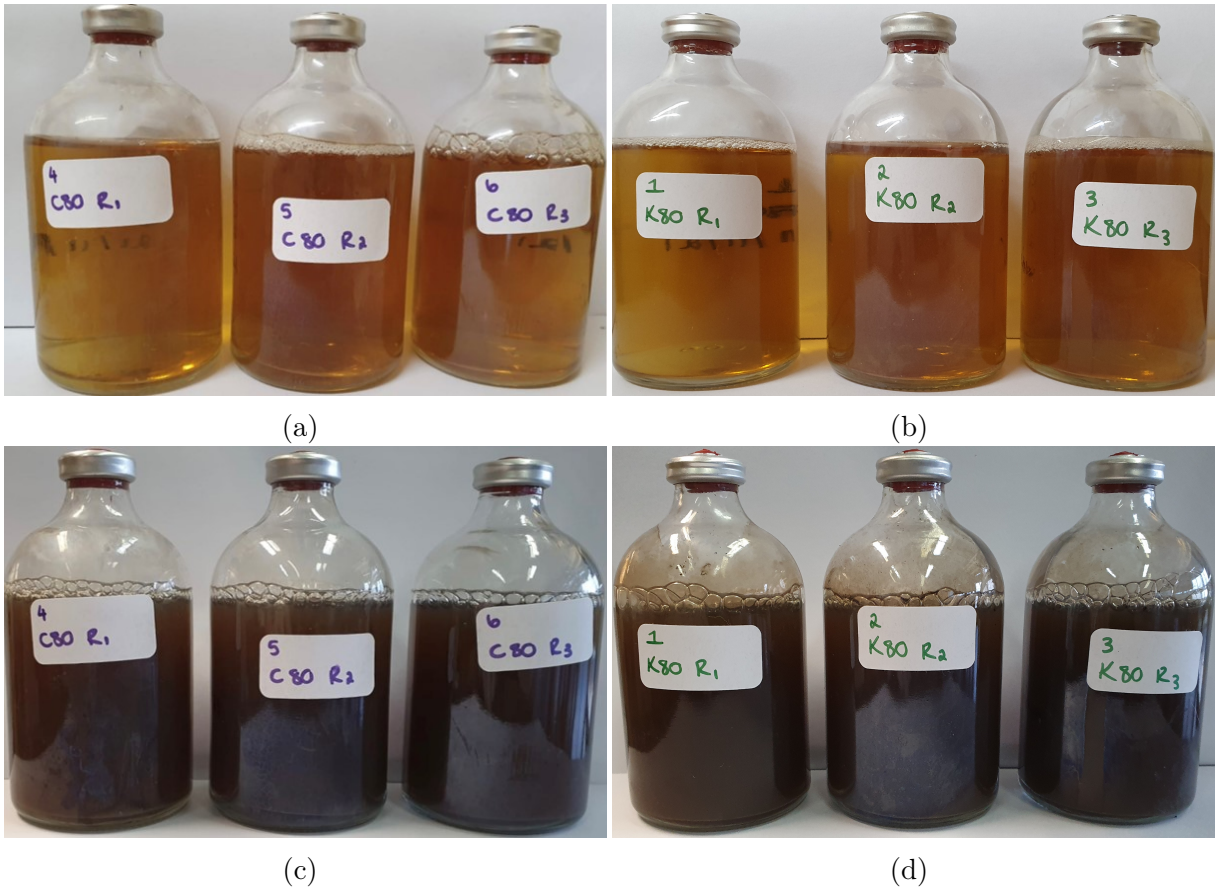


(a) (b)

(c) (d)

Figure 10: The bioreactors of (a) *P. bifermentans* and (b) *K. pneumoniae* at 0 h and the rapid visual changes observed for (c) *P. bifermentans* and (d) *K. pneumoniae* after 17 h.

### 4.2.3 Microbial growth measurements

The metabolic activity of both strains and the consortium is shown in Figure 11. This data shows a different pattern in metabolic activity for the two isolated cultures when compared to the bacterial consortium. This could be an indication that the cultures utilise different precipitation mechanisms when they are isolated compared to when they are contained in the consortium. The metabolic activities of the individual strains do not differ greatly.

A peak value in the metabolic activity is observed for both strains at approximately 65 h, with a steady decline observed thereafter. This decline is a possible indication of substrate depletion within the batch reactors. The decline for the microbial consortium is observed much sooner than the individual strains at approximately 50 h. This could be an indication that the consortium reaches substrate depletion sooner, possibly due to the competing species present in the system. This depletion coincides with results published on the microbial consortium from which the strains were isolated where a plateau in microbial activity is reached after 2 d (Hörstmann, Brink & Chirwa, 2020).

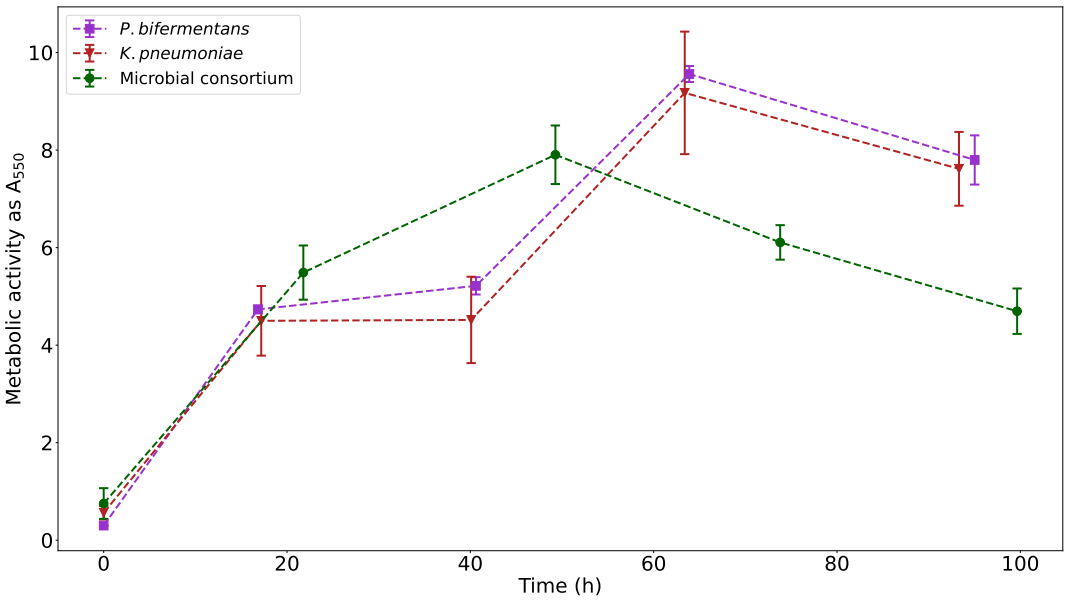


Figure 11: The metabolic activity of *P. bifermentans*, *K. pneumoniae* and the microbial consortium as observed over approximaterRly 100 h of the long duration precipitation study.

### 4.2.4 Residual Pb(II) concentration

The lead removal profiles of *K. pneumoniae*, *P. bifermentans* and the microbial consortium are shown in Figure 12. The amount of Pb(II) removed by *K. pneumoniae* is slightly higher than the consortium possibly indicating that *K. pneumoniae* is inhibited by other microbes when part of the consortium. It is noted that *P. bifermentans* is the least efficient at Pb(II) removal, but still has a significant removal with an approximate final Pb(II) concentration value of 13 mg $L^{-1}$.

The microbial consortium reached a final Pb(II) concentration value of approximately 4.5 mg $L^{-1}$. There is a significant decrease in Pb(II) concentration in samples containing *P. bifermentans* in the initial sample which is an indication of a rapid biosorption or other detoxification mechanism employed by *P. bifermentans*. Overall, the rate of Pb(II) removal for *K. pneumoniae* is faster than for *P. bifermentans* and the consortium. The plateau of the removal curve is reached at the same point at the first peak in metabolic activity for the individual strains and as the peak in metabolic activity for the consortium.

These results correlate with previous research on the continuous bioremoval of Pb(II) using the same microbial consortium from which the individual strains in this study were isolated, where a decrease in Pb(II) concentration is related to an increase in metabolic activity (Chimhundi *et al*, 2021).

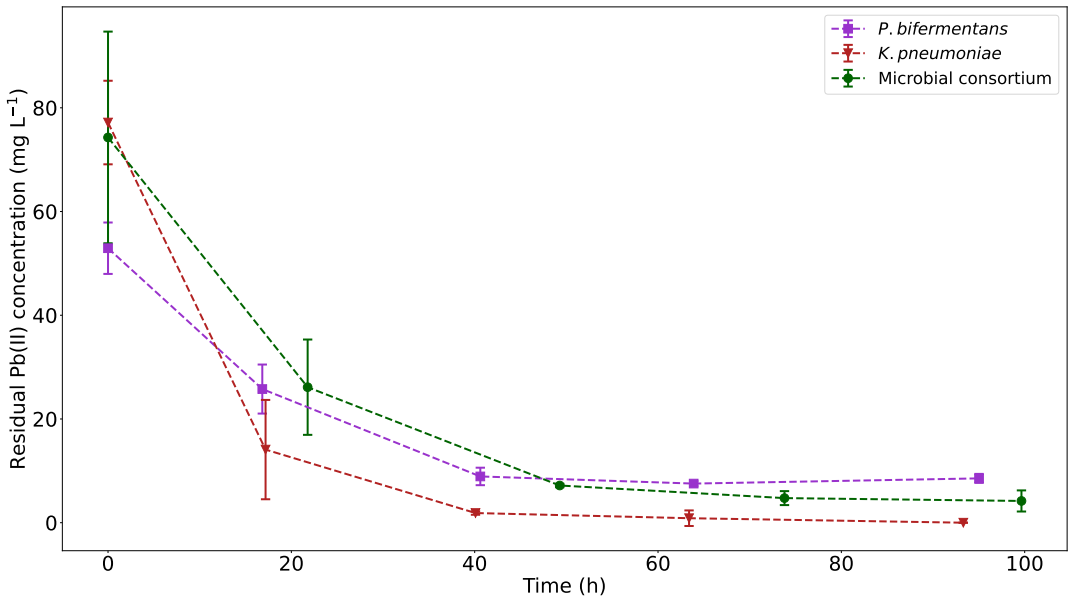


Figure 12: The lead removal profiles of *P. bifermentans*, *K. pneumoniae* and the microbial consortium over approximately 100 h of the long duration precipitation study.

In order to determine if altering the bacterial species does in fact have an effect on the microbial precipitation of lead, a statistical inference analysis was performed based on the methods outlined by D'Agostino Sr, Sullivan & Beiser (2006)[239] for two independent populations with unknown variances.

Initially, a $F$ distribution was calculated to be used to determine if the variances of the two populations are equal. A confidence internal of 95 % was used for the $F$ test and from this is was concluded that the variances are equal. Thereafter a $t$ test statistic was calculated for each data point. The $t$ test statistic was calculated using

$$t = \frac{\overline{X}_1 - \overline{X}_2}{S_p\sqrt{\frac{1}{n_1} + \frac{1}{n_2}}} \tag{1}$$

where $\overline{X}_1$ and $\overline{X}_2$ are the average of the three runs of the two populations, $n_1$ and $n_2$ are the sample sizes which are equal to three for all analysis and $S_p$ is the pooled estimate of the common standard deviation given by

$$S_p = \sqrt{\frac{(n_1 - 1)s_1^2 + (n_2 - 1)s_2^2}{n_1 + n_2 - 2}} \tag{2}$$

where $s_1$ and $s_2$ are the sample standard deviations of the two populations. The populations were compared using the following combinations: *K. pneumoniae* and *P. bifermen-*

*tans*, *K. pneumoniae* and the consortium and, the consortium and *P. bifermentans*.

The null and alternative hypothesis used were

$$H_0 : \mu_1 = \mu_2 \tag{3}$$

and

$$H_1 : \mu_1 \neq \mu_2 \tag{4}$$

which indicates that if there is a statistically significant difference between the two averages of the populations, the change in bacterial species does have an effect on the microbial precipitation of lead. The degrees of freedom are given by

$$df = n_1 + n_2 - 2 \tag{5}$$

and since $n_1$ and $n_2$ are both always equal to three because three replicates of each experiment were done, the degrees of freedom was always equal to four.

A confidence interval of 95 % was used and the critical value of the $t$ distribution at this confidence level and at four degrees of freedom was equal to 2.776. The null hypothesis can therefore be rejected if:

$$t > 2.776 \text{ or } t < -2.776$$

The value of the $t$ statistic and the resulting conclusions from the statistical inference analysis are shown in Table 13. From this analysis it is shown that there is a significant difference in the means between the populations for *K. pneumoniae* and *P. bifermentans*, which indicates that two different bacterial strains are present and are employing different mechanisms of lead bioprecipitation. It is also an indication that *K. pneumoniae* did have a higher rate of precipitation than *P. bifermentans*. There is no significant difference between *K. pneumoniae* and the consortium, as well as between *P. bifermentans* and the consortium. This could be due to the presence of both *K. pneumoniae* and *P. bifermentans* in the microbial consortium.

Table 13: The results of the statistical inference analysis to determine if there is a difference in the means of the populations indicating whether the bacterial species has a significant effect on the microbial precipitation of lead.

| Time interval | *P. bifermentans* and *K. pneumoniae* | *K. pneumoniae* and consortium | *P. bifermentans* and consortium |
|---|---|---|---|
| | | Calculated $t$ | |
| 1 | 3.772 | 2.559 | -2.511 |
| 2 | 5.442 | 4.340 | -2.168 |
| 3 | 5.127 | 2.095 | -2.513 |
| 4 | 18.25 | 5.547 | -7.243 |
| | | Conclusion | |
| 1 | Reject $H_0$ | Do not reject $H_0$ | Do not reject $H_0$ |
| 2 | Reject $H_0$ | Reject $H_0$ | Do not reject $H_0$ |
| 3 | Reject $H_0$ | Do not reject $H_0$ | Do not reject $H_0$ |
| 4 | Reject $H_0$ | Reject $H_0$ | Reject $H_0$ |

The final percentage removal of Pb(II) is shown in Table 14 to compare the effectiveness of each strain. It is clear from this data that *K. pneumoniae* was slightly more efficient at Pb(II) removal when compared to *P. bifermentans* and the consortium as the concentration of Pb(II) reached levels undetectable by the analytical instrumentation after 93 h. A percentage removal of 94.4 ± 1.88 % is recorded for the consortium after 100 h and a percentage removal of 83.8 ± 1.70 % is recorded for *P. bifermentans* after 95 h.

Table 14: The average percentage of Pb(II) removed from the reactors of each run at the final sampling time for the long duration study.

| Strain | Time elapsed (h) | Pb(II) removed (%) |
|---|---|---|
| *P. bifermentans* | 95 | 83.8 ± 1.70 |
| *K. pneumoniae* | 93 | 100[1] |
| Microbial consortium | 100 | 94.4 ± 1.88 |

[1] Taken to be 100 % since values were too low to be detected by the analytical instrumentation.

### 4.2.5 Nitrate concentration

The nitrate concentration was determined to establish whether the precipitation and metabolic activity is dependent on the concentration of nitrates available in the system. The nitrate concentration for the experimental runs over 100 h is shown in Figure 13.

The nitrate concentration decreases over time which correlates to an increase in metabolic activity as observed in Figure 11. The nitrate concentration remains stable thereafter for the individual strains even though a second exponential growth is observed for the individual strains. This is an indication that the metabolic activity of the strains is not dependent on the nitrate concentration. The nitrates are not depleted for the individual strains and is it therefore likely that nitrates are not a limiting substrate for growth in the individual strains.

The initial drop in nitrates of the individual strains is comparable to data previously published based on the microbial consortium from which the strains used in this study were isolated, where a drop of approximately 100 mg $L^{-1}$ occurs after 1.5 d (Hörstmann, Brink & Chirwa, 2020). This drop is equivalent to the magnitude of the drop observed in Figure 13.

The trend observed for the consortium differs from that stated for the individual strains

in that an initial decrease is observed with a plateau reached in concentration after 20 h. This correlates with an increase in growth as observed between 0 and 40 h. After this time, a drop in growth is observed which does not correlate to the nitrate concentration.

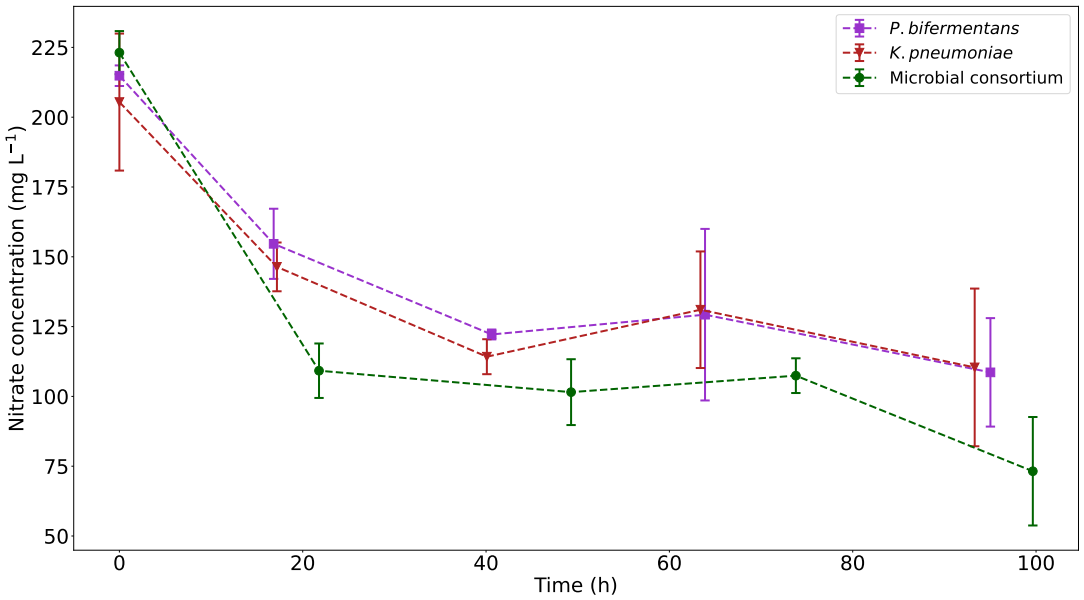


Figure 13: The nitrate concentration of *K. pneumoniae*, *P. bifermentans* and the microbial consortium as observed over approximately 100 h of the long duration precipitation study.

## 4.3 Conclusions

It was possible to isolate the two strains of interest, *K. pneumoniae* and *P. bifermentans* from the microbial consortium and both strains were identified using 16S rDNA sequencing.

The visual changes in the experiment indicated the presence of lead precipitate in the solution in under 18 h for both strains. There was a slight colour difference between the two strains which could indicate that the identity of the lead precipitate varies between the strains. This point will be investigated further in Chapter 5.

The residual Pb(II) concentrations indicated that both strains are able to precipitate Pb(II) over the 100 h period investigated, with the majority of precipitation occurring in under 18 h. Using statistical analysis it was concluded that there is a significant difference in the values of residual Pb(II) concentration between the two strains, indicating that the strains possibly utilise different precipitation mechanisms.

The metabolic activity of the strains and the consortium indicate that the strains undergo a different metabolic mechanism when not part of the consortium. The metabolic activity

of the two strains did not differ greatly. The nitrate concentration of the samples over time indicated that nitrates are almost depleted for the microbial consortium over the 100 h period with a definite decrease observed towards the end of the period. This is not true for the individual strains and could indicate that the metabolic growth of the strains is not dependent on the nitrate concentration.

The long duration study provided a proof of concept regarding the microbial precipitation of Pb(II) from solution using bacterial strains isolated from an industrially obtained microbial consortium. It is concluded that in the long term study, *K. pneumoniae* was slightly more efficient than *P. bifermentans* at the bioprecipitation of Pb(II). A short term study is required to further analyse the precipitation mechanism.

# 5 Bioprecipitation of lead using *P. bifermentans* and *K. pneumoniae*: short duration study

The lead removal efficiency of the two isolated strains, *P. bifermentans* and *K. pneumoniae*, was investigated over a shorter period with an increased amount of sampling intervals. This was done to gain a greater understanding of the precipitation mechanism since it was observed that a large percentage of precipitation occurs in under 18 h for both strains. The study was done over 30 h with nine sampling intervals.

The work presented in this chapter has been accepted for publication in *International Journal of Molecular Sciences* under the title "Microbial Precipitation of Pb(II) with Wild Strains of *Paraclostridium bifermentans* and *Klebsiella pneumoniae* Isolated From an Industrially Obtained Microbial Consortium".

## 5.1 Experimental

The experiments were conducted in anaerobic batch reactors prepared as described in Chapter 3.2.3 in triplicate with four varying initial Pb(II) concentrations, 80 mg $L^{-1}$, 250 mg $L^{-1}$, 500 mg $L^{-1}$ and 900 mg $L^{-1}$.

The metabolic activity of the samples was determined immediately after each sampling interval using the method described in Chapter 3.2.4. The nitrate and residual Pb(II) concentrations were determined using the methods described in Chapter 3.2.5 and Chapter 3.2.7 respectively.

The extracellular and intracellular Pb(II) concentrations were determined using the method described in Chapter 3.2.8. The precipitate identity was determined using XPS, with the samples prepared using the method in Chapter 3.2.9.

## 5.2 Results and discussions

### 5.2.1 Visual changes

A visual change was observed throughout the experiments as the precipitation of Pb(II) occurs. The visual changes observed for the experiments involving *P. bifermentans* are shown in Figure 14, and indicate that precipitation only occurs after 12 h. The visual changes observed for the experiments involving *K. pneumoniae* are shown in Figure 15

and indicate that the precipitation mechanism occurs sooner for these experiments than for experiments involving *P. bifermentans*, with a dark precipitate forming at around 6 h in samples containing 80 and 250 mg $L^{-1}$ initial Pb(II) concentration. The precipitate is formed later in experiments containing 500 mg $L^{-1}$ initial Pb(II) concentration.

Not all reactors containing 900 mg $L^{-1}$ initial Pb(II) concentration underwent a colour change. This could be due to the Pb(II) concentration being too high for bacterial growth and the data for an initial Pb(II) concentration of 900 mg $L^{-1}$ is therefore not discussed further.

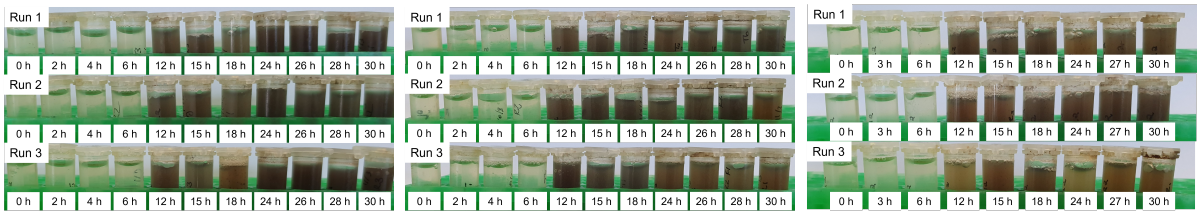


(a) (b) (c)

Figure 14: The visual changes observed for each experiment in triplicate containing *P. bifermentans* over 30 h for (a) 80 mg $L^{-1}$, (b) 250 mg $L^{-1}$ and (c) 500 mg $L^{-1}$ initial Pb(II) concentration.

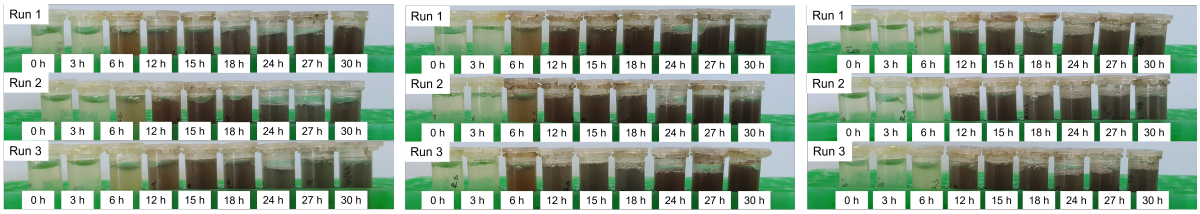


(a) (b) (c)

Figure 15: The visual changes observed for each experiment in triplicate containing *K. pneumoniae* over 30 h for (a) 80 mg $L^{-1}$, (b) 250 mg $L^{-1}$ and (c) 500 mg $L^{-1}$ initial Pb(II) concentration.

### 5.2.2 Microbial growth measurements

The metabolic activity of both strains at the varying initial concentrations of Pb(II) is shown in Figure 16. These values are compared to previously published data obtained from the microbial consortium from which the strains were isolated (Hörstmann, Brink & Chirwa, 2020).

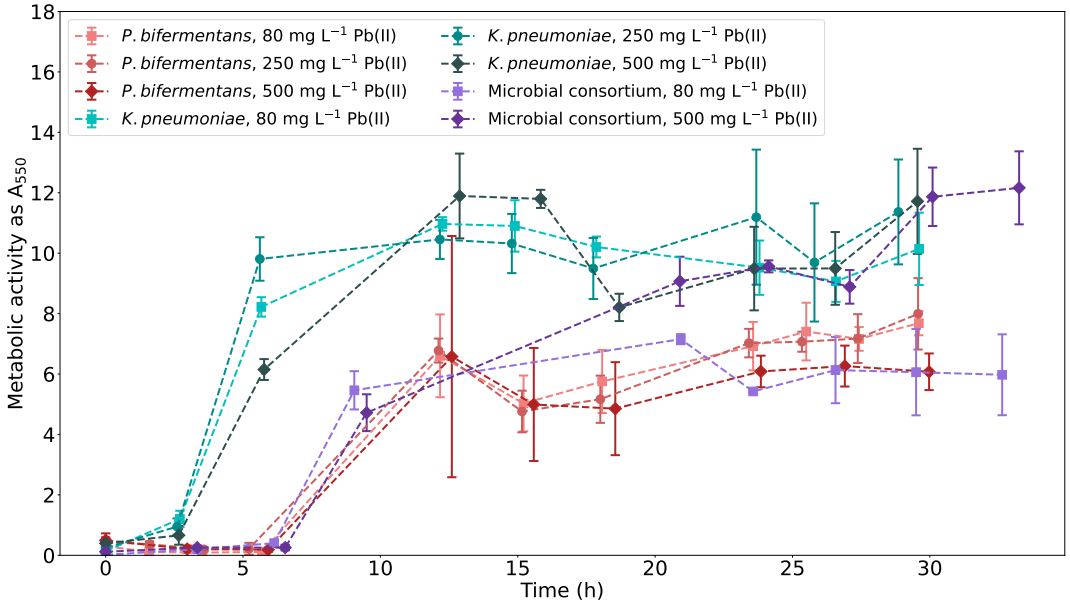


Figure 16: The metabolic activity as $A_{550}$ for both *P. bifermentans* and *K. pneumoniae* with varying initial Pb(II) concentrations compared with previously published data on the consortium from which the strains were isolated (Hörstmann, Brink & Chirwa, 2020).

From Figure 16, a lag phase is observed for all bacterial strains with a longer lag phase noted for *P. bifermentans*. This could be an indication that *K. pneumoniae* is better adapted to the initial toxicity of Pb(II). The lag phase noted in the data on the microbial consortium is near identical to the lag phase of *P. bifermentans*. This is a possible indication that *K. pneumoniae* is inhibited while in the consortium by other strains of the consortium such as *P. bifermentans*.

From these results it is observed that *K. pneumoniae* has a higher metabolic activity than *P. bifermentans* and the consortium for all initial Pb(II) concentrations. This is a possible indication that *K. pneumoniae* is better suited to the toxic environment created by the presence of Pb(II). The strain has a faster exponential growth phase at all initial Pb(II) concentrations than *P. bifermentans* and the consortium, with the rate of initial growth decreasing with an increase in initial Pb(II) concentration. The metabolic activity values reached by the microbial consortium are lower than those reached by *K. pneumoniae* which could be an indication that *K. pneumoniae* is inhibited by other microorganisms when part of the consortium.

The pattern of metabolic activity displayed by *P. bifermentans* is similar for all initial concentrations of Pb(II), which could indicate that the mechanism of precipitation utilised by *P. bifermentans* does not differ for varying Pb(II) concentrations. An initial exponential growth is observed in samples containing *P. bifermentans* with a second increase observed after 20 h. This correlates with previous research done on the consortium

using simulated LB broth where it was concluded that the second exponential growth is attributed to the increased nutrient concentrations of the broth (Hörstmann, Brink & Chirwa, 2020).

The metabolic activity values of the consortium were similar to the initial values recorded for *P. bifermentans*, and thereafter these values tended to the metabolic activity readings recorded for *K. pneumoniae*. This could be an indication that *P. bifermentans* inhibits the growth of *K. pneumoniae* in the consortium, which would then limit the initial overall metabolic activity.

### 5.2.3 Residual Pb(II) concentration

The residual Pb(II) concentration for both *P. bifermentans* and *K. pneumoniae* is shown in Figure 17 and is compared with previously published data on the consortium (Hörstmann, Brink & Chirwa, 2020). The results indicate once more that *K. pneumoniae* is slightly more efficient than *P. bifermentans* at Pb(II) bioprecipitation. Both strains were able to precipitate a larger fraction of Pb(II) than the consortium at 80 mg $L^{-1}$ initial Pb(II) concentration but a faster removal rate was observed for the consortium for samples containing 500 mg $L^{-1}$ initial Pb(II) concentration. The amount of Pb(II) removed by *P. bifermentans* decreases as the initial Pb(II) concentration increases.

Both strains have the same initial concentrations of Pb(II) for the experiments, but a decrease in Pb(II) concentration is observed in the first reading. This reading was taken approximately 10 min after inoculation. This could be indicative of a rapid detoxification mechanism since a drop in Pb(II) concentration is observed followed by an increase in Pb(II) concentration. The same occurrence was noted in previous research on the microbial consortium (Hörstmann, Brink & Chirwa, 2020; Cilliers *et al*, 2022). It was also noted in previous research that approximately 62 % of Pb(II) is removed from solution after 3 h by the microbial consortium after metabolic inhibition of the bacteria with $NaN_3$ 91. In the same study, a drop of approximately 50 % of Pb(II) concentration is observed after approximately 15 min. The observation of a drop in Pb(II) concentration in this study can therefore be attributed to biosorption of Pb(II) by metabolically inactive bacteria. The experiments in this study were inoculated using frozen precultures and therefore the likelihood of the presence of metabolically inactive bacteria is not significant. In addition, the nitrate concentrations measured at the start showed statistically insignificant differences using a t-statistic inference with a 95 % confidence interval, and therefore supports the assertion that the same initial Pb(II) concentrations were used. The main source of nitrates in the reactors were $Pb(NO_3)_2$ and therefore this acts as an internal standard. The statistical inference analysis was conducted using the methods

described in Chapter 4.2.4, and the value of the $t$ statistic and the resulting conclusions from the statistical inference analysis are shown in Table 15. The null hypothesis is not rejected for any calculated $t$ value and it can be concluded that there is no statistically significant difference in the initial nitrate concentration between experimental conditions.

Table 15: The calculated $t$ statistics of the inference analysis.

| Initial Pb(II) concentration (mg $L^{-1}$) | Populations to be compared | $t$ |
|---|---|---|
| 80 | *P. bifermentans* and *K. pneumoniae* | -0.3324 |
| | *P. bifermentans* and microbial consortium | -1.341 |
| | *K. pneumoniae* and microbial consortium | -0.6174 |
| 250 | *P. bifermentans* and *K. pneumoniae* | -0.6207 |
| 500 | *P. bifermentans* and *K. pneumoniae* | -0.2274 |
| | *P. bifermentans* and microbial consortium | -0.5171 |
| | *K. pneumoniae* and microbial consortium | -0.4058 |

In order to further compare the efficiency of the strains, the final percentage removal of Pb(II) is compared in Table 16. From this data is is clear that *K. pneumoniae* is more efficient at Pb(II) microbial precipitation than *P. bifermentans* at two of the three initial Pb(II) concentrations investigated.

Table 16: The percentage Pb(II) removed for each strain at the varying initial Pb(II) concentrations at the final sampling time of 30 h.

| Strain | Initial Pb(II) concentration (mg $L^{-1}$) | Percentage of Pb(II) removed (%) |
|---|---|---|
| *P. bifermentans* | 80 | 86.1 ± 4.61 |
| *P. bifermentans* | 250 | 55.6 ± 6.58 |
| *P. bifermentans* | 500 | 19.2 ± 32.5 |
| *K. pneumoniae* | 80 | 91.1 ± 0.302 |
| *K. pneumoniae* | 250 | 27.4± 12.4 |
| *K. pneumoniae* | 500 | 41.5 ± 6.59 |

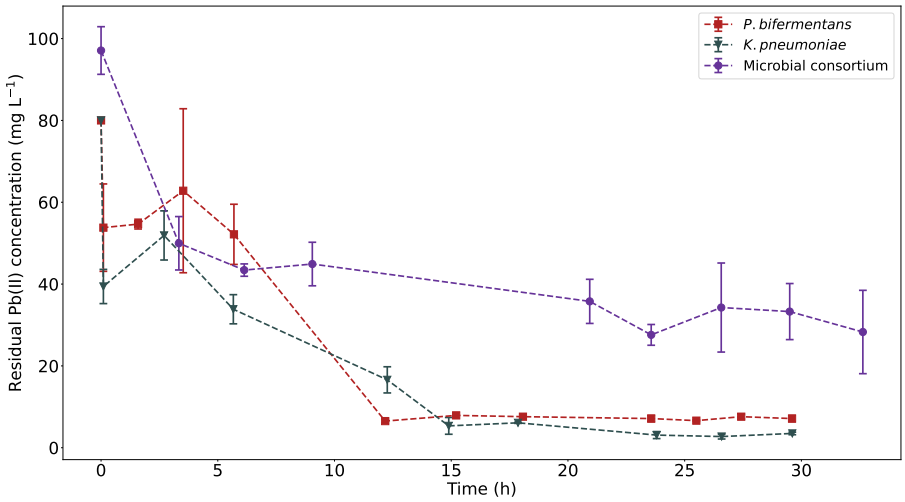


(a)

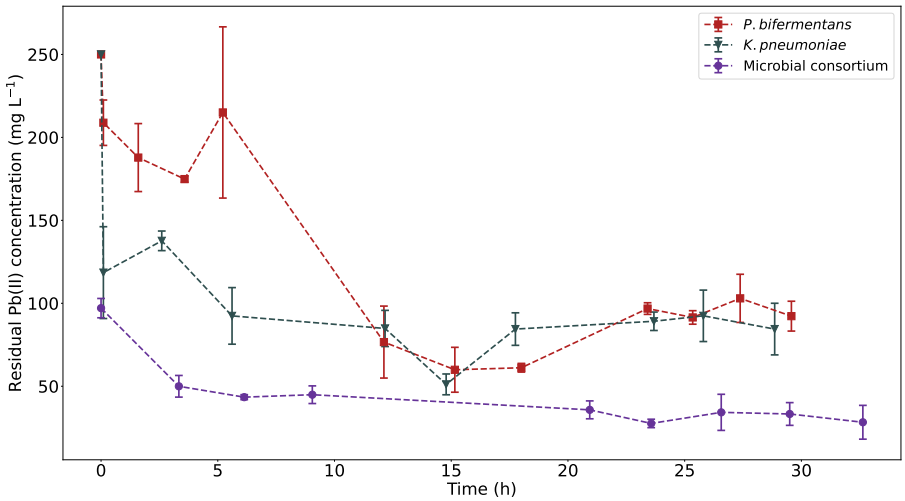


(b)

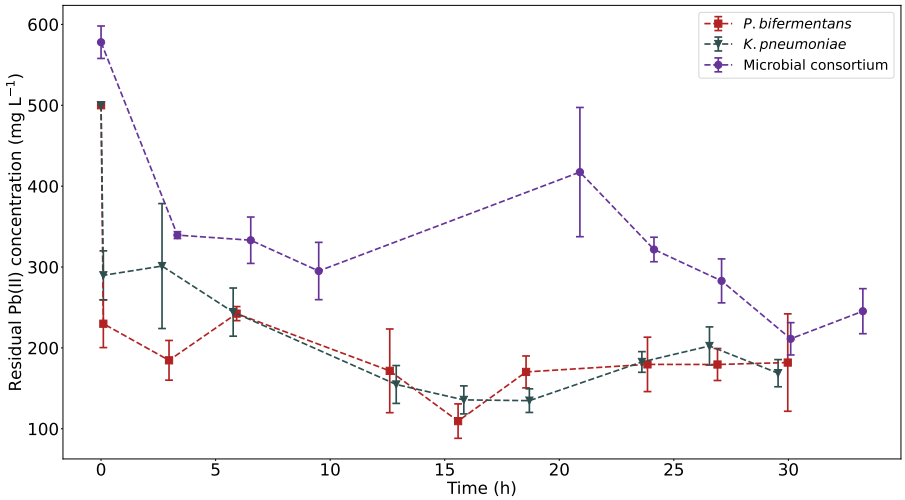


(c)

Figure 17: The residual Pb(II) concentration over time for experiments containing both *P. bifermentans* and *K. pneumoniae* with (a) 80 mg L$^{-1}$, (b) 250 mg L$^{-1}$ and (c) 500 mg L$^{-1}$ initial Pb(II) concentration, compared to previously published data on the microbial consortium from which the strains were isolated (Hörstmann, Brink & Chirwa, 2020).

### 5.2.4 Nitrate concentration

The nitrate concentration over the duration of the experiment is shown in Figure 18. The nitrate concentration does not tend to zero, indicating that nitrates are not a limiting substrate for microbial growth in the individual strains as mentioned in Chapter 4.2.5. Microbial growth is therefore possibly dependent on the nutrient rich medium used. A more in depth analysis using the first derivatives of the curves would need to be conducted to effectively conclude that microbial growth is not dependent on the nitrate concentration. The initial decrease in nitrates observed could be due to an anaerobic respiration mechanism employed by the bacteria, such as denitrification.

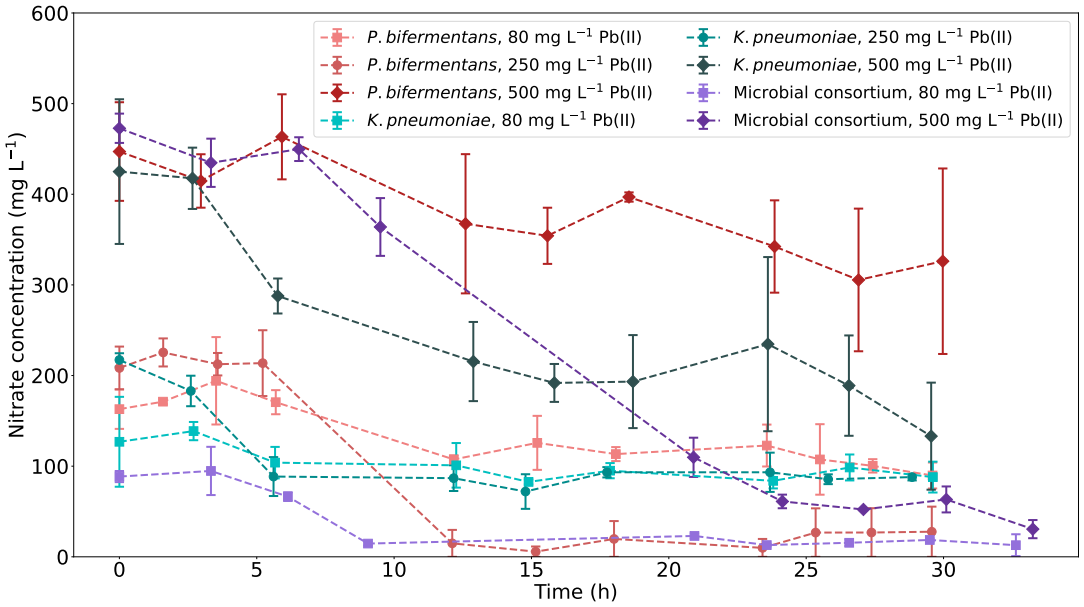


Figure 18: The nitrate concentration over time for both *P. bifermentans* and *K. pneumoniae* with varying initial Pb(II) concentrations, compared to previously published data on the microbial consortium from which the strains were isolated (Hörstmann, Brink & Chirwa, 2020).

The change in nitrates remains constant between the strains for an initial Pb(II) concentration of 80 mg $L^{-1}$, while *P. bifermentans* has a lower final value of nitrate concentration for 250 mg $L^{-1}$ initial Pb(II) concentration than *K. pneumoniae*. *K. pneumoniae* has a lower final nitrate concentration than *P. bifermentans* for experiments containing 500 mg $L^{-1}$. This could illustrate that the mechanisms of respiration used by the bacteria varies if the amount of Pb(II) in the reactor varies.

In a previous study on the effects of nitrate concentration on microbial precipitation of Pb(II) using the microbial consortium from which the strains used in this study were isolated, it was concluded that the lack of nitrates in the sample has no significant effect

on the bioprecipitation rate of Pb(II) in the sample. It is argued that the denitrification bacteria present in the consortium and therefore responsible for the drop in nitrate concentration observed for the microbial consortium in Figure 18, are not responsible for the bioprecipitation of lead (Cilliers *et al*, 2022).

### 5.2.5 Comparison between metabolic activity measurements, nitrate concentration and residual Pb(II) concentration

A comparison between metabolic activity, nitrate concentration and residual Pb(II) concentration for all experimental conditions is shown in Figure 19 and Figure 20 for *P. bifermentans* and *K. pneumoniae* respectively. The nitrate concentration decreases as an increase in metabolic activity is observed, possibly indicating a relationship between these entities. This decrease in nitrates is less considerable in samples containing 500 mg $L^{-1}$ initial Pb(II) concentration for both *P. bifermentans* and *K. pneumoniae*.

A decrease in Pb(II) concentration is observed for all experimental conditions when an increase in metabolic activity occurs. This is an indication that the precipitation mechanism is possibly dependent on the metabolic activity of the sample.

A drop in nitrate concentration occurs at approximately the same time as the drop in Pb(II) concentration, contributing to the idea that Pb(II) precipitation is metabolically dependent and that the microbial growth is dependent on the nitrate concentration.

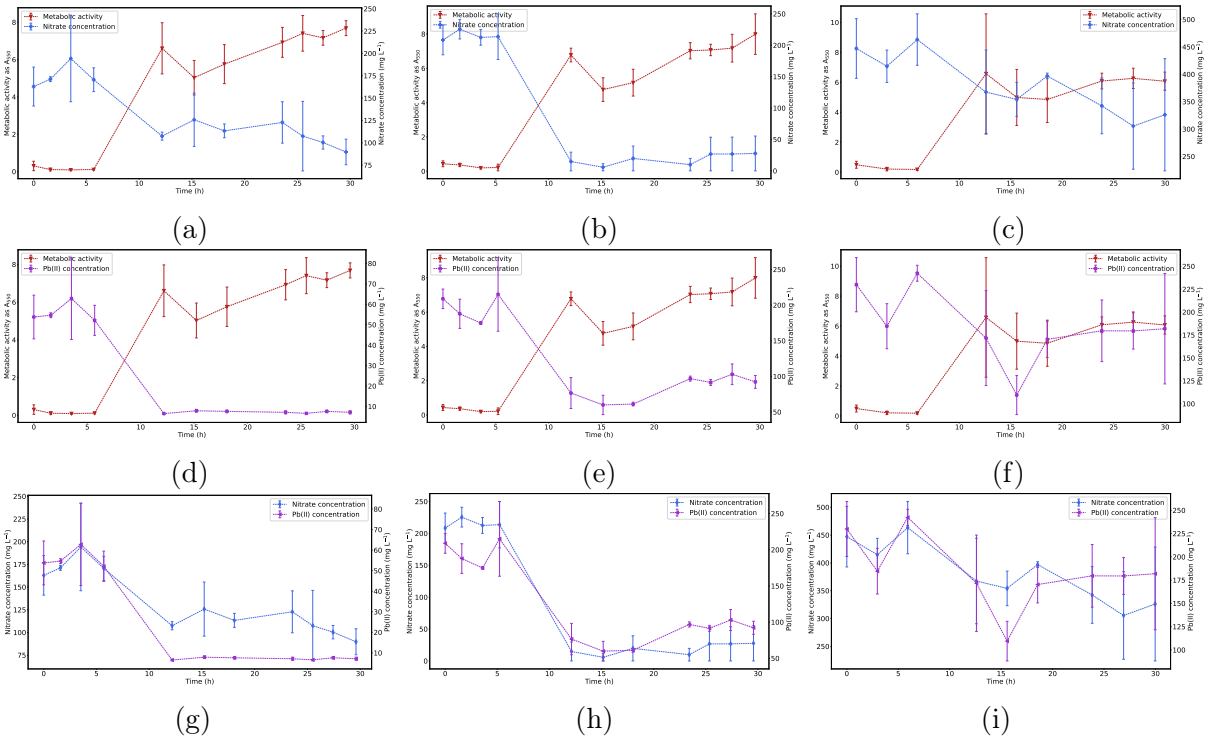


Figure 19: A comparison between metabolic activity as $A_{550}$ and the nitrate concentration for (a) 80 mg $L^{-1}$, (b) 250 mg $L^{-1}$, (c) 500 mg $L^{-1}$ initial Pb(II) concentration. A comparison between metabolic activity as $A_{550}$ and residual Pb(II) concentration for (d) 80 mg $L^{-1}$, (e) 250 mg $L^{-1}$, (f) 500 mg $L^{-1}$ initial Pb(II) concentration. A comparison between nitrate concentration and residual Pb(II) concentration of (g) 80 mg $L^{-1}$, (h) 250 mg $L^{-1}$ and (i) 500 mg $L^{-1}$ initial Pb(II) concentration for *P. bifermentans*.

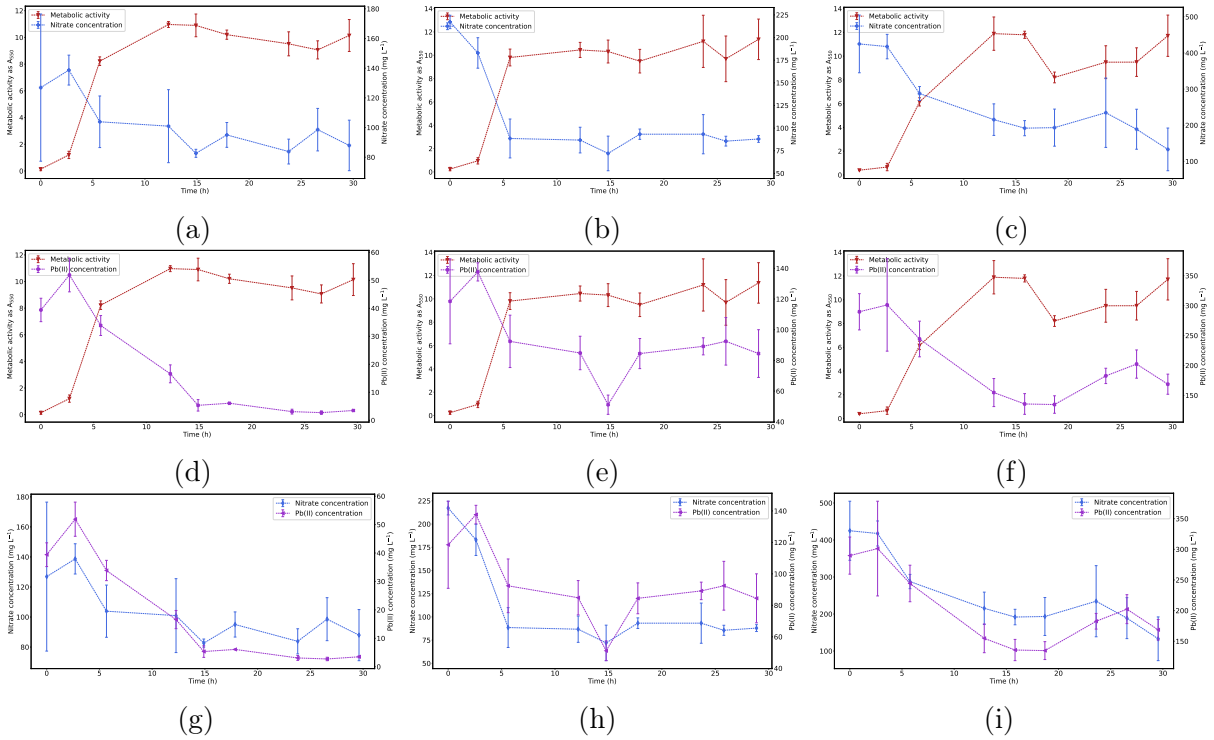


Figure 20: A comparison between metabolic activity as $A_{550}$ and the nitrate concentration for (a) 80 mg $L^{-1}$, (b) 250 mg $L^{-1}$, (c) 500 mg $L^{-1}$ initial Pb(II) concentration. A comparison between metabolic activity as $A_{550}$ and residual Pb(II) concentration for (d) 80 mg $L^{-1}$, (e) 250 mg $L^{-1}$, (f) 500 mg $L^{-1}$ initial Pb(II) concentration. A comparison between nitrate concentration and residual Pb(II) concentration of (g) 80 mg $L^{-1}$, (h) 250 mg $L^{-1}$ and (i) 500 mg $L^{-1}$ initial Pb(II) concentration for *K. pneumoniae*.

To further analyse the relationships between the measured data, a four part sigmoidal curve was fitted on the data using GraphPad Prism version 9.4.0. This was done to obtain the first derivatives of the curves describing metabolic activity, nitrate concentration and residual Pb(II) concentration to compare the derivatives of these curves to establish if a relationship exists between these entities. The fitted curves are shown in Figure 21, and the derivatives of the curves are compared in Figure 22 and Figure 23 for *P. bifermentans* and *K. pneumoniae* respectively. From these curves it is clear that no relationship exists between the nitrate concentration, lead concentration and metabolic activity.

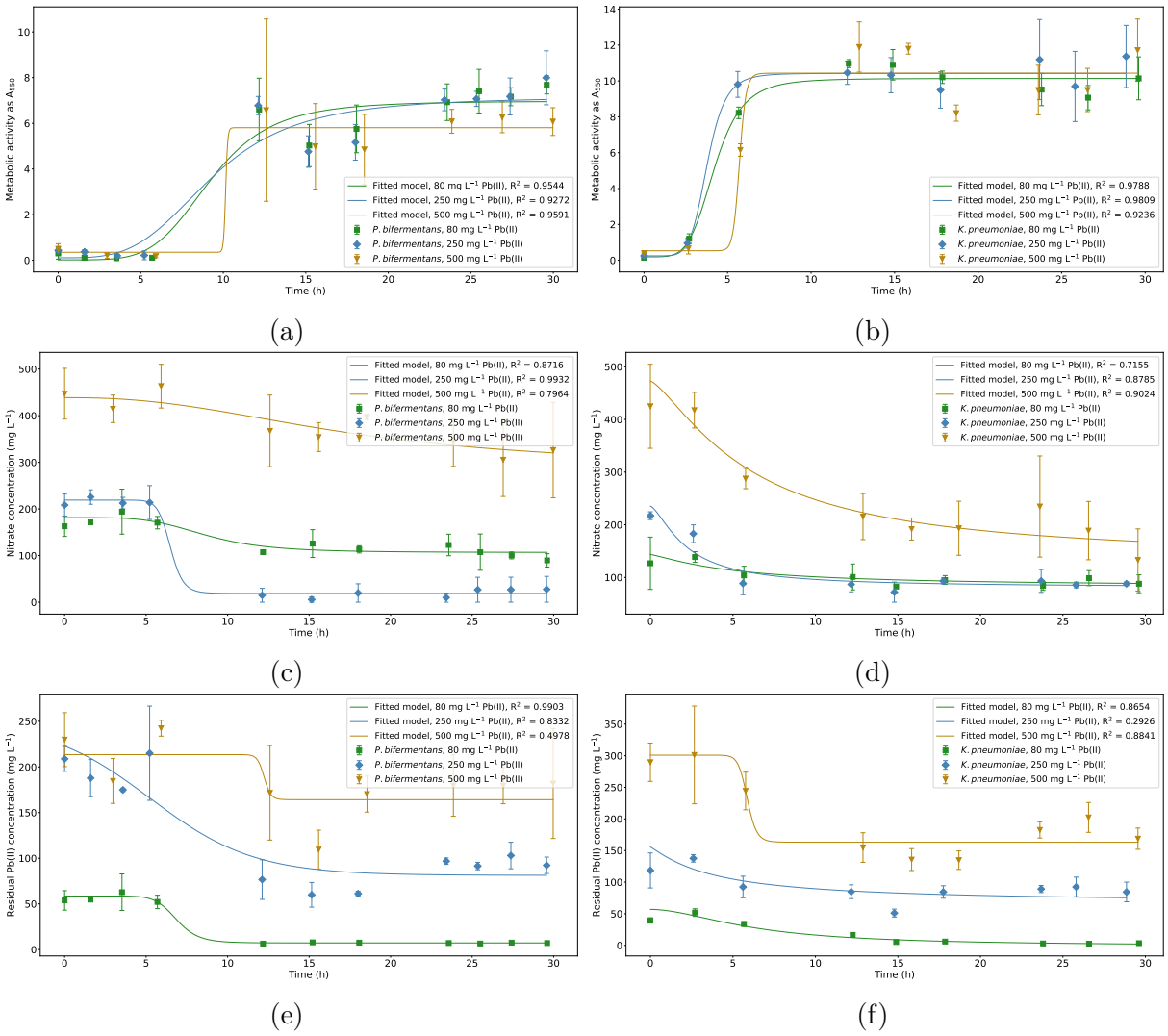


Figure 21: The fitted curves using a four part sigmoidal curve for metabolic activity of (a) *P. bifermentans* and (b) *K. pneumoniae*, nitrate concentration of (c) *P. bifermentans* and (d) *K. pneumoniae* and residual Pb(II) concentration of (e) *P. bifermentans* and (f) *K. pneumoniae*.

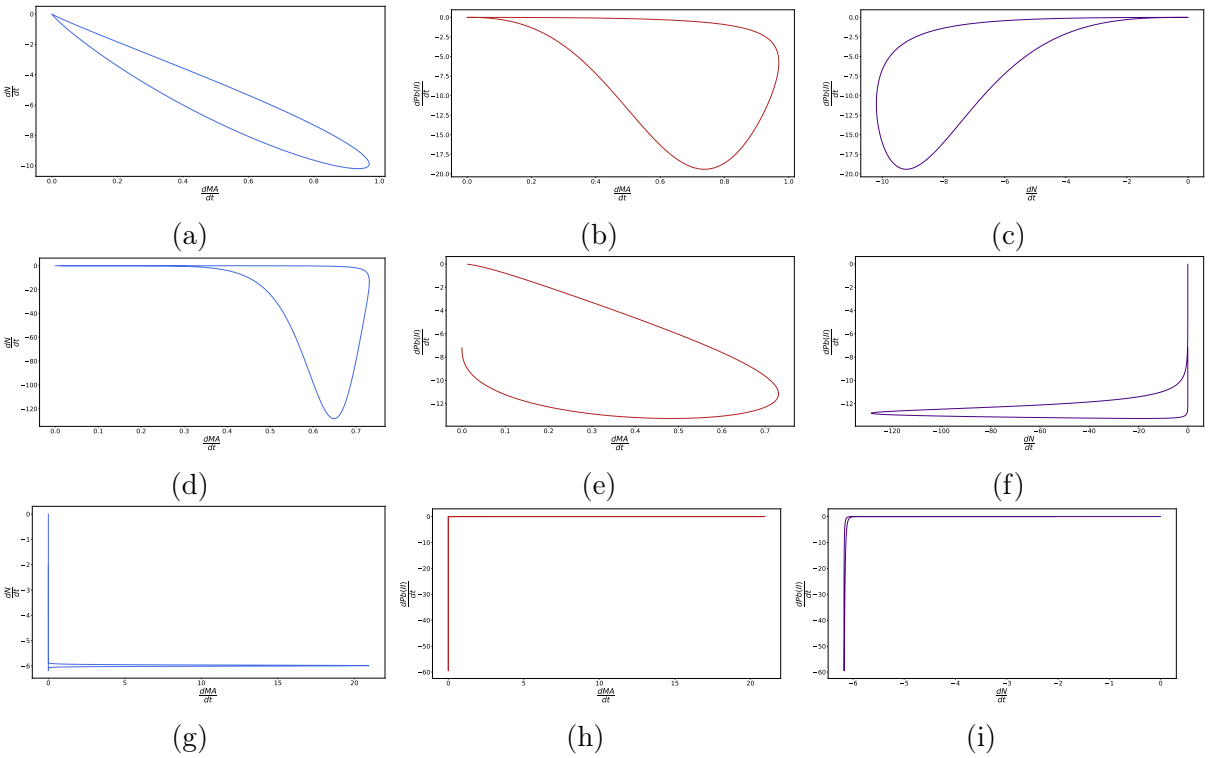

Figure 22: The comparison between the first derivative curves of *P. bifermentans* for (a) metabolic activity and nitrate concentration, (b) metabolic activity and residual Pb(II) concentration, (c) nitrate and lead concentration for 80 mg $L^{-1}$ initial Pb(II) concentration, (d) metabolic activity and nitrate concentration, (e) metabolic activity and residual Pb(II) concentration, (f) nitrate and residual Pb(II) concentration for 250 mg $L^{-1}$ initial Pb(II) concentration, (g) metabolic activity and nitrate concentration, (h) metabolic activity and residual Pb(II) concentration, (i) nitrate and residual Pb(II) concentration for 500 mg $L^{-1}$ initial Pb(II) concentration.

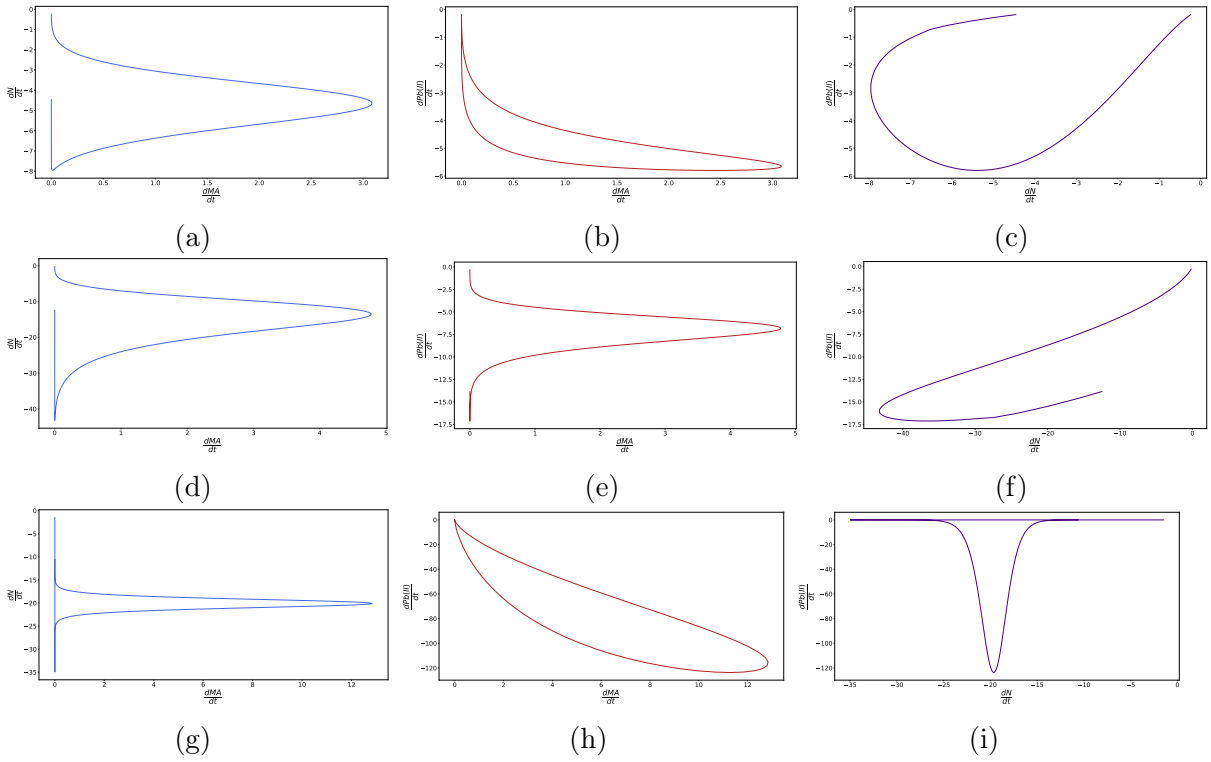

Figure 23: The comparison between the first derivative curves of *K. pneumoniae* for (a) metabolic activity and nitrate concentration, (b) metabolic activity and residual Pb(II) concentration, (c) nitrate and lead concentration for 80 mg $L^{-1}$ initial Pb(II) concentration, (d) metabolic activity and nitrate concentration, (e) metabolic activity and residual Pb(II) concentration, (f) nitrate and residual Pb(II) concentration for 250 mg $L^{-1}$ initial Pb(II) concentration, (g) metabolic activity and nitrate concentration, (h) metabolic activity and residual Pb(II) concentration, (i) nitrate and residual Pb(II) concentration for 500 mg $L^{-1}$ initial Pb(II) concentration.

The fitted data consisting of residual Pb(II) concentration, nitrate concentration and metabolic activity, was compared with the first derivative of these curves and is shown in Figure 24 and Figure 25 for *P. bifermentans* and *K. pneumoniae* respectively. From Figure 24a, Figure 24d and Figure 24g it can be seen that the rate of metabolic activity reaches a peak as the metabolic activity of the samples increases, this occurs for all initial Pb(II) concentrations investigated and is a possible indication that the initial Pb(II) concentration does not affect the metabolic growth mechanism of *P. bifermentans*. This is comparable with results recorded for *K. pneumoniae* where a similar trend is observed in Figure 25a, Figure 25d and Figure 25g.

From Figure 24b, Figure 24e and Figure 24h an initial increase in the rate of change in nitrate concentration is observed, possibly indicating a rapid initial uptake of nitrates in the microbe. This rate is more rapid in the results for *K. pneumoniae* in Figure 25b, Figure 25e and Figure 25h, with the peak observed at a high concentration of nitrates. This indicates that the microbe did not make much use of the nitrates for the majority

of the experiment. It is therefore possible that *P. bifermentans* is more dependent on nitrates than *K. pneumoniae*.

The rate of change in residual Pb(II) concentration for *P. bifermentans* as shown in Figure 24c, Figure 24f and Figure 24i indicates that the mechanism of bioprecipitation for *P. bifermentans* remains similar for varying initial Pb(II) concentrations. A maximum rate of change in Pb(II) concentration is observed for each initial Pb(II) concentration. This is not the case for *K. pneumoniae* in Figure 25c, Figure 25f and Figure 25i where the trend of the rate of change in Pb(II) concentration differs for each initial Pb(II) concentration. This is a possible indication that the mechanism of precipitation for *K. pneumoniae* is dependent on the initial Pb(II) concentration.

The points discussed above relate to the mechanisms of precipitation utilised by the bacteria. These observations coincide with recently published work by this research team on the mechanisms of precipitation where the effect of nitrates was investigated (Cilliers *et al*, 2022). The results of the study indicated that bacteria usage of nitrates occurred most prominently at lower Pb(II) concentrations and that the denitrifying bacteria present in the microbial consortium were most likely not responsible for Pb(II) removal. This conclusion was attributed to the fact that Pb(II) removal was not inhibited by a lack of nitrates in the sample. By using TEM and SEM, it was indicated that at lower concentrations of Pb(II), the Pb(II) in the sample was precipitated extracellularly while at higher concentrations of Pb(II) and intracellular precipitation mechanism occurred. The intracellular precipitation was concluded to be due to the production of metallothionein, a low molecular weight metal-bonding protein that is responsible for intracellular lead sequestration and the transportation, storage and detoxification of Pb(II). From an XRD analysis it was concluded that four compounds were present in the samples. These included: pyromorphite, lead sulphide, elemental lead and elemental sulphur. The authors stated that the presence of pyromorphite was due to the biotransformation of PbS to pyromorphite. A smaller amount of pyromorphite was detected in samples containing 80 mg $L^{-1}$ Pb(II), possibly indicating that denitrifying bacteria is present at lower Pb(II) concentrations and cause a higher amount of sulphur released via the enzyme nitrate reductase.

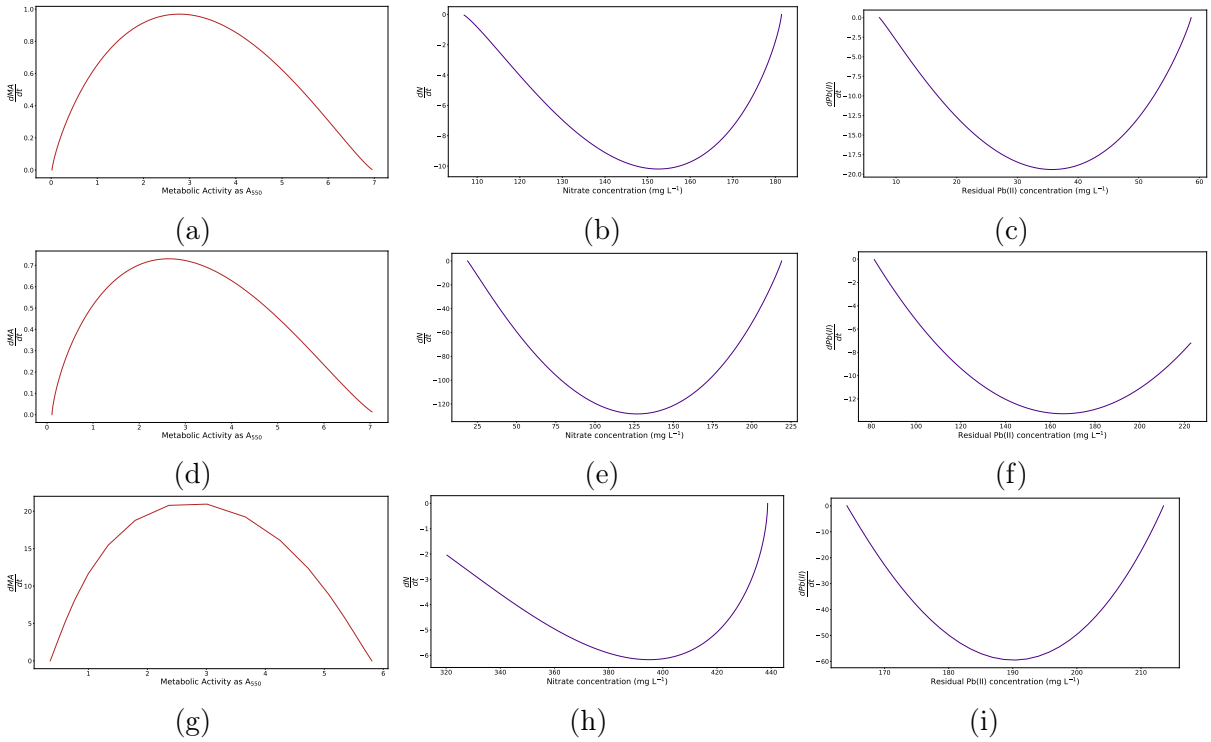


Figure 24: The comparison between the metabolic activity and the rate of change in metabolic activity for *P. bifermentans* with (a) 80 mg $L^{-1}$, (d) 250 mg $L^{-1}$ and (g) 500 mg $L^{-1}$ initial Pb(II) concentration. The comparison between the nitrate concentration and the rate of change in nitrate concentration for *P. bifermentans* with (b) 80 mg $L^{-1}$, (e) 250 mg $L^{-1}$ and (h) 500 mg $L^{-1}$ initial Pb(II) concentration. The comparison between the residual Pb(II) concentration and the rate of change in Pb(II) concentration for *P. bifermentans* with (c) 80 mg $L^{-1}$, (f) 250 mg $L^{-1}$ and (i) 500 mg $L^{-1}$ initial Pb(II) concentration

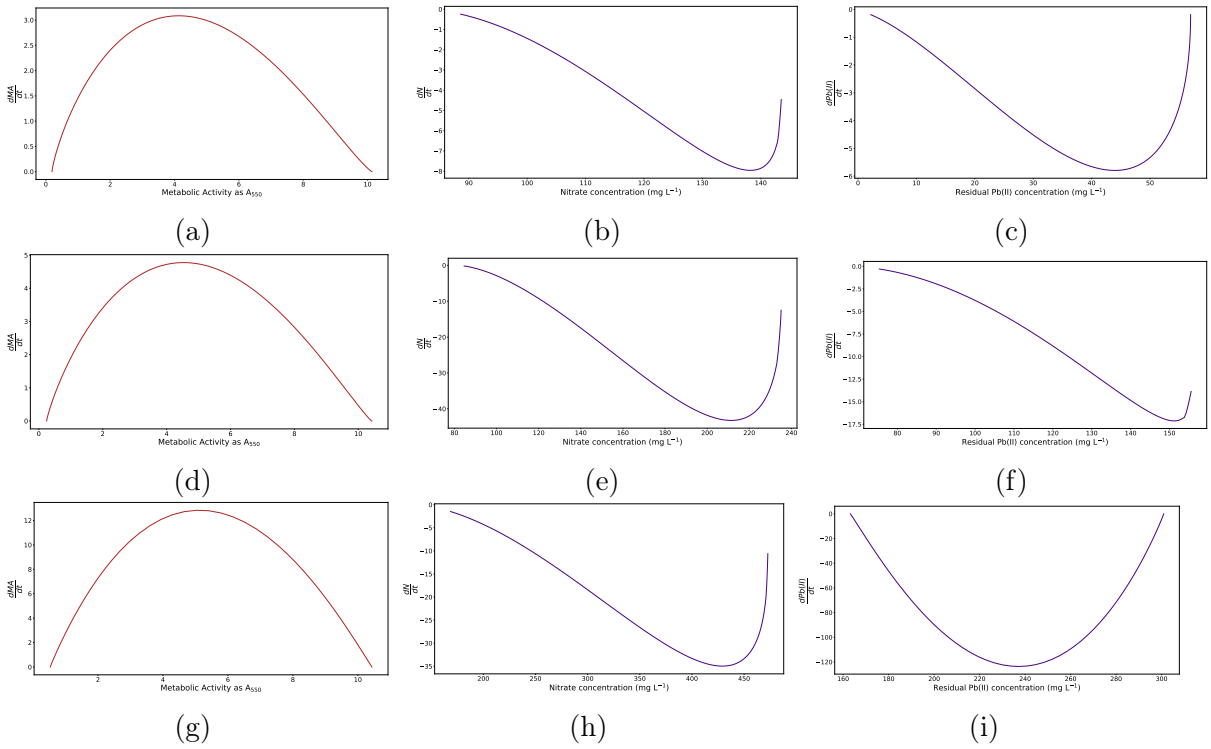


Figure 25: The comparison between the metabolic activity and the rate of change in metabolic activity for *K. pneumoniae* with (a) 80 mg $L^{-1}$, (d) 250 mg $L^{-1}$ and (g) 500 mg $L^{-1}$ initial Pb(II) concentration. The comparison between the nitrate concentration and the rate of change in nitrate concentration for *K. pneumoniae* with (b) 80 mg $L^{-1}$, (e) 250 mg $L^{-1}$ and (h) 500 mg $L^{-1}$ initial Pb(II) concentration. The comparison between the residual Pb(II) concentration and the rate of change in Pb(II) concentration for *K. pneumoniae* with (c) 80 mg $L^{-1}$, (f) 250 mg $L^{-1}$ and (i) 500 mg $L^{-1}$ initial Pb(II) concentration

### 5.2.6 Extracellular and Intracellular Pb(II) concentration

The percentage composition of the samples in terms of extracellular, intracellular and solution Pb(II) concentration is shown in Figure 26 for both strains at two initial Pb(II) concentrations. An obvious change in solution Pb(II) concentration is noted across the time intervals, with a decrease occurring. It is expected that this is due to the precipitation of Pb(II). The majority of the Pb(II) is initially found in the extracellular portion of the cells with this amount decreasing over time. This is indicative of an adsorption mechanism that occurs within the first 6 h of the experiment. This adsorption is attributed to a rapid detoxification mechanism and has been observed in previous research on the microbial consortium from which the strains were isolated, as discussed in Chapter 5.2.3. There is a decrease in Pb(II) removal with an increase in initial Pb(II) concentrations.

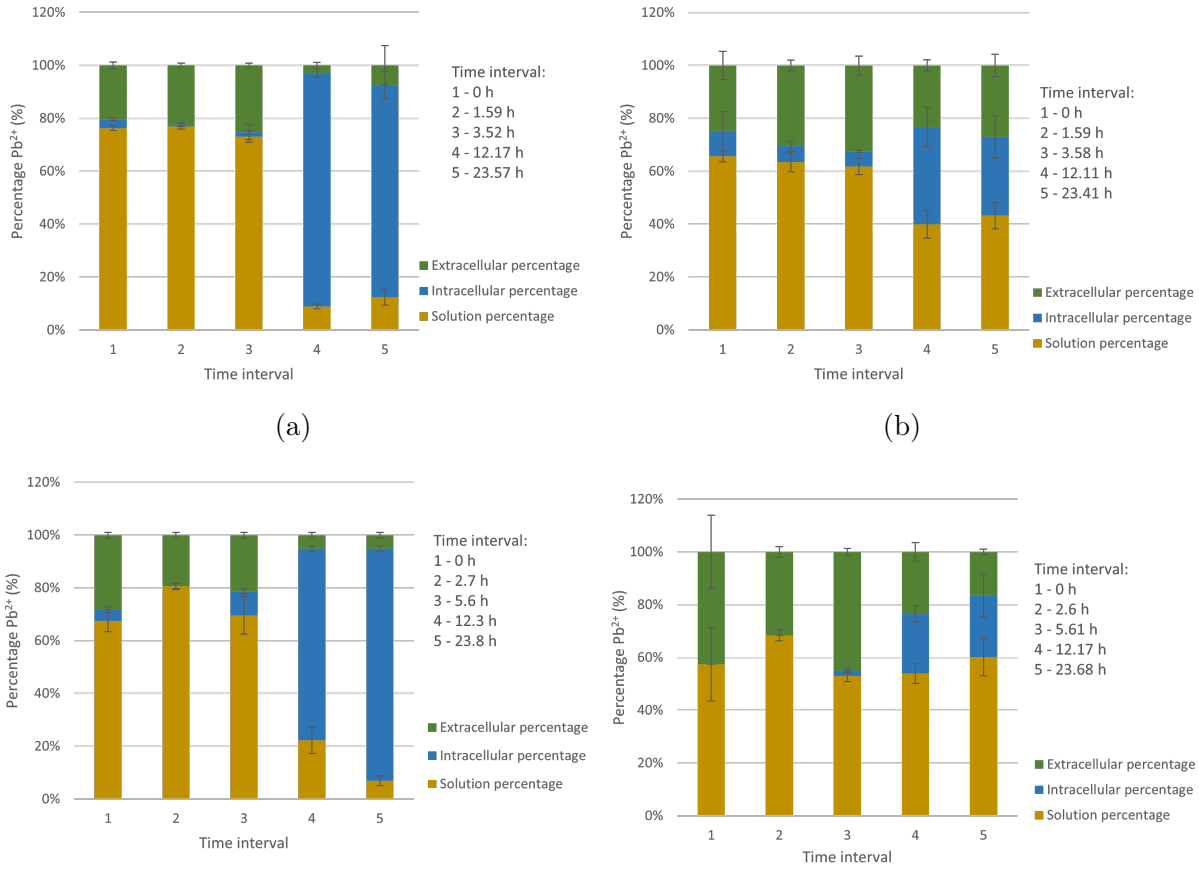


Figure 26: The percentage composition of the samples in terms of extracellular, intracellular and solution Pb(II) concentration for *P. bifermentans* at (a) 80 mg $L^{-1}$ and (b) 250 mg $L^{-1}$ initial concentration Pb(II) and *K. pneumoniae* at (c) 80 mg $L^{-1}$ and (d) 250 mg $L^{-1}$ initial concentration Pb(II).

### 5.2.7 Specific growth rate

The specific growth rate of the bacteria for each experimental condition was calculated using

$$\frac{dMA}{dt} = \mu \times MA \tag{6}$$

where $\frac{dMA}{dt}$ is the first derivative of the metabolic activity curve and $\mu$ is the specific growth rate in $d^{-1}$. The specific growth rate was calculated using the fitted metabolic activity curves in Figure 21 and the derivative of this curve. The specific growth rate calculation was done using GraphPad Prism version 9.4.0. The values of $\mu$ calculated over time for each experimental condition is shown in Figure 27.

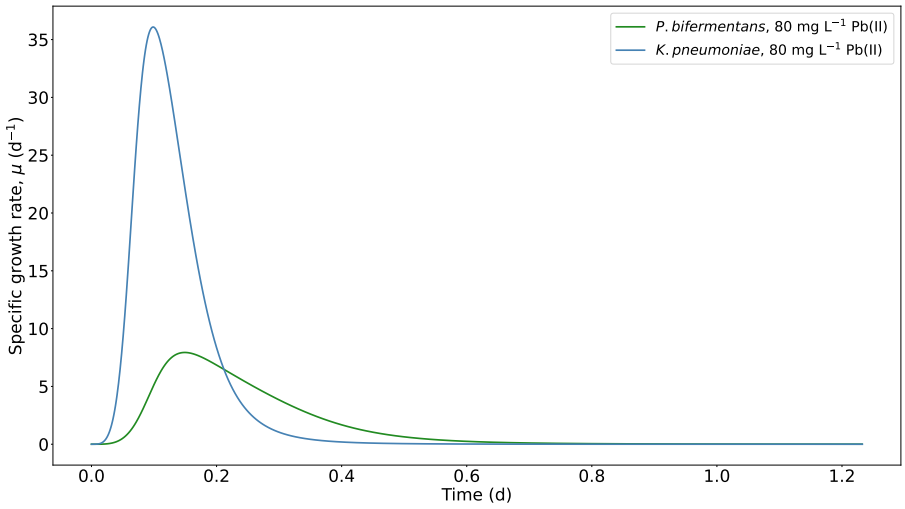


(a)

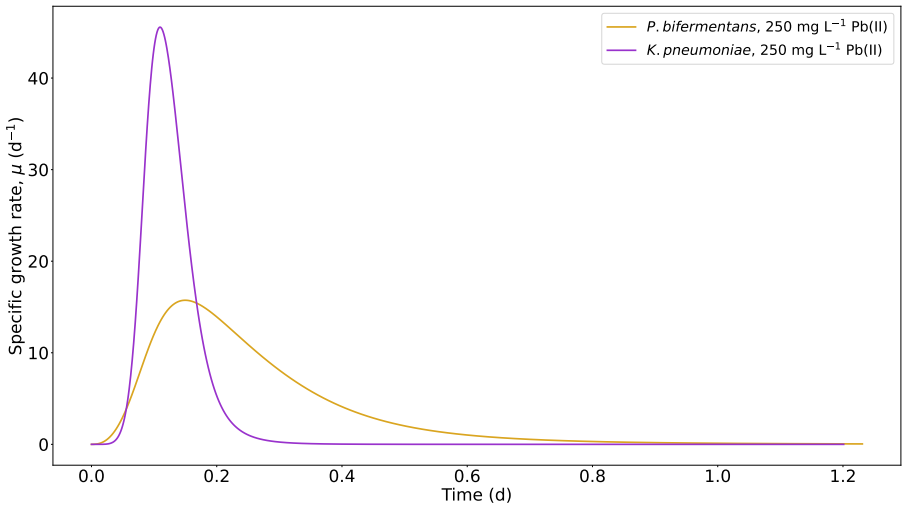


(b)

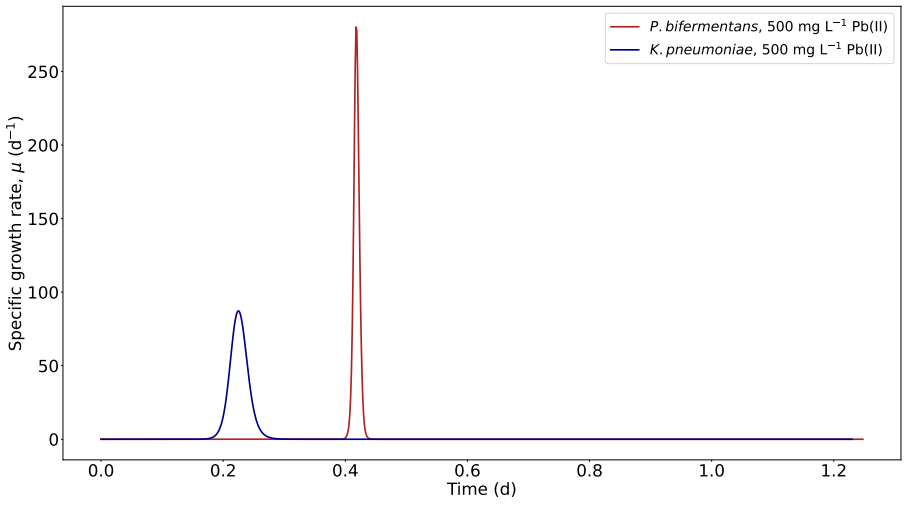


(c)

Figure 27: The specific growth rate, $\mu$, over time for *P. bifermentans* and *K. pneumoniae* with (a) 80 mg L$^{-1}$, (b) 250 mg L$^{-1}$ and (c) 500 mg L$^{-1}$ initial Pb(II) concentration.

The generation time of the bacteria was calculated using

$$t_g = \frac{\ln(2)}{\mu_{max}} \tag{7}$$

where $t_g$ is the generation time in d and $\mu_{max}$ is the maximum specific growth rate in $d^{-1}$. The values of $\mu_{max}$ and $t_g$ for each experimental condition are shown in Table 17.

Table 17: The value of the maximum specific growth rate ($\mu_{max}$) and the generation time ($t_g$) for all the experimental conditions observed for both strains.

| Strain | Initial Pb(II) concentration (mg $L^{-1}$) | $\mu_{max}$ ($d^{-1}$) | $t_g$ (d) |
|---|---|---|---|
| *P. bifermentans* | 80 | 7.94 | 0.0873 |
| | 250 | 15.2 | 0.0441 |
| | 500 | 280 | 0.00247 |
| *K. pneumoniae* | 80 | 36.1 | 0.0192 |
| | 250 | 45.6 | 0.0152 |
| | 500 | 87.2 | 0.00795 |

From this data is it observed that *K. pneumoniae* has a higher value of $\mu_{max}$ at initial Pb(II) concentrations of 80 and 250 mg $L^{-1}$ but *P. bifermentans* has the higher value of $\mu_{max}$ at 500 mg $L^{-1}$ initial Pb(II) concentration. This could indicate that *K. pneumoniae* is better suited to conditions imposed by lower Pb(II) concentrations but *P. bifermentans* is more metabolically active than *K. pneumoniae* at higher initial Pb(II) concentrations.

### 5.2.8 Precipitate identity

The XPS profiles used in the identification of the Pb-precipitate are shown in Figure 28. The peaks shown in the profiles were identified using the NIST X-ray Photoelectron Spectroscopy Database (National Institute of Standards and Technology, 2002), and the data was convoluted using OriginPro 2022 (OriginLab Corporation, Northampton, Massachusetts, USA).

The results for *P. bifermentans* indicate the precipitate present as PbS and $Pb^0$, these precipitates will contribute greatly to the dark colour observed in the samples. The presence of PbS is likely due to the liberation of $S^{2-}$ ions during the catabolism of

sulphur containing amino acids, such as cysteine and methionine (Brink, Hörstmann & Peens, 2020).

The precipitates present in samples containing *K. pneumoniae* were identified as PbO with either PbCl or $Pb_3(PO_4)_2$. The absence of PbS and $Pb^0$ for *K. pneumoniae* will contribute to the lighter, more brown colour observed in these samples. These results indicate that a different bioprecipitation mechanism is utilised by the strains.

A previous analysis done by Brink, Hörstmann & Peens (2020) on the microbial consortium indicated the presence of significant fractions of PbS in runs done anaerobically. This is an indication that *P. bifermentans* is active in the consortium at anaerobic conditions. The aerobic runs on the consortium contained a precipitate containing PbO and elemental Pb, which would indicate the possible absence of *P. bifermentans* in these runs.

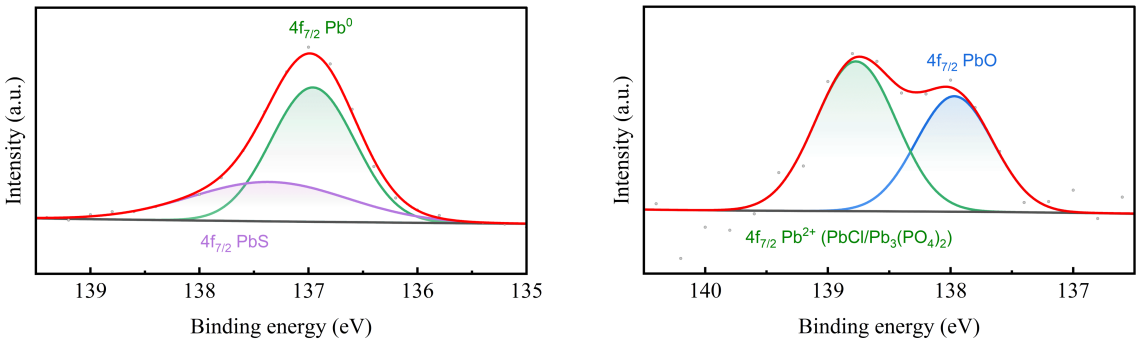


(a) (b)

Figure 28: The XPS profiles of the Pb-species for samples containing 80 mg $L^{-1}$ initial Pb(II) concentration with (a) *P. bifermentans* and (b) *K. pneumoniae*.

## 5.3 Conclusions

The visual changes observed in the experiments for both *P. bifermentans* and *K. pneumoniae* at varying initial Pb(II) concentrations indicated the presence of lead precipitate in under 12 h. The colour difference between the two precipitate products of the strains was once again noted as in Chapter 4. The microbial growth measurements in the form of metabolic activity indicated that *K. pneumoniae* has a higher metabolic activity than *P. bifermentans* and the consortium. This is a possible indication that *K. pneumoniae* is better suited than the other strains to the toxic lead environment. The values for metabolic activity reached by the consortium are lower than those of *K. pneumoniae*, and it is determined that *K. pneumoniae* is possibly inhibited by the consortium. The growth of *P. bifermentans* remains similar for all varying initial Pb(II) concentrations,

which could possibly indicate that the precipitation mechanism utilised by the strains is either not metabolically dependent or is independent on the initial Pb(II) concentration.

The residual Pb(II) concentration measurements indicated that *K. pneumoniae* is once more slightly more efficient at the bioprecipitation of Pb(II) with percentage removals of 86.1 ± 4.61 % and 91.1 ± 0.302 % recorded in samples containing 80 mg $L^{-1}$ initial Pb(II) concentration after 30 h for *P. bifermentans* and *K. pneumoniae* respectively.

The nitrate concentration was not depleted in experiments containing *K. pneumoniae* and *P. bifermentans* and it is determined that the microbial growth is therefore not limited to the nitrate concentration but rather to the concentration of the constituents found in the nutrient broth. A comparison between metabolic activity, nitrate concentration and residual Pb(II) concentration using the first derivative of a fitted curve of this data indicated that the rate of change in the entities do not have a direct relationship. It is therefore concluded that the microbial growth is not dependent on the nitrate concentration and that precipitation is not dependent on the microbial growth or the nitrate concentration.

The determination of the extracellular and intracellular Pb(II) concentration led to deductions that a rapid detoxification mechanism such as biosorption, is present in both *P. bifermentans* and *K. pneumoniae* within the first 6 h of the experiment.

The specific growth calculated for the experiments showed that *K. pneumoniae* has a faster exponential phase at 80 and 250 mg $L^{-1}$ initial Pb(II) concentrations but *P. bifermentans* depicts a faster exponential growth at 500 mg $L^{-1}$ initial Pb(II) concentration.

The precipitate identities determined with the use of XPS concluded that samples containing *P. bifermentans* had the precipitate present as PbS and $Pb^0$, while samples containing *K. pneumoniae* has the precipitate present as PbO and either PbCl or $Pb_3(PO_4)_2$. This explains the colour difference observed in the samples as PbS and $Pb^0$ would contribute to the dark colour observed in samples containing *P. bifermentans*.

The short-term study greatly improved the understanding of the mechanisms of Pb(II) removal from solution employed by both *P. bifermentans* and *K. pneumoniae*. This research can be used to further the application of the system to an industrial scale. Further research can be done on the application of the system, such as the utilisation of a continuous reactor system.

# 6 Bioprecipitation of lead using *P. bifermentans* and *K. pneumoniae*: an investigation into exponential growth and the influence of Pb(II)

This experiment was conducted in collaboration with the Carl and Emily Fuchs Institute of Microelectronics as part of a study on non-destructive impedance monitoring of bacterial metabolic activity. This research is a step towards inline monitoring of bacterial activity in projects associated with the biorecovery of Pb(II). This research has been published in *Sensors* under the title "Non-Destructive Impedance Monitoring of Bacterial Metabolic Activity Towards Continuous Lead Biorecovery" (Andrews *et al*, 2022).

The work described in this chapter focuses on the exponential growth of the bacteria and the influence of Pb(II) on growth.

## 6.1 Experimental

The experiment was structured to do measurements of metabolic growth over the exponential phase and the stationary phase. From previous experiments it was observed that the exponential phase of *K. pneumoniae* occurs between 0 and 5 h and the exponential phase of *P. bifermentans* occurs only after 6 h. The stationary phase for both strains is observed at around 24 h. Four samples were taken hourly during the stationary phase and three samples were taken hourly during the stationary phase.

The reactors were set up as anaerobic reactors using the method stipulated in Chapter 3.2.3. The measurement for metabolic growth was done as colony forming units (CFU). The samples were diluted in sterile distilled water and plated using the spread plate method described in Chapter 3.2.10. The plates were incubated in anaerobic conditions for 96 h and the number of colony forming units was determined per plate.

Colony forming units were used as the method of growth due to the difficulty of conducting metabolic activity measurements hourly. A correlation was obtained between CFU, metabolic activity and $OD_{600}$ to calculate predicted values of metabolic activity and $OD_{600}$. This was done by setting up an experiment in triplicate with reactors containing 80 mg $L^{-1}$ initial Pb(II) concentration for both strains. Three measurements were taken for metabolic activity, $OD_{600}$ and CFU using the methods described in Chapter 3.2. A linear regression study was then conducted to obtain the correlations between the data sets. The residual Pb(II) measurements were obtained using the method described in Chapter 3.2.7.

## 6.2 Results and discussions

### 6.2.1 Visual changes

The visual changes observed during the experiments involving both *P. bifermentans* and *K. pneumoniae* are shown in Figure 29. The formation of the dark precipitate is observed in all experiments. The colour difference between the precipitates of the strains is clear at the sample taken at 6 h after inoculation where *P. bifermentans* is darker than *K. pneumoniae*. This relates to the difference in precipitate identity as discussed in Chapter 5.

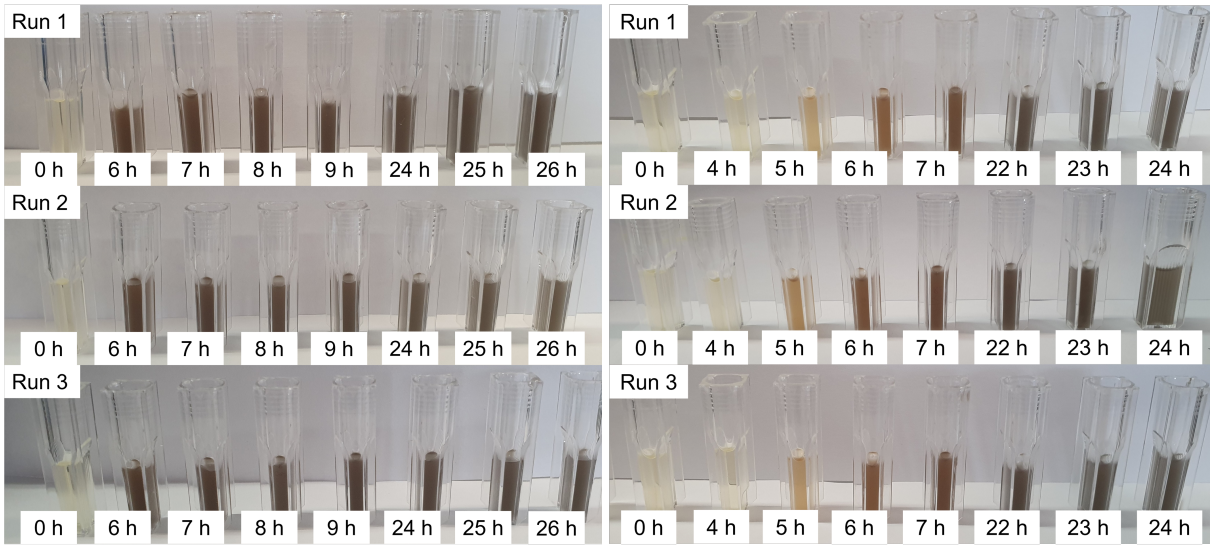


(a) (b)

Figure 29: The visual results of the experiment involving (a) *P. bifermentans* and (b) *K. pneumoniae* with 80 mg $L^{-1}$ initial concentration Pb(II).

### 6.2.2 Microbial growth measurements

The microbial growth measurements are shown in Figure 30 as colony forming units and from this point onwards the value of growth reported as log(CFU $ml^{-1}$) is referred to as the "CFU count", unless otherwise stated. From these results it is observed that both strains perform better in the presence of Pb(II), with *K. pneumoniae* reaching a similar maximum value of CFU count as *P. bifermentans*.

The similarities in the growth trends for *K. pneumoniae* with and without added Pb(II) could signify that the Pb(II) in solution markedly increases the growth of *K. pneumoniae*, likely due to the availability of Pb(II) as anaerobic respiration co-substrate and therefore

resulting in increased ATP production as concluded by Hörstmann, Chirwa, *et al* (2021) on work done on the microbial consortium from which the strains were isolated.

In contrast, *P. bifermentans* shows an initial increase in CFU count up to a maximum at approximately 9 h followed by a decrease to the end of the experiment. This is an indication that *P. bifermentans* experiences a substrate depletion at around 9 h as opposed to sufficient substrate supply for *K. pneumoniae*.

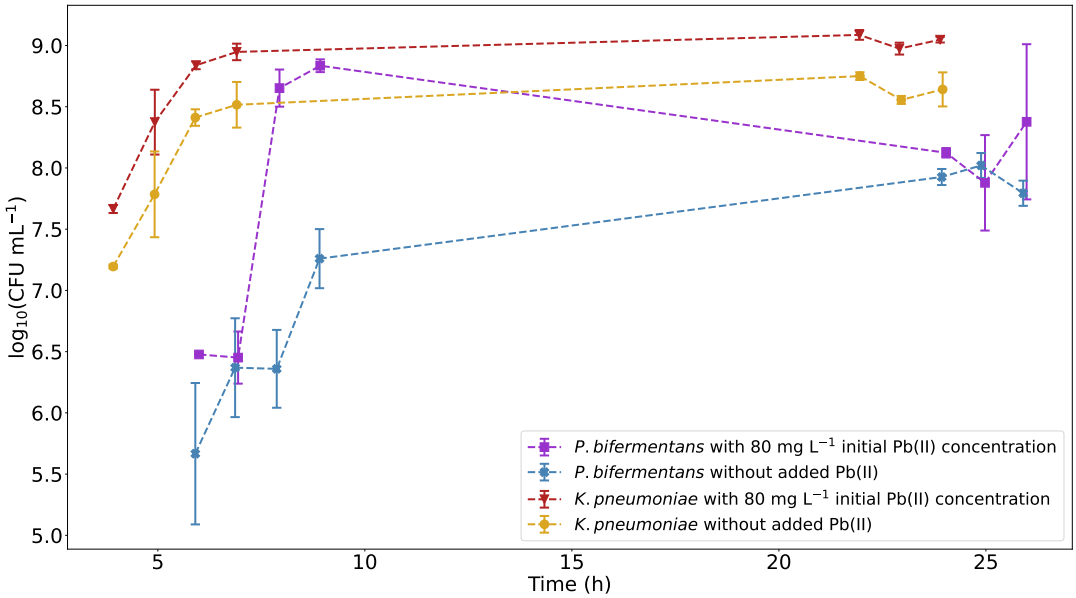


Figure 30: Microbial growth of *P. bifermentans* and *K. pneumoniae* measured as CFU count for experiments containing no added Pb(II) and experiments containing 80 mg $L^{-1}$ initial concentration Pb(II).

### 6.2.3 Residual Pb(II) concentration

The residual Pb(II) measurements for both strains is shown in Figure 31. Initial measurements as shown in Chapter 5, indicated that precipitation occurs sooner in *K. pneumoniae* than in *P. bifermentans*, which is why the experiments were started at a later stage for *P. bifermentans*. From the residual Pb(II) data it is evident that for this experiment the opposite was observed, with precipitation occurring in reactors containing *P. bifermentans* in under 6 h with a faster removal rate than *K. pneumoniae*.

The Pb(II) concentrations for *P. bifermentans* reach a minimum after 9 h which corresponds to the maximum value recorded for CFU count. The Pb(II) removal for *K. pneumoniae* continues for the duration of the experiment which correlates with the continued increase in CFU count observed in Figure 30. Both strains reach a similar final value for Pb(II) concentration.

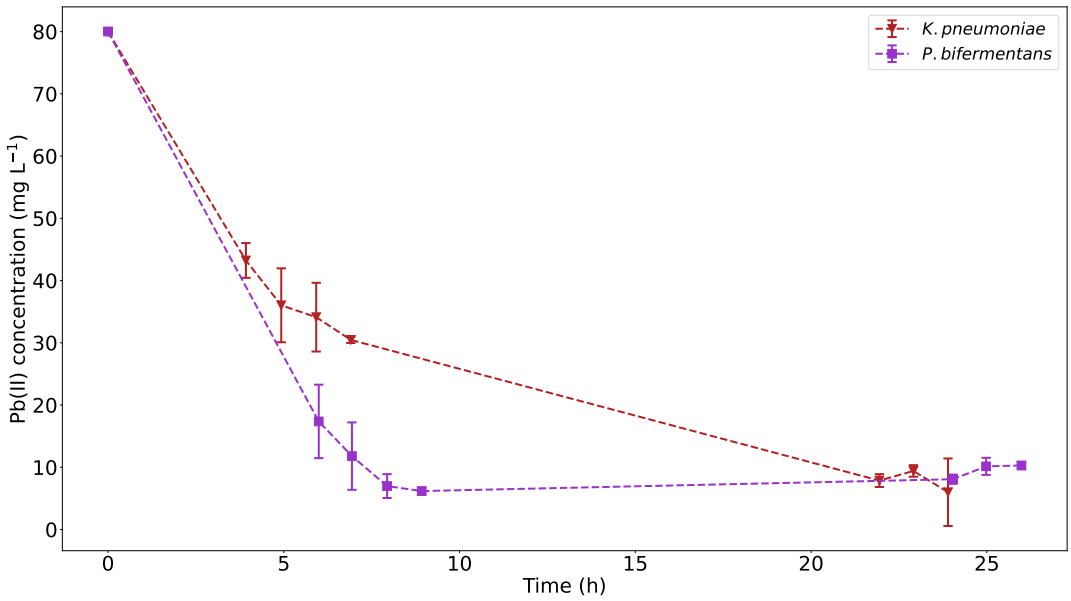


Figure 31: Residual Pb(II) concentration for experiments containing *P. bifermentans* and *K. pneumoniae* with 80 mg L$^{-1}$ initial concentration Pb(II).

### 6.2.4 Correlation between CFU count, $OD_{600}$ and metabolic activity

Due to the nature of the experiment, it would be difficult to measure the metabolic activity of the reactors as done in previous experiments since samples were taken every hour and metabolic activity measurements take at least two hours to complete. An experiment was therefore conducted to determine if a correlation exists between metabolic activity, $OD_{600}$ and CFU count. It is not advisable to use $OD_{600}$ for growth measurements in samples containing Pb(II) as the dark colour caused by the precipitate interferes with the readings.

The relationship between metabolic activity and CFU count for both *K. pneumoniae* and *P. bifermentans* with 80 mg L$^{-1}$ initial Pb(II) concentration is shown in Figure 32. Adequate correlations are obtained for both cases, with the correlation coefficient for *K. pneumoniae* equal to 0.9992 and the correlation coefficient for *P. bifermentans* equal to 0.8876.

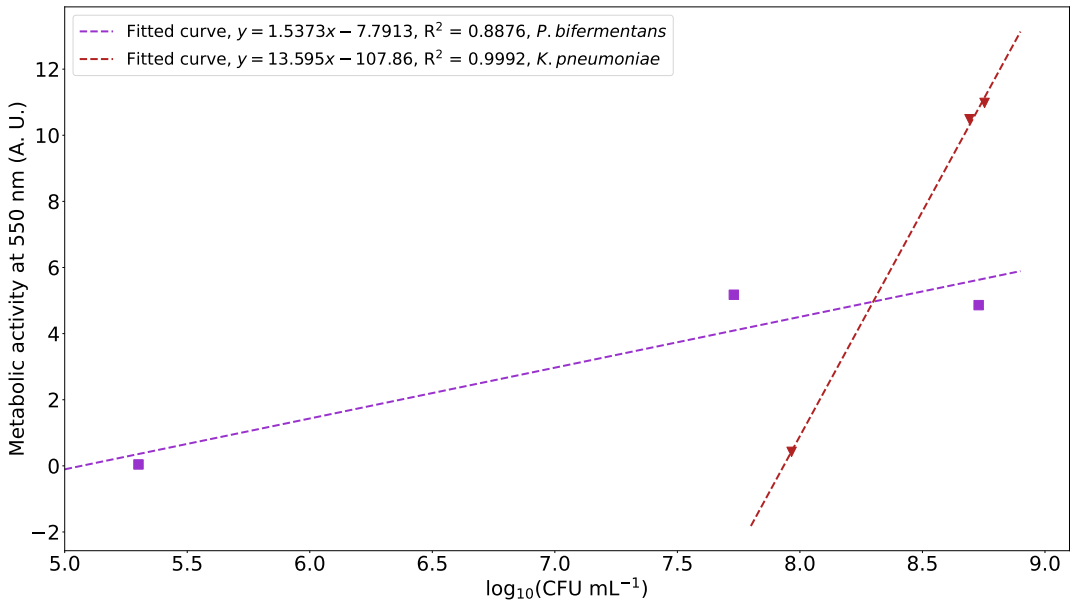


Figure 32: The relationship between metabolic activity and CFU count for *P. bifermentans* and *K. pneumoniae* with 80 mg L$^{-1}$ initial concentration Pb(II).

The relationship between metabolic activity, CFU count and $OD_{600}$ for *P. bifermentans* is shown in Figure 33. Adequate correlations are obtained in both cases with a correlation coefficient of 0.9699 for the relationship between CFU count and metabolic activity and a correlation coefficient of 0.7358 for the relationship between CFU count and $OD_{600}$.

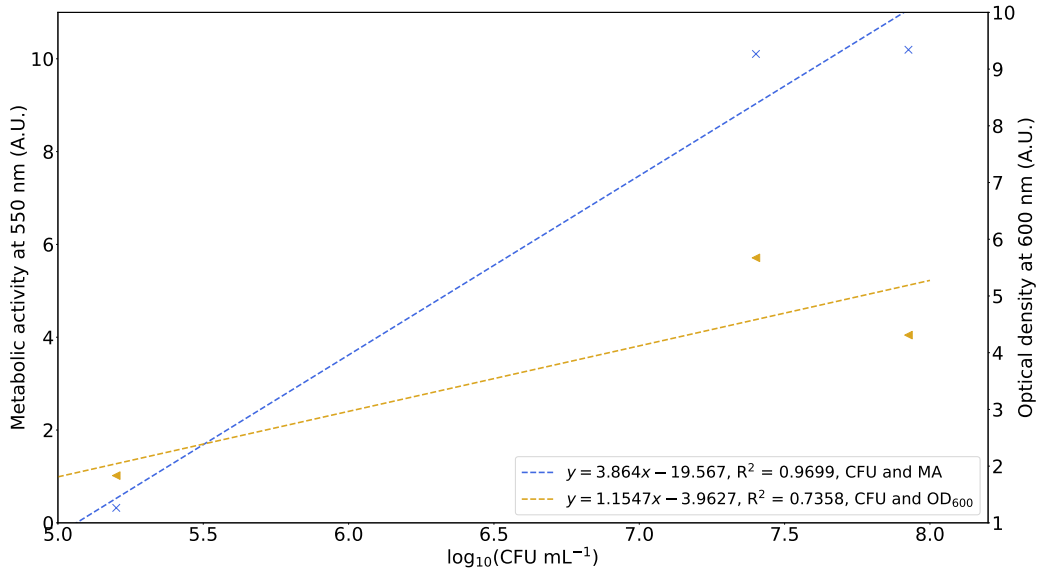


Figure 33: The relationship between metabolic activity and CFU count as well as $OD_{600}$ and CFU count for *P. bifermentans* with no added Pb(II).

The relationship between metabolic activity, CFU count and $OD_{600}$ for *K. pneumoniae* with no added Pb(II) is shown in Figure 34. A poor correlation is obtained for the

relationship between CFU count and metabolic activity with a correlation coefficient of 0.3688 and since a correlation coefficient of 0.9033 is calculated for the relationship between CFU count and $OD_{600}$, it is recommended that this relationship be used.

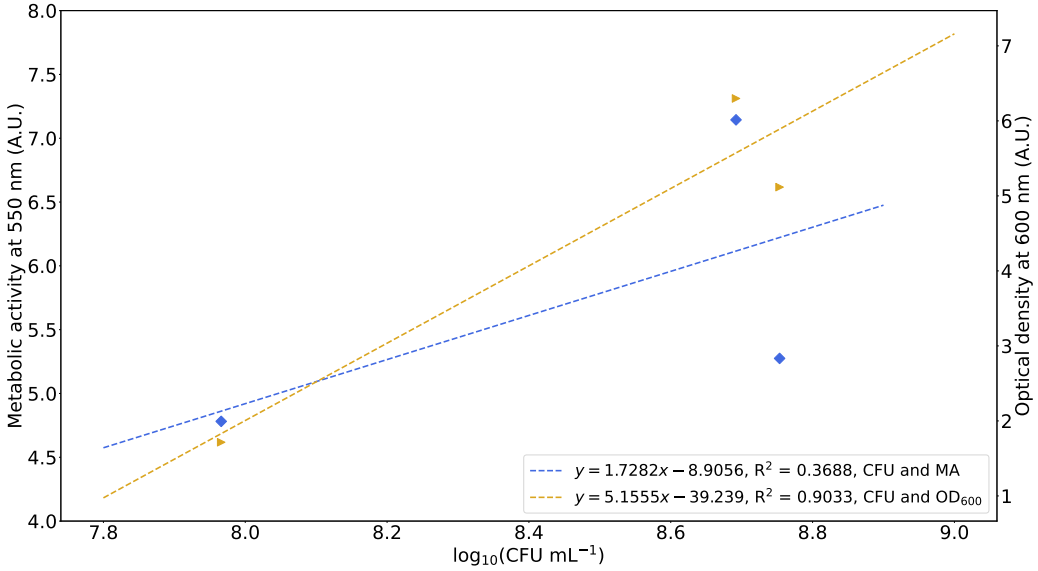


Figure 34: The relationship between metabolic activity and CFU count as well as $OD_{600}$ and CFU count for *K. pneumoniae* with no added Pb(II).

The linear regression equations for each strain with and without added Pb(II) providing a relationship between the growth measurements CFU count, $OD_{600}$ and metabolic activity can be seen in Table 18.

Table 18: Linear regression equations for a correlation between CFU, MA and $OD_{600}$

| Strain | Parameters | Equation | Correlation coefficient, $R^2$ |
|---|---|---|---|
| *P. bifermentans* with 80 mg $L^{-1}$ initial Pb(II) concentration | CFU and MA | $y = 1.5373x - 7.7913$ | 0.8876 |
| *P. bifermentans* without Pb(II) | CFU and MA | $y = 3.8640x - 19.567$ | 0.9699 |
| *P. bifermentans* without Pb(II) | CFU and $OD_{600}$ | $y = 1.1547x - 3.9627$ | 0.7358 |
| *K. pneumoniae* with 80 mg $L^{-1}$ initial Pb(II) concentration | CFU and MA | $y = 13.595x - 107.86$ | 0.9992 |
| *K. pneumoniae* without Pb(II) | CFU and MA | $y = 1.7282x - 8.9056$ | 0.3688 |
| *K. pneumoniae* without Pb(II) | CFU and $OD_{600}$ | $y = 5.1555x - 39.293$ | 0.9003 |

### 6.2.5 Predicted values for metabolic activity and $OD_{600}$

The values for metabolic activity and $OD_{600}$ calculated from the obtained correlation equations for samples with 80 mg $L^{-1}$ initial concentration Pb(II) and without added Pb(II) are shown in Figure 35 and Figure 36 respectively. It is observed that the data for metabolic activity and $OD_{600}$ follow the same trends as observed for CFU count as expected due to the high correlation values obtained. This observation is not true for the metabolic activity for *K. pneumoniae* because of the poor correlation obtained. These values are easier to compare with previous research and create a wider range of data available for future studies.

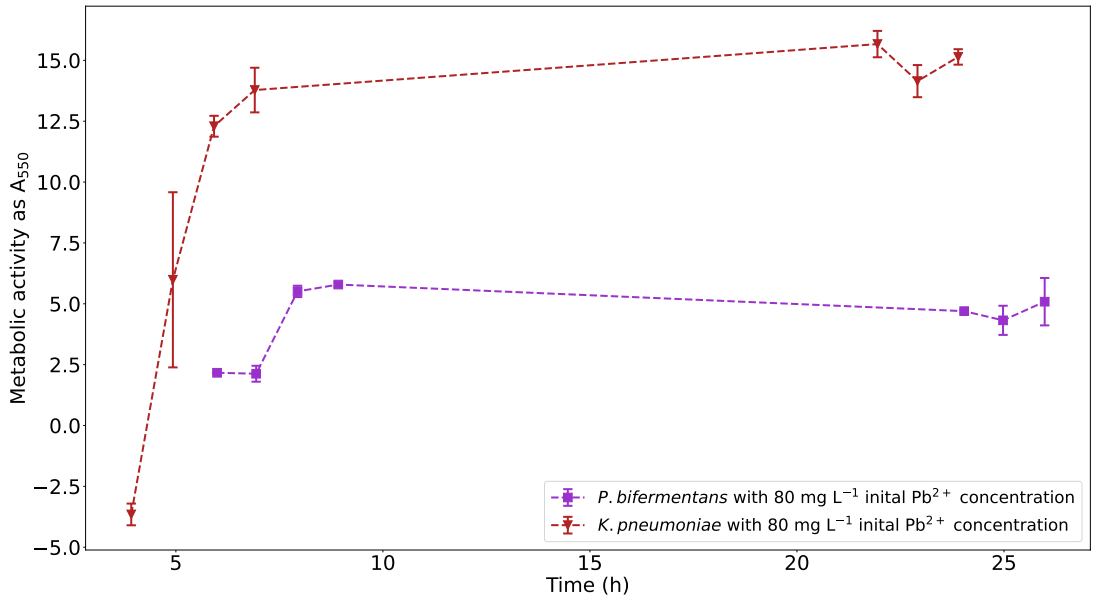


Figure 35: The predicted values of metabolic activity for *P. bifermentans* and *K. pneumoniae* with 80 mg $L^{-1}$ initial concentration Pb(II).

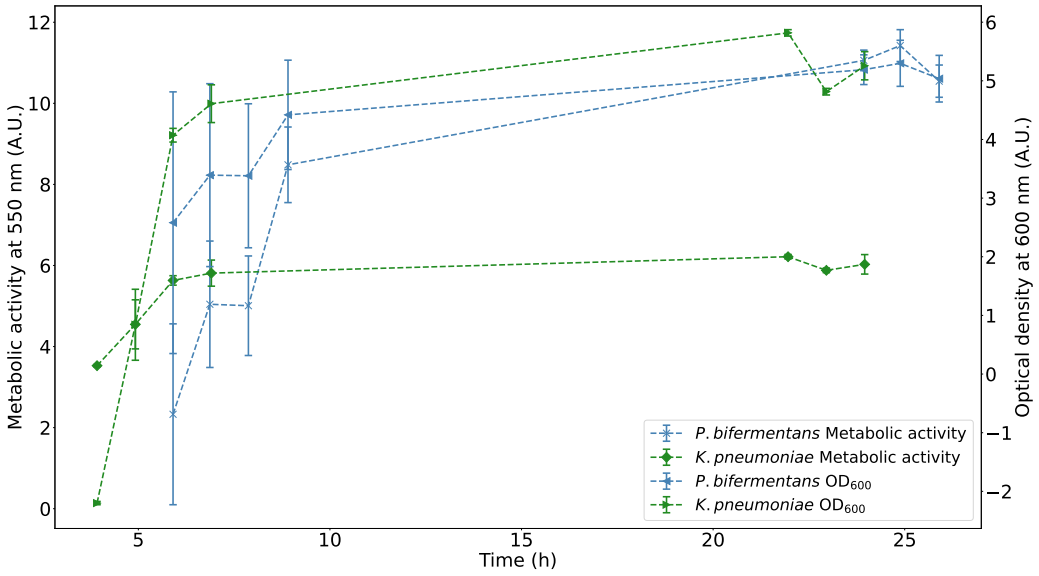


Figure 36: The predicted values for metabolic activity and $OD_{600}$ for *P. bifermentans* and *K. pneumoniae* with no added Pb(II).

### 6.2.6 Specific growth rate

The specific growth rate was calculated using a logistic fit on GraphPad Prism version 9.4.0. The rate constant determined by the software was considered to be equivalent to the maximum specific growth rate, $\mu_{max}$. The fitted curves are shown in Figure 37 along with the 95 % confidence interval calculated by the software. The maximum specific growth rate, $\mu_{max}$, with the confidence interval and the correlation coefficient of the fit are shown in Table 19.

Table 19: The maximum specific growth rate, $\mu_{max}$, and the confidence interval and correlation coefficient of the fit for each experimental condition.

| Strain | Initial Pb(II) concentration (mg $L^{-1}$) | $\mu_{max}$ ($d^{-1}$) | Confidence interval | $R^2$ |
|---|---|---|---|---|
| *P. bifermentans* | 80 | 2.53 | 1.60 – 4.06 | 0.977 |
| *P. bifermentans* | No added Pb(II) | 0.907 | 0.701 – 1.19 | 0.992 |
| *K. pneumoniae* | 80 | 0.388 | 0.144 – 0.703 | 0.962 |
| *K. pneumoniae* | No added Pb(II) | 0.723 | 0.503 – 1.27 | 0.974 |

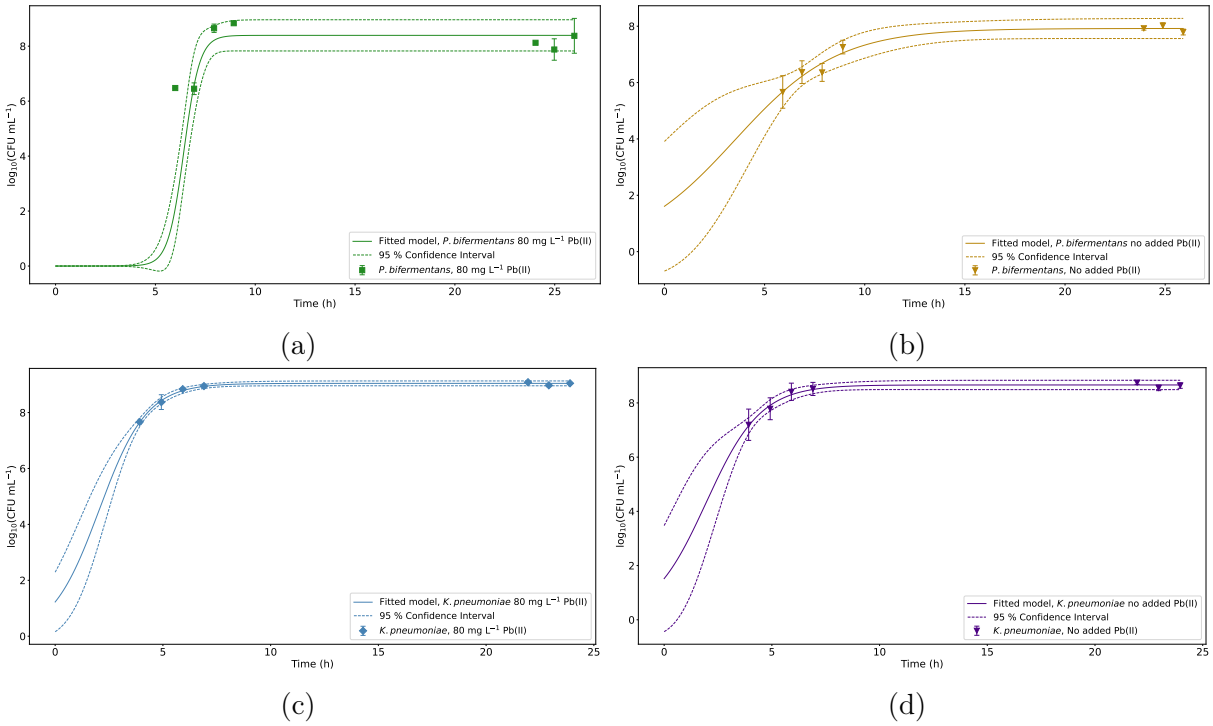


Figure 37: The fitted curves of the CFU count for experiments containing *P. bifermentans* with (a) 80 mg $L^{-1}$ Pb(II) and (b) no added Pb(II) and experiments containing *K. pneumoniae* with (c) 80 mg $L^{-1}$ Pb(II) and (d) no added Pb(II).

The value of $\mu_{max}$ for *P. bifermentans* for no added Pb(II) is higher than the value for *K. pneumoniae* with no added Pb(II), which indicates that *P. bifermentans* has a faster exponential growth. The value of the maximum specific growth rate for *P. bifermentans* with added Pb(II) is much higher than that of *K. pneumoniae* and correlates with the rapid exponential growth observed in Figure 30. The value of $\mu_{max}$ for *P. bifermentans* with added Pb(II) was higher than for no added Pb(II) which is an indication that *P. bifermentans* grows faster when Pb(II) is present. This is not true for *K. pneumoniae* where the value of $\mu_{max}$ is lower in experiments with added Pb(II). The confidence interval indicates that the possible range in which the true value of $\mu_{max}$ lies is narrow in all experimental conditions, especially in the sections that contain the experimental data. This is an indication that the fit of CFU count would be sensitive to changes in the value of $\mu_{max}$. The results indicate a significant difference in the maximum specific growth of the experiments. This is proof that the microbes utilise a different growth mechanism when compared to each other as well as when in the presence of Pb(II).

## 6.3 Conclusions

The visual differences between samples containing *P. bifermentans* and *K. pneumoniae* indicated that a different lead precipitate is present. This was confirmed in Chapter 5 where the identity of the precipitate was shown using XPS.

The microbial growth indicated that *P. bifermentans* utilises a different growth pattern or mechanism when Pb(II) is added compared to when the sample contains no added Pb(II). The mechanism of growth for *K. pneumoniae* with and without added Pb(II) does not differ. It was also concluded that *K. pneumoniae* has more viable cells during the experiment than *P. bifermentans*.

The residual Pb(II) measurements indicated no apparent difference in the amount of Pb(II) removed between the strains with both strains reaching approximately the same final Pb(II) concentration. It was noted that *P. bifermentans* has a faster initial removal rate.

It was possible to establish a correlation between CFU count, $OD_{600}$ and metabolic activity using linear regression. The correlation between CFU count and metabolic activity for *K. pneumoniae* was poor but all other correlations were acceptable. From these correlations it was possible to calculate predicted values for metabolic activity and $OD_{600}$ which ensures that the experiment is comparable with literature.

The specific growth rate was calculated for each experiment and it was concluded that *P. bifermentans* has a higher value of maximum specific growth than *K. pneumoniae* for experiments with no added Pb(II). The value of maximum specific growth for *P. bifermentans* with 80 mg $L^{-1}$ initial Pb(II) concentration was higher than the value for *K. pneumoniae*. The values of maximum specific growth rate for *P. bifermentans* with added Pb(II) was higher than for no added Pb(II), this was not the case for *K. pneumoniae*, which indicates that *P. bifermentans* is better suited for the toxic environment caused by the Pb(II). This conclusion contradicts what was noted in Chapter 5. The narrow confidence interval indicates that the fit of CFU count is sensitive to changes in the value of the maximum specific growth rate, and from this is it observed that the estimated value of $\mu_{max}$ is close to the true value.

The study provided insight into the exponential growth phase of the bacteria and provided information to establish a correlation between commonly used growth measurements.

# 7 General conclusions and recommendations

General conclusions of the study and recommendations In this study the mechanisms of bioprecipitation of two strains isolated from a microbial consortium was investigated. The long-duration study was conducted over 5 d in Chapter 4 which investigated the abilities of the strains to precipitate Pb(II) from solution. These results indicated that lead precipitate was present in solution in under 18 h. It was determined that there was a statistical difference in the amount of Pb(II) precipitated by the strains which indicated that the mechanisms of precipitation vary. A colour difference was evident between the two strains and this could be indicative of a difference in the precipitate identity of the lead compounds.

Since precipitation was observed in under 18 h, a short-duration study was conducted to further investigate the mechanisms as described in Chapter 5. The short-duration study indicated that precipitation occurs in samples containing *K. pneumoniae* at a faster rate than samples containing *P. bifermentans*. It was also determined that nitrates were not required for microbial growth and precipitation. An XPS analysis of the precipitate found in samples indicated that the strains did precipitate different lead compounds, as previously suspected.

The exponential growth was further analysed in Chapter 6 which indicated that the strains exhibit varying behaviour when exposed to Pb(II) than when not. The mechanism of growth for *P. bifermentans* differs when Pb(II) is added to solution. The mechanism of growth for *K. pneumoniae* did not differ but it was noted that *K. pneumoniae* is better suited to the toxic environment imposed by the presence of Pb(II) since the microbial growth with Pb(II) was higher than without.

Further studies are recommended to determine the exact removal mechanisms employed by the strains. These studies could include the use of SEM and TEM to visually determine if the precipitation of Pb(II) occurs extracellularly or intracellularly. Ion chromatography could be employed to determine changes in ionic compound concentrations such as sulphates and nitrates. The system can be applied to a continuous reactor and this would be a step towards application on an industrial scale.

# 8 References


Akpor, O, Ohiobor, G and Olaolu, T (2014) "Heavy metal pollutants in wastewater effluents: Sources, effects and remediation" *Advances in Bioscience and Bioengineering*, *4*, 37–43 DOI: 10.11648/j.abb.20140204.11.

Andrews, G, Neveling, O, De Beer, D, Chirwa, E, Brink, H and Joubert, T (2022) "Non-destructive Impedance Monitoring of Bacterial Metabolic Activity towards Continuous Lead Biorecovery" *Sensors*, *22*, DOI: https://doi.org/10.3390/s22187045.

Arbabi, M, Hemati, S and Amiri, M (2015) "Removal of lead ions from industrial wastewater: A review of Removal methods" *International Journal of Epidemiologic Research*, *2*, 105–109.

Ashurst, J and Dawson, A (2021) *Klebsiella pneumoniae*, 1st ed. StatPearls Publishing, Treasure Island, FL URL: https://www.ncbi.nlm.nih.gov/books/NBK519004/.

Ayangbenro, A, Olanrewaju, O and Babalola, O (2018) "Sulfate-Reducing Bacteria as an Effective Tool for Sustainable Acid Mine Bioremediation" *Frontiers in Microbiology*, *9*, 1–10 DOI: 0.3389/fmicb.2018.01986.

Baysal, A, Ozbek, N and Akman, S (2013) "Determination of Trace Metals in Waste Water and Their Removal Processes", in: *Waste Water - Treatment Technologies and Recent Analytical Developments*, Einschlag, F (Ed.), Intech Press DOI: 10.5772/52025 URL: https://www.intechopen.com/books/waste-water-treatment-technologies-and-recent-analytical-developments/determination-of-trace-metals-in-waste-water-and-their-removal-processes (visited on 02/08/2021).

Brink, H, Hörstmann, C and Feucht, C (2019) "Microbial Pb(II) Precipitation: Minimum Inhibitory Concentration and Precipitate Identity" *Chemical Engineering Transactions*, *74*, 1453–1458 DOI: 10.3303/CET1974243.

Brink, H, Hörstmann, C and Peens, J (2020) "Microbial Pb(II)-precipitation: the influence of oxygen on Pb(II)-removal from aqueous environment and the resulting precipitate identity" *International Journal of Environmental Science and Technology*, *17*, 409–420 DOI: https://doi.org/10.1007/s13762-019-02502-4.

Brink, H, Lategan, M, Naudé, K and Chirwa, E (2017) "Lead Removal Using Industrially Sourced Consortia: Influence of Lead and Glucose Concentrations" *Chemical Engineering Transactions*, *57*, 409–415 DOI: 10.3303/CET1757069.

Brink, H and Mahlangu, Z (2018) "Microbial Lead(II) Precipitation: The Influence of Growth Substrate" *Chemical Engineering Transactions*, *64*, 439–444 DOI: 10.3303/CET1864074.

Chemtech International (2020) *Advantages and Disadvantages of Electrocoagulation Water Treatment* URL: https://chemtech-us.com/advantages-and-disadvantages-of-electrocoagulation-water-treatment/ (visited on 02/11/2021).

Chimhundi, J, Hörstmann, C, Chirwa, E and Brink, HG (2021) "Microbial Removal of Pb(II) Using an Upflow Anaerobic Sludge Blanket (UASB) Reactor" *Catalysts*, *11*, 1–15 DOI: 10.3390/catal11040512.

Christensen, DG, Orr, JS, Rao, CV and Wolfe, AJ (2017) "Increasing growth yield and decreasing acetylation in Escherichia coli by optimizing the carbon-to-magnesium ratio in peptide-based media" *Applied and Environmental Microbiology*, *83*, (6) ISSN: 10985336 DOI: 10.1128/AEM.03034-16.

Cilliers, C, Neveling, O, Tichapondwa, S, Chirwa, E and Brink, H (2022) "Microbial Pb(II)-bioprecipitation: Characterising Responsible Biotransformation Mechanisms" *Journal of Cleaner Production*, *374*, DOI: https://doi.org/10.1016/j.jclepro.2022.133973.

Cui, Y, Gong, X, Shi, Y and Wang, Z (2017) "Salinity effect on production of PHA and EPS by *Haloferax mediterranei*" *RSC Advances*, *7*, DOI: 10.1039/C7RA09652F.

D'Agostino Sr, R, Sullivan, L and Beiser, A (2006) *Introductory Applied Biostatistics*, 1st ed. Cengage Learning, Belmont, CA, USA.

Department of Mineral Resources: Republic of South Africa (2019) *South Africa's Mineral Industry* Report Arcadia, South Africa.

Department of Water Affairs (2013) *Revision of general authorisations in terms of section 39 of the national water act, 1998, (Act no. 36 of 1998)* Government Gazette South Africa.

Didar-Ul Islam, S (2019) "Electrocoagulation (EC) technology for wastewater treatment and pollutants removal" *Sustainable Water Resources Management*, *5*, 359–380 DOI: 10.1007/s40899-017-0152-1.

Dongre, R (2020) "Lead: Toxicological Profile, Pollution Aspects and Remedial Solutions", in: *Lead Chemistry*, Chooto, P (Ed.), Intech Press DOI: 10.5772/intechopen.93095 URL: https://www.intechopen.com/books/lead-chemistry/lead-toxicological-profile-pollution-aspects-and-remedial-solutions (visited on 02/08/2021).

EMEW Clean Technologies (2016) *Electrowinning 101: What is electrowinning?* URL: https://blog.emew.com/electrowinning-101-what-is-electrowinning (visited on 02/08/2021).

Esmaeili, H and Foroutan, R (2015) "Investigation into ion exchange and adsorption methods for removing heavy metals from aqueous solutions" *International Journal of Biology, Pharmacy, and Allied Sciences*, *4*, 620–629.

Fu, F and Wang, Q (Mar. 2011) "Removal of heavy metal ions from wastewaters: A review" *Journal of Environmental Management*, *92*, (3): 407–418 ISSN: 03014797 DOI: 10.1016/j.jenvman.2010.11.011.

Fuller, R (2009) "Lead Exposures from Car Batteries—A Global Problem" *Environ Health Perspect. 117*, DOI: 10.1289/ehp.0901163.

García, R and Báez, A (2012) "Atomic Absorption Spectrometry (AAS)", in: *Atomic Absorption Spectrometry*, Farrukh, M (Ed.), Intech Press DOI: 10.5772/25925 URL: https://www.intechopen.com/books/atomic-absorption-spectroscopy/atomic-absorption-spectrometry-aas- (visited on 03/28/2021).

Hendriks, J, Oubrie, A, Castresana, J, Urbani, A, Gemeinhardt, S and Saraste, M (2000) "Nitric oxide reductases in bacteria" *Biochimica et Biophysica Acta*, *1459*, 266–273 DOI: 10.1016/S0005-2728(00)00161-4.

Hörstmann, C and Brink, H (2019a) "Microbial Pb(II) Precipitation: The Effects of Aeration Conditions and Glucose Presence on a Lead-Mine Consortium" *Chemical Engineering Transactions*, *76*, 1291–1296 DOI: 10.3303/CET1976216.

Hörstmann, C and Brink, H (2019b) "Microbial Pb(II) Precipitation: The Influence of Aqueous Zn(II) and Cu(II)" *Chemical Engineering Transactions*, *74*, 1447–1452 DOI: 10.3303/CET1974242.

Hörstmann, C, Brink, H and Chirwa, E (2020) "Pb(II) Bio-Removal, Viability, and Population Distribution of an Industrial Microbial Consortium: The Effect of Pb(II) and Nutrient Concentrations" *Sustainability*, *6*, DOI: https://doi.org/10.3390/su12062511.

Hörstmann, C, Chirwa, E and Brink, H (2021) "Insight into the metabolic profiling of Pb(II) removal microorganisms" *Molecules*, *26*, DOI: 10.3390/molecules26134008.

Hörstmann, C, Naidoo, S, Brink, H and Chirwa, E (2020) "Microbial Pb(II) Precipitation: Yeast Extract Autolyzed from *Saccharomyces Cerevisiae* as a Sustainable Growth Substrate" *Chemical Engineering Transactions*, *79*, 421–426 DOI: 10.3303/CET2079071.

Hubicki, Z and Kołodyńska, D (2011) "Selective Removal of Heavy Metal Ions from Waters and Waste Waters Using Ion Exchange Methods", in: *Ion Exchange Technologies*, Kilislioglu, A (Ed.), Intech Press DOI: 10.5772/51040 URL: https://www.intechopen.com/books/ion-exchange-technologies/selective-removal-of-heavy-metal-ions-from-waters-and-waste-waters-using-ion-exchange-methods (visited on 02/08/2021).

Hwang, J and Oweimreen, G (2003) "The Solubility Product of PbCl2 from Electrochemical Measurements" *Journal of Chemical Education*, *80*, 1051–1052 DOI: https://doi-org.uplib.idm.oclc.org/10.1021/ed080p1051.

Iloms, E, Ololade, O, Ogola, H and Selverajan, R (2020) "Investigating Industrial Eluent Impact on Municipal Wastewater Treatment Plant in Vaal, South Africa" *International Journal of Environmental Research and Public Health*, *17*, 1–18 DOI: 10.3390/ijerph17031096.

Interchim (2015) *LB Broth (Miller's LB Broth)* URL: https://www.interchim.fr/ft/N/N1398A.pdf (visited on 03/03/2021).

Kang, CH, Kwon, YJ and So, JS (2016) "Bioremediation of heavy metals by using bacterial mixtures" *Ecological Engineering*, *89*, 64–69 DOI: 10.1016/j.ecoleng.2016.01.023.

Knowles, R (1982) "Denitrification" *Microbiological reviews*, *46*, 43–70.

Kupcsik, L (2011) "Estimation of Cell Number Based on Metabolic Activity: The MTT Reduction Assay", in: *Mammilian Cell Viability*, Stoddart, M (Ed.), Humana Press DOI: ttps://doi-org.uplib.idm.oclc.org/10.1007/978-1-61779-108-6_3.

Kutsuna, R, Miyoshi-Akiyama, T, Mori, K, Hayashi, M, Tomida, J, Morita, Y, Tanaka, K and Kawamura, Y (2018) "Description of *Paraclostridium bifermentans* subsp. *muricolitidis* subsp. nov., emended description of *Paraclostridium bifermentans* (Sasi Jyothsna et al., 2016), and creation of *Paraclostridium bifermentans* subsp. *bifermentans* subsp. nov" *Microbiology and Immunology*, *63*, 1–10 ISSN: 0385-5600 DOI: 10.1111/1348-0421.12663.

Lal, A and Cheeptham, N (2007) *Eosin-Methylene Blue Agar Plates Protocol* American Society for Microbiology URL: www.asmscience.org.

Lenntech (2021) *Lead - Pb* URL: https://www.lenntech.com/periodic/elements/pb.htm (visited on 02/08/2021).

Li, X, Peng, W, Jia, Y, Lu, L and Fan, W (2016) "Bioremediation of lead contaminated soil with *Rhodobacter sphaeroides*" *Chemosphere*, *156*, 228–235 DOI: 10.1016/j.chemosphere.2016.04.098.

Linke, H, Sánchez-Cordero, S and Hoffman, H (1980) "Isolation of a salt tolerant pleomorphic Klebsiella strain from a case of diabetic periodontitis" *Microbios. 27*, 107–115.

Lombó, CG, Posadas, Y, Quintanar, L and Eugenia, M (2013) "Neurotoxicity linked to dysfunctional metal ion homeostasis and xenobiotic metal exposure: Redox signaling and oxidative stress" *Antioxidants Redox Signal.* 1–114 DOI: https://doi.org/10.1089/ars.2017.7272.

MacWilliams, M and Liao, M (2006) *Luria Broth (LB) and Luria Agar (LA) Media and Their Uses Protocol* American Society for Microbiology.

Miller, DL, Brazer, S, Murdoch, D, Reller, LB and Ralph, G (2001) *Significance of Clostridium tertium Bacteremia in Neutropenic and Nonneutropenic Patients: Review of 32 Cases*: pp. 975–978.

Morena-Vivián, C, Cabello, P, Martínez-Luque, M, Blasco, R and Castillo, F (1999) "Prokaryotic Nitrate Reduction: Molecular Properties and Functional Distinction among

Bacterial Nitrate Reductases" *Journal of bacteriology*, *181*, 6573–6584 DOI: 10.1128/JB.181.21.6573-6584.1999.

Naik, M and Dubey, S (2013) "Lead resistant bacteria: Lead resistance mechanisms, their applications in lead bioremediation and biomonitoring" *Ecotoxicology and Environmental Safety*, *98*, 1–7 DOI: https://doi.org/10.1016/j.ecoenv.2013.09.039.

National Institute of Standards and Technology (2002) *NIST X-ray Photoelectron Spectroscopy Database, NIST Standard Reference Database Number 20* URL: doi:10.18434/T4T88K (visited on 08/17/2022).

Neveling, O, Veenhuyzen, B van, Cilliers, C, Chirwa, E and Brink, H (2022) "Microbial Pb(II) Removal by Precipitation and Adsorption Mechanisms with *Klebsiella Pneumoniae* Isolated from an Industrially Obtained Consortium" *Chemical Engineering Transactions*, *92*, DOI: 10.3303/CET2292018.

Nosier, S and Sallam, S (2000) "Removal of lead ions from wastewater by cementation on a gas-sparged zinc cylinder" *Separation and Purification Technology*, *18*, 93–101 DOI: https://doi.org/10.1016/S1383-5866(99)00052-0.

Oaikhena, E, Makaije, D, Denwe, S, Namadi, M and Haroun, A (2016) "Bioremediation Potentials of Heavy Metal Tolerant Bacteria Isolated from Petroleum Refinery Effluent" *American Journal of Environmental Protection*, *5*, 29–34 DOI: 10.11648/j.ajep.20160502.12.

Ogbu, K, Anyika, K, Ochai, S, Gyendeng, J and Olaolu, O (2017) "Determination of bacterial load in dog milk with its associated risk factors in Jos, Plateau State" *World Journal of Pharmaceutical and Medical Research*, *3*, (10): 130–134 ISSN: 2455-3301 URL: https://www.researchgate.net/publication/320780727.

Parker, N, Schneegurt, M, Thi Tu, A, Lister, P and Forster, B (2016) *Microbiology*, 1st ed. OpenStax, Houston, Texas URL: https://openstax.org/books/microbiology/pages/1-introduction.

Pauleta, S, Dell'Acqua, S and Moura, I (2013) "Nitrous oxide reductase" *Coordination Chemistry Reviews*, *257*, 332–349 DOI: 10.1016/j.ccr.2012.05.026.

Peens, J, Wu, Y and Brink, H (2018) "Microbial Pb(II) Precipitation: The Influence of Elevated Pb(II) Concentrations" *Chemical Engineering Transactions*, *64*, 583–588 DOI: 10.3303/CET1864098.

Perpetuo, E, Barbieri, C and Nascimento, C (2011) "Engineering Bacteria for Bioremediation" *Progress in Molecular and Environmental Bioengineering - From Analysis and Modeling to Technology Applications*, DOI: 10.5772/19546.

Pfennig, N and Biebl, H (1976) "*Desulfuromonas acetoxidans* gen. nov. and sp. nov., a new anaerobic, sulfur-reducing, acetate-oxidizing bacterium" *Archives of Microbiology*, *110*, 3–12 DOI: 10.1007/BF00416962.

Rai, A, Ramana, CV, Uppada, J and Sasikala, C (2020) "*Paraclostridium*", in: *Bergey's Manual of Systematics of Archaea and Bacteria*, Rainey, FA (Ed.), Elsevier DOI: 10.1002/9781118960608.gbm01635.

Rigoletto, M, Calza, P, Gaggero, E, Malandrino, M and Fabbri, D (2020) "Bioremediation Methods for the Recovery of Lead-Contaminated Soils: A Review." *Applied Science*, *2*, DOI: https://doi:10.3390/app10103528.

Rinaldo, S and Cutruzzolá, F (2007) "Chapter 3 - Nitrite Reductases in Denitrification", in: *Biology of the Nitrogen Cycle*, Bothe, H, Ferguson, S and Newton, W (Eds.), Elsevier ISBN: 9780444528575 DOI: 10.1016/B978-044452857-5.50004-7 URL: https://www.sciencedirect.com/science/article/pii/B9780444528575500047 (visited on 02/24/2021).

Sanders, ER (May 2012) "Aseptic laboratory techniques: Plating methods" *Journal of Visualized Experiments*, (63): 1–18 ISSN: 1940087X DOI: 10.3791/3064.

Shamuyarira, K and Gumbo, J (2014) "Assessment of Heavy Metals in Municipal Sewage Sludge: A Case Study of Limpopo Province, South Africa" *International Journal of Environmental Research and Public Health*, *11*, 2569–2579 DOI: 10.3390/ijerph110302569.

Skoog, D, Holler, F and Crouch, S (2018) *Principles of Instrumental Analysis*, 7th ed. Cengage Learning, Boston, MA ISBN: 978-1-305-57721-3.

Slonczewski, JL and Foster, JW (2011) *Microbiology: An Evolving Science*, 2nd ed. W. W. Norton, New York: p. 166 ISBN: 9780393934472.

Snodgrass, R (1986) "Lead in South Africa" *Journal of the South African Institute of Mining and Metallurgy*, *86*, 97–111.

Stanković, V (2007) "Metal Removal from Effluents by Electrowinning and a new Design Concept in Wastewater Purification Technology" *Chemical and Biochemical Engineering Quarterly*, *1*, 33–45.

Sylwan, I and Thorin, E (Apr. 2021) "Removal of heavy metals during primary treatment of municipal wastewater and possibilities of enhanced removal: A review" *Water (Switzerland)*, *13*, (8) ISSN: 20734441 DOI: 10.3390/w13081121.

Tankeshwar, A (2019) *Klebsiella pneumoniae: Properties, Diseases and Laboratory Diagnosis* URL: https://microbeonline.com/klebsiella-pneumoniae-properties-virulence-diseases-diagnosis/ (visited on 03/02/2021).

Tao, Y and Zhang CLü, T (2020) "Removal of Pb(II) Ions from Wastewater bu Using Magnetic Nanoparticles" *Applied Science*, *10*, DOI: https://dio.org/10.3390/app10030948.

Tiquia-Arashiro (2018) "Lead absorption mechanisms in bacteria as strategies for lead bioremediation" *Applied Microbiology and Biotechnology*, *102*, 5437–5444 DOI: 10.1007/s00253-018-8969-6.

Tsuji, A, Kaneko, Y, Takahashi, K, Ogawa, M and Goto, S (1982) "The Effects of Temperature and pH on the Growth of Eight Enteric and Nine Glucose Non-Fermenting Species of Gram-Negative Rods" *Microbiology and Immunology*, *26*, 15–24 DOI: https://doi.org/10.1111/j.1348-0421.1982.tb00149.x.

van Veenhuyzen, B, Chirwa, E and Brink, HG (2021) "Microbial Pb(II) Precipitation: the Role of Biosoprtion as a Pb(II) REmoval Mechanism" *Chemical Engineering Transactions*, *86*, 181–186 DOI: 10.3303/CET2186031.

Zarei, O, Dastmalchi, S and Hamzeh-Mivehroud, M (2016) "A Simple and Rapid Protocol for Producing Yeast Extract from *Saccharomyces cerevisiae* Suitable for Preparing Bacterial Culture Media" *Iranian Journal of Pharmaceutical Research*, *15*, 907–913.

Zhang, K, Zhang, D, Li, X and Xue, Y (2021) "Biomineraization of lead in wastewater: Bacterial reutilization and metal recovery" *Journal of Hazardous Materials*, *421*, DOI: 10.1016/j.jhazmat.2021.126765.

Zumft, W (1997) "Cell Biology and Molecular Basis of Denitrification" *Microbiology and molecular biology reviews*, *61*, 533–616.

# A Appendix

This appendix contains the results of the 16S rDNA analysis done by Inqaba Biotech (South Africa) for *P. bifermentans* and *K. pneumoniae* as below:

- *P. bifermentans* as "Isolation 3"
- *K. pneumoniae* as "EMB1R1"

inqaba biotec™

*Africa's Genomics Company*

# 16S REPORT

| | |
|---|---|
| Client's Name: | Olga Neveling |
| Institute: | University of Pretoria |
| Client's Address: | Pretoria |
| Report Compiled By: | Inqaba Biotechnical Industries (Pty) Ltd |

## BACKGROUND:

Some bacterial isolates cannot be taxonomically identified from phenotypic characteristics. Bacterial isolates can be characterised by sequencing the 16S rDNA. The universal primers 27F and 1492R are used to amplify the 16S target region (Lane et al 1991; Turner et al 1999).

## MATERIAL AND METHODS:

Genomic DNA was extracted from the cultures received using the Quick-DNA™ Fungal/Bacterial Miniprep Kit (Zymo Research, Catalogue No. D6005). The 16S target region was amplified using OneTaq® Quick-Load® 2X Master Mix (NEB, Catalogue No. M0486) with the primers presented in Table 1. The PCR products were run on a gel and gel extracted with the Zymoclean™ Gel DNA Recovery Kit (Zymo Research, Catalogue No. D4001). The extracted fragments were sequenced in the forward and reverse direction (Nimagen, BrilliantDye™ Terminator Cycle Sequencing Kit V3.1, BRD3-100/1000) and purified (Zymo Research, ZR-96 DNA Sequencing Clean-up Kit™, Catalogue No. D4050). The purified fragments were analysed on the ABI 3500xl Genetic Analyzer (Applied Biosystems, ThermoFisher Scientific) for each reaction for every sample, as listed in Section 1. CLC Bio Main Workbench v7.6 was used to analyse the .ab1 files generated by the ABI 3500XL Genetic Analyzer and results were obtained by a BLAST search (NCBI).

BLASTN 2.2.31+

Reference: Stephen F. Altschul, Thomas L. Madden, Alejandro A. Schäffer, Jinghui Zhang, Zheng Zhang, Webb Miller, and David J. Lipman (1997), "Gapped BLAST and PSI-BLAST: a new generation of protein database search programs", Nucleic Acids Res. 25:3389-3402.

Table 1: 16S Primers sequences

| Name of Primer | Target | Sequence (5' to 3') |
|---|---|---|
| 16S-27F | 16S rDNA sequence | AGAGTTTGATCMTGGCTCAG |
| 16S-1492R | 16S rDNA sequence | CGGTTACCTTGTTACGACTT |

inqaba biotec™

*Africa's Genomics Company*

# 16S REPORT

## RESULTS:

Figure 1: A photographic image of an agarose gel indicating the amplification of the 16S target region.

inqaba biotec™

*Africa's Genomics Company*

# 16S REPORT

## RESULTS:

BLAST: The BLAST results correspond to the similarity between the sequence queried and the biological sequences within the NCBI database.

| | |
|---|---|
| Name of sample | Isolation 3 from Plate 4 |
| Request ID | FRMWPP86016 |
| Predicted Organism | *Paraclostridium bifermentans* |
| GenBank Accession | CP032452.1 |

inqaba biotec™

*Africa's Genomics Company*

# 16S REPORT

## CONCLUSION:

| Name of sample | BLAST prediction |
|---|---|
| Isolation 3 from Plate 4 | *Paraclostridium bifermentans* |

Dr Erika Viljoen
Genomics Scientist

24/07/2021
Date

Dr Christiaan Labuschagne
Genomics Manager

Date

inqaba biotec™

*Africa's Genomics Company*

# 16S REPORT

| | |
|---|---|
| Client's Name: | Carla Cilliers |
| Institute: | University of Pretoria |
| Client's Address: | |
| Report Compiled By: | Inqaba Biotechnical Industries (Pty) Ltd |

## BACKGROUND:

Some bacterial isolates cannot be taxonomically identified from phenotypic characteristics. Bacterial isolates can be characterised by sequencing the 16S rDNA. The universal primers 27F and 1492R are used to amplify the 16S target region (Lane et al 1991; Turner et al 1999).

## MATERIAL AND METHODS:

Genomic DNA was extracted from the cultures received using the Quick-DNA™ Fungal/Bacterial Miniprep Kit (Zymo Research, Catalogue No. D6005). The 16S target region was amplified using OneTaq® Quick-Load® 2X Master Mix (NEB, Catalogue No. M0486) with the primers presented in Table 1. The PCR products were run on a gel and gel extracted with the Zymoclean™ Gel DNA Recovery Kit (Zymo Research, Catalogue No. D4001). The extracted fragments were sequenced in the forward and reverse direction (Nimagen, BrilliantDye™ Terminator Cycle Sequencing Kit V3.1, BRD3-100/1000) and purified (Zymo Research, ZR-96 DNA Sequencing Clean-up Kit™, Catalogue No. D4050). The purified fragments were analysed on the ABI 3500xl Genetic Analyzer (Applied Biosystems, ThermoFisher Scientific) for each reaction for every sample, as listed in Section 1. CLC Bio Main Workbench v7.6 was used to analyse the .ab1 files generated by the ABI 3500XL Genetic Analyzer and results were obtained by a BLAST search (NCBI).

BLASTN 2.2.31+

Reference: Stephen F. Altschul, Thomas L. Madden, Alejandro A. Schäffer, Jinghui Zhang, Zheng Zhang, Webb Miller, and David J. Lipman (1997), "Gapped BLAST and PSI-BLAST: a new generation of protein database search programs", Nucleic Acids Res. 25:3389-3402.

Table 1: 16S Primers sequences

| Name of Primer | Target | Sequence (5' to 3') |
|---|---|---|
| 16S-27F | 16S rDNA sequence | AGAGTTTGATCMTGGCTCAG |
| 16S-1492R | 16S rDNA sequence | CGGTTACCTTGTTACGACTT |

inqaba biotec™

*Africa's Genomics Company*

# 16S REPORT

## RESULTS:

Figure 1: A photographic image of an agarose gel indicating the amplification of the 16S target region.

inqaba biotec™

*Africa's Genomics Company*

# 16S REPORT

## RESULTS:

BLAST: The BLAST results correspond to the similarity between the sequence queried and the biological sequences within the NCBI database.

| | |
|---|---|
| Name of sample | B80EMB2-A |
| Request ID | 8ZXCJW3U01N |
| Predicted Organism | *Klebsiella pneumoniae* |
| GenBank Accession | CP071086.1 |

| | |
|---|---|
| Name of sample | B80EMB2-B |
| Request ID | 8ZXCU9WR01N |
| Predicted Organism | *Klebsiella pneumoniae* |
| GenBank Accession | CP039974.1 |

| | |
|---|---|
| Name of sample | EMB1-R1 |
| Request ID | 8ZXD2MAM01N |
| Predicted Organism | *Klebsiella pneumoniae* |
| GenBank Accession | CP039974.1 |

| | |
|---|---|
| Name of sample | EMB1-R2 |
| Request ID | 8ZXD948G01N |
| Predicted Organism | *Clostridium sp., [Clostridium] bifermentans* |
| GenBank Accession | FJ638499.1, JX267081.1 |

Print Date: 5/5/2021

inqaba biotec™

*Africa's Genomics Company*

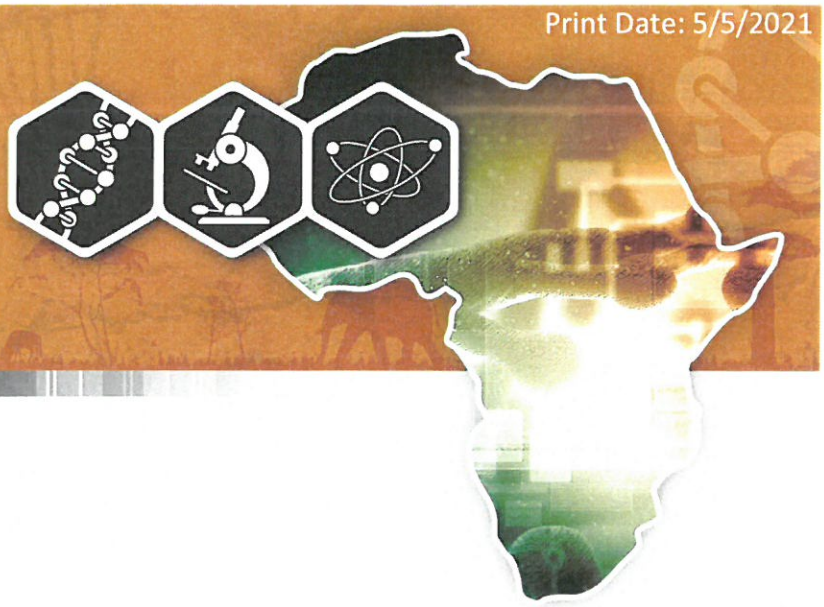

# 16S REPORT

## CONCLUSION:

| Name of sample | BLAST prediction |
|---|---|
| B80EMB2-A | *Klebsiella pneumoniae* |
| B80EMB2-B | *Klebsiella pneumoniae* |
| EMB1-R1 | *Klebsiella pneumoniae* |
| EMB1-R2 | *Clostridium sp., [Clostridium] bifermentans* |

Dr Erika Viljoen
Genomics Scientist

5/5/2021
Date

Dr Christiaan Labuschagne
Genomics Manager

Date